UC Davis

UC Davis Electronic Theses and Dissertations

Title

Novel Genomic Rearrangements Derived from Haploid Induction and Their Potential Use in Plant Breeding

Permalink

https://escholarship.org/uc/item/82p824qh

Author

Ordonez Aquino, Benny Julissa

Publication Date

2023

Peer reviewed|Thesis/dissertation

eScholarship.org Powered by the California Digital Library
University of California

NOVEL GENOMIC REARRANGEMENTS DERIVED FROM HAPLOID INDUCTION CROSSES AND THEIR POTENTIAL USE IN PLANT BREEDING

By
BENNY JULISSA ORDONEZ AQUINO
DISSERTATION

Submitted in partial satisfaction of the requirements for the degree of
DOCTOR OF PHILOSOPHY
In

Integrative Genetics and Genomics
in the

OFFICE OF GRADUATE STUDIES

of the

UNIVERSITY OF CALIFORNIA

DAVIS

Approved:

_____
Luca Comai, Chair

_____
Joanna Chiu

_____
Fereydoun Hormozdiari

Committee in Charge
2023

ABSTRACT

Novel Genomic Rearrangements Derived from Haploid Induction and Their Potential Use in Plant Breeding

By
Benny Ordonez

Potatoes (*Solanum tuberosum* L.) rank among the world's leading staple crops due to their high demand and nutritional value. They are autotetraploid with tetrasomic inheritance, and exhibit high heterozygosity, posing challenges for genetic studies and crop improvement efforts. Moreover, the limited genetic diversity in modern cultivated potatoes makes them vulnerable to diseases and restricts opportunities for increasing productivity. In contrast, wild relatives and landraces display superior phenotypes for many valuable traits and could provide genetic variation absent in cultivated varieties. A method for efficient transfer of these traits to the cultivated pool could help alleviate these limitations. Unfortunately, interspecific hybridization is often hindered by crossing barriers. A promising alternative for harnessing the diversity of potato relatives is through the haploid induction system and its byproducts.

In potatoes, haploid induction occurs between tetraploid cultivars and specific diploid lines acting as haploid inducers (HIs). The resulting products from this cross include not only the desired dihaploids, but also triploids, tetraploids, and aneuploids, originating from both the 4x parent and the haploid inducer. Despite their crucial role in the production of dihaploids, haploid inducers (HIs) have not seen significant improvements from a breeding standpoint. Potato breeders prefer HIs that flower profusely and yield many dihaploids. They dislike HIs that generate more instances of extrachromosomal DNA—specifically additional and/or rearrangement HI chromosomes— in the dihaploids.

In this study, we compare the haploid induction rate (*HIR*) of two well-known IvP HIs alongside a new haploid inducer named PL-4, conducting haploid induction crosses using forty elite 4x breeding lines as pistillate parents. Our findings highlight PL-4 as a superior HI, exhibiting an overall higher *HIR* (11.6%) compared to IvP101 and IvP35 (6.8% and 4.3%, respectively). Additionally, PL-4 demonstrates broad pistillate parent compatibility, irrespective of their cytoplasm type. This suggests that PL-4 can be a valuable asset in a large-scale dihaploid production scheme.

As diploid potato breeding advances, the need to understand the diverse karyotypic variations resulting from haploid induction crosses becomes increasingly crucial. While genome instability has been observed among the products of haploid induction in *Arabidopsis thaliana*, the associated instability in potatoes remains relatively unexplored. The progeny of potato haploid induction may serve as a reservoir for novel rearrangements, including extrachromosomal DNA. The characterization of these novel chromosomal elements could provide tools for precision genome engineering by serving as platforms to introduce new traits and enhance the overall potato genetic landscape.

To comprehensively assess the byproducts of haploid induction, our examination began with a thorough analysis of various seed types, followed by detailed phenotypic assessment. We employed IvP48, a HI previously known for harboring residual HI DNA in the resulting progeny. To minimize bias towards well-developed seeds, all seed types underwent *in vitro* germination. Noteworthy among our findings is the characterization of a new type—shriveled seeds—which encompasses seeds with compromised or partially collapsed endosperm, in addition to the more commonly observed spotted and spotless seeds in this cross. This novel category exhibits an enrichment of aneuploidy types. In summary, our analysis of the dihaploid lines unveiled 15%

maternal aneuploidy, with chromosome 8 displaying the most frequent variation in dosage. This observed pattern is attributed to a previously identified translocation between chromosome 7 and chromosome 8 in the Red Polenta cultivar used as the pistillate parent. Similarly to what is observed in the progeny of haploid induction crosses in *Arabidopsis thaliana,* there is a potential chromothriptic case among the dihaploids that requires further investigation.

Minichromosomes (minis), stand out as the most intriguing byproducts of haploid induction, yet their potential in potato research remains largely unexplored. Remarkably, minis in potato have yet to receive comprehensive study. To help fill this gap, we investigated an *A. thaliana* line harboring a minichromosome, named *mini1a*, presenting the first comprehensive characterization of minis resulting from Arabidopsis haploid induction crosses. Our investigation of *mini1a* has revealed distinctive characteristics, including a meiotic transmission rate of approximately 28% and a confirmed circular structure through cytological examination. Subsequent sequencing revealed the formation of mini-subtypes, showcasing structural variations, particularly in the centromeric regions. Notably, in certain instances, *mini1a* led to detrimental effects on fertility. The assessment of *mini1a*'s mitotic stability, utilizing a visual trait, yielded inconclusive results, which we attributed to potential silencing of the mini genes. However, a more detailed characterization is still required. Our findings highlight challenges in utilizing minis as vectors for chromosome engineering. Despite their promising potential, successful implementation may encounter obstacles, as evidenced in our study.

In conclusion, this dissertation advances our comprehension of crucial elements in haploid induction, unraveling novel insights for both potato and Arabidopsis. The identification of a new

haploid inducer and the exploration of unique chromosome rearrangements, particularly minichromosomes, emerge as pivotal contributions. These findings not only expand our knowledge but may also open avenues for harnessing these novel elements as powerful tools in crop improvement.

Dedicated to my mom, the most incredible person I've ever known. If she had the same opportunities I've had, her contributions to the world would have been boundless.
I deeply admire her unwavering determination to break the chains of poverty and shape our destiny. She is the rock that has uplifted our generations.

ACKNOWLEDGEMENTS

Finishing this thesis has been one of the most challenging yet fulfilling journeys in my entire life, and none of it would be possible without the support and encouragement from numerous people.

First and foremost, I want to express my gratitude to my Ph.D. advisor, Dr. Luca Comai, for his continued support, encouragement, and guidance throughout my time in his lab. Many challenges arose during my time here. Dr. Comai believed in me and provided available assistance by writing support letters and emails when needed. Thanks to him, I have grown as a researcher but also as an individual, grateful for the trust he placed in my abilities.

I extend my gratitude to my thesis committee members, Dr. Joanna Chiu and Dr. Fereydoun Hormozdiari, and also Dr. Isabelle Henry for lending their expertise and guidance. Special thanks to Dr. Nicole Kingsley for helping me during one of the hardest times of my PhD journey.

I would like to extend my heartfelt appreciation to my former mentor Dr. Meredith Bonierbale, who has been a role model and provides constant support since I joined the International Potato Center. Meredith is an outstanding female scientist, and I know that I can always rely on her as a professional mentor and friend. Thanks to Dr. Awais Khan for suggesting my participation in the grant for potato haploid induction which led me to pursue this PhD.

I would like to acknowledge the members of the Comai lab who shared their journey with me: Dr. Nampun Hungsaprug, Dr. Livingstone Nganga, Dr. Kirk Amundson, Dr. Weier Guo, Dr. Peter Lynagh, Dr. Han Tan, Paul Osuna-Kleist, Helen Tsai, Sergio Silva and Meric Lieberman. Many thanks to my undergrad students, including Kevin Morimoto, Sara Jovanovich, Christine Chen, Tram Ngo, Lisa Chou, Laila Canosa, Fangchen Liu, Winky Wong and Cecilia Yung. You are all exceptional and bright scientists, and it has been a pleasure working with each of you. I hope I was able to effectively share and impart my practical knowledge.

I am also grateful to my IGG ‘Callipygies’ friends: Dr. Daniela Soto, Dr. Julie Chow, Dr. Ellen Gregory, Dr. Kyle Lewald and Dr. Noemi Sierra. These friends are among the best I met when I joined the IGG PhD program.

To my family, specifically my mom, Benita, and my sister, Diana, who have been my support system during both happy and challenging times. Endless thanks to my husband, Sean Cusick, for his trust, support, and unwavering belief in me, and to my son, Piero, who is my constant inspiration every day.

TABLE OF CONTENTS

List of Tables

List of Figures

Chapter 1

Introduction

Background

Potato (*Solanum tuberosum* L,) is the third most important crop for human consumption worldwide (Kearney, 2010). Due to its high nutritional content and adaptability, potato plays a critical role in ensuring food security. However, potato breeding has faced slower progress compared to other crops due to polyploidy, tetrasomic inheritance and high heterozygosity (Halterman et al. 2016; Jansky, 2009). To address the need for improved performance of potato varieties in the face of emerging climate change, the introduction of novel traits at an accelerated rate is imperative. One promising innovative approach could be the utilization of extrachromosomal DNA, such as additional chromosomes and/or rearranged chromosomes. These natural plant chromosome vectors (NPCVs) offer the potential to introduce valuable traits and novel genetic variation into breeding programs. This is particularly relevant in potato because potato breeding relies heavily on the production of dihaploids and extrachromosomal DNA can arise from the outcomes of haploid induction crosses.

Haploid induction is a process used in breeding programs to produce dihaploids (2n=2x=24) from tetraploids. Dihaploids have the advantage of being genetically simpler for breeding purposes. Haploid induction is used extensively in potato. Instability induced by this cross leads to the production not only of dihaploids but also of triploids, tetraploids, and aneuploids, originating from both the pistillate parent and the haploid inducer (HI). This comprehensive spectrum of genomic variations significantly amplifies the value of haploid induction outcomes as a potential reservoir of extrachromosomal DNA that can be harnessed for precision genome engineering.

In potato, dihaploids are generated through one of two pathways: by using the *phureja*-inducing

lines via gynogenesis, or by *in vitro* culture of anthers or microspores via androgenesis. For gynogenesis, selected diploid accessions of *Solanum tuberosum* Group Phureja (Hutten et al. 1995) known as Haploid Inducers (HI), are used as pollinators of 4x cultivars. The alternative pathway to generate dihaploids consists in *in vitro* culture of microspores or anthers. This approach is cumbersome and requires expertise in tissue culture techniques. As a result, breeders often prefer the use of HIs due to their easy implementation and faster development of dihaploids from existing 4x lines into their breeding programs.

Haploid Induction in potato

The mechanism governing potato haploid induction was previously attributed to a single fertilization event via parthenogenesis, but new independent findings point to genome elimination as a mechanism. One of the first hints of egg fertilization by the HI came from Clulow et al. (1991) who reported the presence of HI chromosomes in dihaploids. In addition, disparate molecular and cytological markers have suggested that, in some cases, a partial genomic contribution by the HI was retained (Clulow et al. 1993; Clulow & Rousselle-Bourgeois, 1997; Ercolano et al. 2004; Straadt and Rasmussen, 2003; Wilkinson et al. 1995). Recently, genomic investigations have probed the basis of haploid induction although the exact mechanism remains elusive. For instance, Pham et al. (2019) reported that most dihaploids displayed ubiquitous paternal (HI) single nucleotide polymorphisms (SNP). The authors suggested that widespread recombination took place before the HI genome was eliminated and that the dihaploids were chimeric. However, this study did not provide clear molecular or phenotypic evidence of stable chromosome addition or introgression. Later, Amundson et al. (2021), including myself as a coauthor, assessed a large set of dihaploids for the presence of HI DNA. Our findings did not support parthenogenesis as the

mechanism for potato haploid induction, because approximately 1% of dihaploids displayed chromosomal addition from the HI. We found no evidence of widespread recombination between parental genomes. Instead, our data were compatible with another explanation: we hypothesized that defects in the sperm resulted in incomplete fusion of sperm and egg. This "pseudofertilization" could lead to delivery of cytoplasmic factors that trigger parthenogenetic growth and, in rare cases, contamination by HI chromosomes.

Notwithstanding the incomplete understanding of the genetic mechanisms involved, breeders are keen on exploring potential improvements in this area. In this regard, the new potato diploid inbred-line-based breeding strategy, described as Potato 2.0 (Stokstad, 2019) has emerged as a focal point, placing haploid induction into the spotlight. This strategy aims to develop diploid homozygous inbred lines and F1 hybrids (Jansky et al. 2016). However, the primary challenge of this strategy lies in the requirement for efficient production of dihaploids from tetraploid elite lines (Ordoñez et al. 2021). Both the elucidation of the haploid induction mechanism and the selection of improved haploid inducers, potentially leveraging mechanistic insights, would play crucial roles in expediting this new strategy.

Haploid Inducers

Haploid Inducers (HI) have not undergone significant improvements since the release of the IvP inducers by the Institute of Plant Breeding (IvP) at Wageningen in the '70s. The selection of the IvP HI lines was primarily based on their dominant 'homozygous' anthocyanin spot marker found on the botanical seed, which facilitates the differentiation between dihaploids (non-spotted) and the hybrids (spotted). The most commonly used IvP HIs include IvP35, IvP48 and IvP101.

Previous studies have shown that IvP101 exhibits a significantly higher induction rate (*HIR*) compared to IvP35 and IvP48 (Uijtewaal et al. 1987). However, as highlighted by Breukelen (1981), the detection of the spot marker is subject to false-negative bias due to its position in the embryo. To achieve successful dihaploid production, the availability of a well-flowering HI line is also essential. More recently, a new haploid inducer, PL-4, has emerged as a true game-changer among HIs due to its high induction rate (*HIR*), profuse flowering and broad compatibility for generating dihaploids (see Chapter 2 for more details, refer to Ordoñez et al. 2021).

The role of dihaploids research in the advancement of potato improvement

Since the discovery of haploids in Datura by Blakeslee et al. (1922), plant breeders have recognized the revolutionary potential of this "new" technology for its application in highly heterozygous polyploid outcrossers such as potato. In the context of potato genetics, dihaploids resulting from Haploid Induction are often considered close to "inbred lines" due to overall reduction in heterozygosity. Typically, dihaploids exhibit male sterility, which hinders their flexible use in sexual crossing schemes. This constraint further contributes to the accumulation of specific cytoplasms, leading to a bottleneck effect in the newly generated potato material. Therefore, it becomes crucial to develop dihaploids from 4x breeding lines with a potential fertility restorer mechanism, ensuring their suitability in hybridization schemes (Santayana et al. 2022).

Sexual hybridization with wild relatives has proven to be a valuable approach for incorporating novel traits, such as tolerance and resistance to abiotic and biotic stresses, into potato improvement programs. Dihaploids has been proposed as a genetic bridge for transferring desirable traits from wild relatives into the tetraploid cultivated genepool (Fumia et al. 2022; Bethke et al. 2017). However, the presence of pre- or post-zygotic hybridization barriers among diploids can hinder

the process, as these barriers play a crucial role in maintaining genome integrity and thus influencing the overall breeding process (Camadro et al. 2004; Dinu et al. 2005; Raimondi and Camadro, 2003).

Most of the research conducted using dihaploids has been focused on generating mapping populations to dissect the genetic basis of disease resistance traits. This approach aims to identify the locus responsible for resistance, and haploid induction is utilized to produce homozygous dihaploids specifically for that region. These dihaploids are valuable resources for fine mapping, or for conducting a *de novo* genome assembly. For instance, in a recent study by Akai et al. (2023), dihaploids were generated and their genomes subjected to *de novo* assembly to identify the gene Ry_{chc}, which confers resistance against potato virus Y (PVY). Similar investigations have been conducted for other diseases, such as late blight, potato virus X (PVX), and potato leafroll virus (PLVR), among others.

In other crops, the development of monosomic and disomic lines has proven to be instrumental in transferring desirable genes from wild relatives to cultivated genepools. Unfortunately, in potato, there has been limited progress in generating chromosomal addition lines since the work of Dong et al. (2005). As an alternative approach, researchers have explored somatic hybridization or genetic engineering methods to introduce genes from sexual incompatibility germplasm. Nevertheless, these methods can be cumbersome and face restrictions in certain countries.

Gene pyramiding can greatly benefit breeding programs as well. The discovery of additional HI DNA and maternal chromosomes suggest that HI could also be leveraged to provide pyramiding

platforms. However, to date, no further studies on these additional chromosomes have been conducted apart from those described here (See chapter 3 for more details).

Traditionally, potato breeders have solely focused on examining spotless seeds to identify dihaploids after haploid induction. This single gene marker has led to the oversight of unusual karyotypes. Yet, a better understanding of these chromosomes could determine their potential to accelerate potato breeding and could equip breeders with invaluable tools to overcome the considerable connected challenges.

Genome Instability in haploid induction crosses

The model organism *Arabidopsis thaliana* provides valuable insight into the understanding of genome instability within their haploid induction system. In Arabidopsis, haploid induction involves genome elimination and is mediated by defective centromeric histone 3 (CENH3) (Ravi et al. 2011; Ravi & Chan, 2010). The Arabidopsis progeny of these crosses produce multiple progeny types, e.g. haploids, diploids and aneuploids. Among them, the haploid types can exhibit HI-derived addition (aneuploidy) of three types: *i*) regular chromosomes, *ii*) abnormal chromosomes displaying chromoanagenesis, and *iii*) minichromosomes (Tan et al. 2015; Ishii et al. 2016; Tan et al. 2023). Notably, around one- third of these additions exhibit extensive restructuring of the HI-contributed chromosomes (Britt & Kuppu, 2016; Comai & Tan, 2019). This phenomenon bears resemblance to the cancer-related syndrome known as chromoanagenesis (Holland & Cleveland, 2012), which involves complex and pervasive rearrangements in one or a few chromosomes, typically arising from a single catastrophic event. It is believed to result from damage and repair during the rescue of missegregated chromosomes (Guo et al. 2023).

Minichromosomes

Some of the rearranged chromosomes found within the haploid induction progenies are "minichromosomes" (hereafter "minis"). These minis consist of the centromere of a regular chromosome and small portions of the chromosomal arms. Minis, both linear and circular in structure, have been identified in various species (Schubert, 2001). In maize, circular minis or ring-shaped minis are the result of chromosomal breakage and fusion of the unprotected chromosomal termini (Yu et al. 2007). Interchromatid mitotic crossovers occurring during G2 in these circular minis lead to breakage-fusion-bridge (BFB) cycles and dynamic changes in their structures (McClintock, 1932, 1938, 1941). Regardless of their origin or structure, the transmission rates of minis can vary during both mitotic and meiotic divisions (Han et al. 2007; Murata et al. 2008). Some minis have been observed to exhibit mitotic stability, while the transmission rates during meiosis ranged from 0 to 28% (Murata et al. 2006, 2013) (see Chapter 4 for more details).

To effectively harness the benefit of natural chromosome vectors in potato breeding, it is essential to establish a strategic framework that integrates innovative approaches into the breeding pipeline. This framework can include the following steps:

1. Generate a significant number of dihaploids (2n=2x=24) using Haploid inducer (HI) lines.
2. Identify any dihaploid carrying additional chromosomes or minis using Next-generation sequencing (NGS), if present.
3. Thoroughly characterize dihaploids carrying additional chromosomes or minis, with focus on their cytological and phenotypic traits to ensure their stability across generations and

desirable traits.

4. Integrate these natural chromosome vectors into broader breeding strategies to fully harness their potential for enhancing potato improvement.

Overall, in potato breeding, there is a need to explore and embrace alternative strategies for incorporating desirable genes and enhancing genetic diversity. By considering the utilization of additional chromosomes or minis, breeders can unlock new possibilities and pave the way for improved potato varieties.

Objectives of the dissertation

1. Examine the genetic and genomic variation that arise in the progeny of potato haploid induction.
2. Explore the phenotypes of the novel rearrangements observed in the progeny of potato haploid induction.
3. Characterize the behavior, structure, and transmission of minichromosomes (minis) obtained from haploid induction in the model plant *Arabidopsis thaliana*.

Dissertation Outline

Chapter 1 is an introduction to haploid induction in potato and discussion of the potential use of their byproducts such as novel chromosomal rearrangements or minichromosomes in potato breeding. These topics outline the scope of the questions addressed in this dissertation.

Chapter 2 examines the frequency of dihaploids observed by using different Haploid Inducers.

Specifically, I asked the following questions: (1) What is the frequency of haploid inducer genome presence in potato dihaploids? (2) Does this vary among haploid inducers and pistillate parents? And finally (3) Is there a better Haploid Inducer in terms of haploid induction rate (HIR)?

Chapter 3 provides a comprehensive exploration of the landscape of novel rearrangements arising from haploid induction crosses in potato. Specifically, I asked the following questions: (1) What is the role of selection in determining the outcome of haploid induction? (2) What is the frequency of aneuploids formed? (3) Is there any particular pattern to the observed novel genomic rearrangements? (5) What are the phenotypic consequences associated with the novel rearrangements?

Chapter 4 explores the nature of a small chromosome, referred to as 'mini', that arose from a haploid induction cross in Arabidopsis, and to document its ability to be inherited through crossing and selfing generations. Specifically, I asked the following questions: (1) Are minis stably inherited through meiosis? (2) Are minis stably inherited through mitosis? (3) Do minis undergo structural changes across generations?

Chapter 5 summarizes the findings of this work.

Literature cited

Akai, K., Asano, K., Suzuki, C., Shimosaka, E., Tamiya, S., Suzuki, T., Takeuchi, T., & Ohki, T. (2023). De novo genome assembly of the partial homozygous dihaploid potato identified PVY resistance gene (Rychc) derived from Solanum chacoense. Breeding Science, advpub, 22078.

Amundson, K. R., Ordoñez, B., Santayana, M., Nganga, M. L., Henry, I. M., Bonierbale, M., Khan, A., Tan, E. H., & Comai, L. (2021). Rare instances of haploid inducer DNA in potato

dihaploids and ploidy-dependent genome instability. The Plant Cell. https://doi.org/10.1093/plcell/koab100

Bethke, P. C., Halterman, D. A., & Jansky, S. (2017). Are we getting better at using wild potato species in light of new tools? Crop Science, 57(3), 1241–1258.

Blakeslee, A. F., Belling, J., Farnham, M. E., & Bergner, A. D. (1922). A Haploid Mutant in the Jimson Weed, ``Datura Stramonium''. Science, 55(1433), 646–647.

Breukelen, V. (1981). Pseudogamic production of dihaploids and monoploids in Solanum tuberosum and some related species. Wageningen.

Britt, A. B., & Kuppu, S. (2016). Cenh3: An Emerging Player in Haploid Induction Technology. Frontiers in Plant Science, 7, 357.

Camadro, E. L., Carputo, D., & Peloquin, S. J. (2004). Substitutes for genome differentiation in tuber-bearing Solanum: interspecific pollen-pistil incompatibility, nuclear-cytoplasmic male sterility, and endosperm. TAG. Theoretical and Applied Genetics. Theoretische Und Angewandte Genetik, 109(7), 1369–1376.

Clulow, S. A., & Rousselle-Bourgeois, F. (1997). Widespread introgression of Solanum phureja DNA in potato (S. tuberosum) dihaploids. Plant Breeding = Zeitschrift Fur Pflanzenzuchtung, 116(4), 347–351.

Clulow, S. A., Wilkinson, M. J., & Burch, L. R. (1993). Solanum phureja genes are expressed in the leaves and tubers of aneusomatic potato dihaploids. Euphytica/ Netherlands Journal of Plant Breeding, 69(1-2), 1–6.

Clulow, S. A., Wilkinson, M. J., Waugh, R., Baird, E., De Maine, M. J., & Powell, W. (1991). Cytological and molecular observations on Solanum phureja-induced dihaploid potatoes. TAG. Theoretical and Applied Genetics. Theoretische Und Angewandte Genetik, 82, 545–551.

Comai, L., & Tan, E. H. (2019). Haploid Induction and Genome Instability. Trends in Genetics: TIG, 35(11), 791–803.

Dinu, I. I., Hayes, R. J., Kynast, R. G., Phillips, R. L., & Thill, C. A. (2005). Novel inter-series hybrids in Solanum, section Petota. TAG. Theoretical and Applied Genetics. Theoretische Und Angewandte Genetik, 110(3), 403–415.

Dong, F., Tek, A. L., Frasca, A. B. L., McGrath, J. M., Wielgus, S. M., Helgeson, J. P., & Jiang, J. (2005). Development and characterization of potato-Solanum brevidens chromosomal addition/substitution lines. Cytogenetic and Genome Research, 109(1-3), 368–372.

Ercolano, M. R., Carputo, D., Li, J., Monti, L., Barone, A., & Frusciante, L. (2004). Assessment of genetic variability of haploids extracted from tetraploid (2n = 4x = 48) Solanum tuberosum. Genome / National Research Council Canada = Genome / Conseil National de Recherches Canada, 47(4), 633–638.

Fumia, N., Pironon, S., Rubinoff, D., Khoury, C. K., Gore, M. A., & Kantar, M. B. (2022). Wild relatives of potato may bolster its adaptation to new niches under future climate scenarios. Food and Energy Security. https://doi.org/10.1002/fes3.360

Guo, W., Comai, L., & Henry, I. M. (2023). Chromoanagenesis in plants: triggers, mechanisms, and potential impact. Trends in Genetics: TIG, 39(1), 34–45.

Halterman, D., Guenthner, J., Collinge, S., Butler, N., & Douches, D. (2016). Biotech Potatoes in the 21st Century: 20 Years Since the First Biotech Potato. American Journal of Potato Research: An Official Publication of the Potato Association of America, 93(1), 1–20.

Han, F., Gao, Z., Yu, W., & Birchler, J. A. (2007). Minichromosome analysis of chromosome pairing, disjunction, and sister chromatid cohesion in maize. The Plant Cell, 19(12), 3853–3863.

Holland, A. J., & Cleveland, D. W. (2012). Chromoanagenesis and cancer: mechanisms and consequences of localized, complex chromosomal rearrangements. Nature Medicine, 18(11), 1630–1638.

Hutten R. C. B., Soppe W. J. J., Hermsen J. G. T., Jacobsen E. (1995). Evaluation of dihaploid populations from potato varieties and breeding lines. Potato Research, 38, 77–86.

Ishii, T., Karimi-Ashtiyani, R., & Houben, A. (2016). Haploidization via Chromosome Elimination: Means and Mechanisms. Annual Review of Plant Biology, 67, 421–438.

Jansky, S. (2009). Chapter 2 - Breeding, Genetics, and Cultivar Development. In J. Singh & L. Kaur (Eds.), Advances in Potato Chemistry and Technology (pp. 27–62). Academic Press.

Jansky, S. H., Charkowski, A. O., Douches, D. S., Gusmini, G., Richael, C., Bethke, P. C., Spooner, D. M., Novy, R. G., De Jong, H., De Jong, W. S., Bamberg, J. B., Thompson, A. L., Bizimungu, B., Holm, D. G., Brown, C. R., Haynes, K. G., Sathuvalli, V. R., Veilleux, R. E., Miller, J. C., … Jiang, J. (2016). Reinventing Potato as a Diploid Inbred Line–Based Crop. Crop Science, 56, 1412–1422.

Kearney, J. (2010). Food consumption trends and drivers. Philosophical Transactions of the Royal Society of London. Series B, Biological Sciences, 365(1554), 2793–2807.

McClintock, B. (1932). A Correlation of Ring-Shaped Chromosomes with Variegation in Zea Mays. Proceedings of the National Academy of Sciences of the United States of America, 18(12), 677–681.

McClintock, B. (1938). The Production of Homozygous Deficient Tissues with Mutant Characteristics by Means of the Aberrant Mitotic Behavior of Ring-Shaped Chromosomes. Genetics, 23(4), 315–376.

McClintock, B. (1941). SPONTANEOUS ALTERATIONS IN CHROMOSOME SIZE AND FORM IN ZEA MAYS. In Cold Spring Harbor Symposia on Quantitative Biology (Vol. 9, Issue 0, pp. 72–81). https://doi.org/10.1101/sqb.1941.009.01.010

Murata, M., Shibata, F., Hironaka, A., Kashihara, K., Fujimoto, S., Yokota, E., & Nagaki, K. (2013). Generation of an artificial ring chromosome in Arabidopsis by Cre/LoxP-mediated recombination. The Plant Journal: For Cell and Molecular Biology, 74(3), 363–371.

Murata, M., Shibata, F., & Yokota, E. (2006). The origin, meiotic behavior, and transmission of a novel minichromosome in Arabidopsis thaliana. Chromosoma, 115(4), 311–319.

Murata, M., Yokota, E., Shibata, F., & Kashihara, K. (2008). Functional analysis of the Arabidopsis centromere by T-DNA insertion-induced centromere breakage. Proceedings of the National Academy of Sciences of the United States of America, 105(21), 7511–7516.

Ordoñez, B., Santayana, M., Aponte, M., Henry, I. M., Comai, L., Eyzaguirre, R., Lindqvist-Kreuze, H., & Bonierbale, M. (2021). PL-4 (CIP596131.4): an Improved Potato Haploid Inducer.

American Journal of Potato Research: An Official Publication of the Potato Association of America. https://doi.org/10.1007/s12230-021-09839-y

Pham, G. M., Braz, G. T., Conway, M., Crisovan, E., Hamilton, J. P., Laimbeer, F. P. E., Manrique-Carpintero, N., Newton, L., Douches, D. S., Jiang, J., & Others. (2019). Genome-wide inference of somatic translocation events during potato dihaploid production. The Plant Genome. https://dl.sciencesocieties.org/publications/tpg/articles/0/0/180079

Raimondi, Camadro. (2003). Crossability relationships between the common potato, Solanum tuberosum spp. tuberosum, and its wild diploid relatives S. kurtzianum And S. ruiz-lealii. Genetic Resources and Crop Evolution, 50, 307–314.

Ravi, M., & Chan, S. W. L. (2010). Haploid plants produced by centromere-mediated genome elimination. Nature, 464(7288), 615–618.

Ravi, M., Shibata, F., Ramahi, J. S., Nagaki, K., Chen, C., Murata, M., & Chan, S. W. L. (2011). Meiosis-specific loading of the centromere-specific histone CENH3 in Arabidopsis thaliana. PLoS Genetics, 7(6), e1002121.

Santayana, M., Aponte, M., Kante, M., Eyzaguirre, R., Gastelo, M., & Lindqvist-Kreuze, H. (2022). Cytoplasmic Male Sterility Incidence in Potato Breeding Populations with Late Blight Resistance and Identification of Breeding Lines with a Potential Fertility Restorer Mechanism. Plants, 11(22). https://doi.org/10.3390/plants11223093

Schubert, I. (2001). Alteration of chromosome numbers by generation of minichromosomes – Is there a lower limit of chromosome size for stable segregation? In Cytogenetic and Genome Research (Vol. 93, Issues 3-4, pp. 175–181). https://doi.org/10.1159/000056981

Stokstad, E. (2019). The new potato. Science, 363, 574–577.

Straadt I.K and Rasmussen O.S. (2003). AFLP analysis of Solanum phureja DNA introgressed into potato dihaploids. Plant Breeding = Zeitschrift Fur Pflanzenzuchtung, 122, 352–356.

Tan, E. H., Henry, I. M., Ravi, M., Bradnam, K. R., Mandakova, T., Marimuthu, M. P., Korf, I., Lysak, M. A., Comai, L., & Chan, S. W. (2015). Catastrophic chromosomal restructuring during genome elimination in plants. eLife, 4. https://doi.org/10.7554/eLife.06516

Uijtewaal, B. A., Huigen, D. J., & Th. Hermsen, J. G. (1987). Production of potato monohapioids (2n = x = 12) through prickle pollination. Theoretical and Applied Genetics, 73, 751–758.

Wilkinson, M. J., Bennett, S. T., Clulow, S. A., & Allainguillaume, J. (1995). Evidence for somatic translocation during potato dihaploid induction. Heredity, 74, 146–151.

Yu, W., Han, F., Gao, Z., Vega, J. M., & Birchler, J. A. (2007). Construction and behavior of engineered minichromosomes in maize. Proceedings of the National Academy of Sciences of the United States of America, 104(21), 8924–8929.

Chapter 2

PL-4 (CIP596131.4): an Improved Potato Haploid Inducer

[Published in: *Am. J. Potato Res.* 98, 255–262]

Benny Ordoñez[1,2,4*], Monica Santayana[2], Mariela Aponte[2], Isabelle M. Henry[1], Luca Comai[1], Raúl Eyzaguirre[2], Hannele Lindqvist-Kreuze[2] and Merideth Bonierbale[2,3]

Author affiliations

1 Plant Biology and Genome Center, University of California, Davis, 1 Shields Avenue, Davis, CA, 95616, USA.

2 International Potato Center (CIP), P.O. Box 1558, Lima 12, Peru.

3 Current Address: Duquesa Business Centre, P.O. Box 157, Manilva, Malaga, Spain 29692.

4 Integrative Genetics and Genomics Graduate Group, University of California, Davis, CA 95616, USA.

*Corresponding author: bordonez@ucdavis.edu

Abstract

Dihaploid production from elite tetraploid cultivars is key to both traditional and novel breeding approaches that seek to simplify potato genetics. For this purpose, efficient and widely compatible haploid inducers (HIs) are needed. We compared PL-4, a new HI developed at the International Potato Center, to known HIs IvP101 and IvP35. By pollination of elite tetraploid breeding lines, we showed that PL-4 performed significantly better and had a homogeneous response regardless of the genetic background of the pistillate parents, on the most important efficiency traits—number of dihaploids per 100 fruits and haploid induction rate.

Moreover, PL-4 exhibited a reduced proportion of hybrid seeds, a convenient trait for efficient screening. In this context, we recommend PL-4 as an enhanced HI for the potato breeding community.

Introduction

The cultivated potato, *Solanum tuberosum* L. (2n = 4x =48), is a tetraploid crop with polysomic inheritance, and high levels of heterozygosity (Bradshaw 2007). Its polyploid nature complicates genetic studies and can limit genetic gains in breeding. To overcome these problematic aspects, a new breeding strategy has been proposed that reinvents potato as a diploid inbred-line based system (Jansky et al. 2016). Breeding at the diploid level involves the reduction of ploidy level via the generation of haploid or "dihaploid" (2n = 2x =24) plants from tetraploid varieties or stocks. The hypothetical benefits include a shorter breeding cycle, faster stacking of traits of interest, and more prolific seed production. This could allow for easier variety generation. A large-scale dihaploid generation is a crucial step of this new potato breeding strategy (Lindhout et al. 2011).

Two methods are used to produce potato dihaploids: anther culture (Rokka et al. 1996) and *in vivo* haploid induction using specific diploid accessions from the Phureja Group of *S. tuberosum* as pollinators (hereafter called 'haploid inducers'). Clones *phu* 1.22 (PI225682), IvP35, IvP48, and IvP101 are haploid inducers (HIs) commonly used in breeding (Peloquin et al. 1996; Hutten et al. 1993; Van Breukelen et al. 1977). These HIs are homozygous dominant for anthocyanin pigments that are visible as an embryo spot on the botanical seed and as nodal bands on the stem of young plants (Hermsen and Verdenius 1973). The presence of this pigmentation marker allows discernment between hybrids and putative dihaploids, starting at the seed stage. Unpigmented embryos or seedlings are the desired dihaploids.

Three hypotheses have been proposed for the mechanism of haploid induction in potatoes: parthenogenesis, parent-specific chromosome elimination and egg-pseudo fertilization (Wangenheim et al. 1960; Clulow et al. 1991; Amundson et al. 2021). The exact mechanism at play has not yet been elucidated.

Haploid induction appears to be a monophyletic trait in potatoes. All documented HI derive from the same diploid taxon/germplasm source, but their efficiency differs among them (Hutten et al. 1993). Potato breeders have been attempting to generate new and better HIs. For example, Ortiz et al. (1993) self-pollinated IvP35 and obtained a clone that reached fivefold the rate of spotless seeds to total seeds of IvP35. Later, CIP breeders crossed IvP35 and IvP101 and identified in the resulting progeny a new HI called PL-4 (CIP596131.4, also known as C96HI-01.4). Their data suggested that PL-4 exhibited a higher haploid induction rate (*HIR*) than both parents, but the supporting experiments employed variable recording methods that lacked replication and complete ploidy analysis (Ortiz and Mihovilovich 2020). To assess the efficiency of PL-4 as a HI, we

evaluated and compared the most important haploid induction traits, under a uniform experimental framework and using a novel mixed model for statistical analysis. We also analyzed the effect of parentals' cytoplasm type due to their relationship with male sterility and the urgent need to incorporate different cytoplasmic types into breeding schemes.

Materials and Methods

PL-4 Reproductive Biology and pollen viability

PL-4 reproductive biology was assessed using descriptors based on (Gomez 2006) and the Crop Ontology Curation Tool (https://www.cropontology.org/, 2011).

HIs plants grown under standard conditions in the screenhouse (see below) were used for pollen fertility evaluation. Pollen viability and frequency of 2n pollen were determined as described previously by Ordoñez et al. (2017).

Haploid Induction

Forty CIP elite 4x breeding lines with different genetic backgrounds and desirable attributes (Supplemental Table S.2.1), were used as pistillate parents in crosses with three HIs, PL-4, IvP101 and IvP35.

Haploid induction crosses were performed during 2015, 2016, and 2017 in screenhouses (average temperature: 19.5ºC day and 11.6ºC night; relative humidity range: 56.8 - 87.4%) located at the CIP's experimental station in the Peruvian Andes (3,216 masl, -12.01039, -75.22411).

Flower buds of the pistillate parents were emasculated, and then pollinated with HI pollen the next day. Each HI was assigned to a separate set of pistillate plants to avoid pollination of the same plant with different HIs.

Fruits were harvested forty-eight days after pollination and the seeds were extracted from mature fruits only. The seed progeny was categorized into two different types: well-developed (spotted and spotless) and shriveled seeds. Only well-developed seeds were recorded in this study. Seeds displaying the HI embryo spot trait were then discarded, while spotless seeds (i.e., putative dihaploids) were treated with 1500 ppm gibberellic acid (GA3) for one day to break dormancy and incubated on a damp filter paper at 17ºC for five days. After emergence, seedlings showing nodal anthocyanin bands were removed. The remaining seedlings were transplanted into Jiffy's strips (Jiffystrips ®) and grown in the screenhouse for further evaluations.

Ploidy Assessment

Ploidy was assessed first by counting chloroplast number in stomata guard cells as described by Ordoñez et al. (2017). In those cases where the average chloroplast count was greater than eight, individuals were assigned as non-conclusive status and ploidy was estimated by flow cytometry. Flow cytometry was performed as previously described by Amundson et al. (2020). Plantlets showing a reduced growth rate that could not be evaluated by chloroplast counting were also included in the flow cytometry assessment.

A schematic diagram of the workflow of this study is shown in Fig. 2.1.

Data Analysis

Two 'productivity' and five 'efficiency' traits were estimated to evaluate the performance of the HIs. The productivity traits were: Fruit set percentage (*FSP*), which is the number of fruits per 100

pollinated flowers and seed set rate (*SS*), which is calculated by dividing the number of well-developed seeds by the number of fruits.

For the purpose of documenting and analyzing the efficiency of haploid induction, the total number of spotted seeds per 100 fruits was referred to as *Spotted100F*; the total number of spotless seeds per 100 fruits was referred to as *Spotless100F*; the total number of dihaploids per 100 pollinations was referred to as *DH100P*; and the total number of dihaploids per 100 fruits was referred to as *DH100F*. Haploid induction rate (*HIR*) was defined as the percentage of dihaploids found in the total number of well-developed seeds generated.

Descriptive statistics showed that variance values for productivity and efficiency traits were different among HIs. Therefore, a heterogeneous variance model was considered. To evaluate the general performance of the HIs, a linear mixed model where HIs are fixed effects and pistillate parents are random effects was used. In addition, to examine the effect of the cytoplasm type of the pistillate parent on the efficiency traits (i.e., *DH100P, DH100F* and *HIR*), a model was adjusted for each HI where the cytoplasm types were considered fixed effects.

The ASReml-R (Butler et al. 2017) and the asremlPlus (Brien 2020) packages for R software 4.0.4 (R Core Team 2020) were used to estimate the models and to perform pairwise comparisons. Significance for the fixed effects was assessed using Wald test. Pearson's correlation coefficients were determined to measure the linear association between the characters obtained by the different HIs (Suppl. Table S.2.3).

Raw datasets are available on Dataverse at

https://data.cipotato.org/dataset.xhtml?persistentId=doi:10.21223/SP9MFB

Results

PL-4 Reproductive Biology and pollen viability

Photographs of representative parts of PL-4 are shown in Fig. 2.2. PL-4 exhibited a moderate flowering degree. The average number of inflorescences per plant was 4 (range 2–5) with 5 flowers (range 3–10) per inflorescence. Pollen production was moderate (3 on a 0–5 scale with 0 being none and 5 abundant), but greater than IvP35 and IvP101. Under our screenhouse conditions, the three HIs displayed moderate pollen viability (range: 65- 80%, Ordoñez et al. 2017). As for 2n pollen production, PL-4 showed a low percentage of 2n pollen, whereas both IvP101 and IvP35 showed no presence of 2n pollen.

Haploid induction

A total of 9705 pollinations were performed between the CIP elite 4x breeding lines and the HIs—IvP35, IvP101 and PL-4, setting a total of 2375 fruits, 21,356 seeds and 1612 dihaploids over the span of three years. The number of flowers pollinated per HI was in the range of 17 – 451 for PL-4 (mean = 102), 16 – 587 for IvP101 (mean = 139) and 16 – 434 for IvP35 (mean = 123). The number of fruits per HI ranged from 0 to 120 in PL-4, from 0 to 103 in IvP101 and from 2 to 185 in IvP35. We found no significant differences in *FSP* among the HIs. In contrast, IvP35 displayed a higher *SS* than IvP101 and PL-4 (Table 2.1). Shriveled seeds were also observed in all the crosses, but it was not feasible to record their number.

Over the course of the three years of experimentation, PL-4 generated a total of 813 dihaploids, while IvP101 and IvP35 had 272 and 527, respectively. PL-4 yielded 193.9 *Spotless100F* while

IvP101 and IvP35 yielded 140.3 and 147.7, respectively. These results suggest no significant differences between the HIs for this variable. Interestingly, IvP35 yielded the most *Spotted100F*, at 820.7 compared to PL-4 and IvP101 with 476.9 and 579.9, respectively. PL-4 produced significantly fewer spotted seeds and exhibited higher *Spotless100F* values. Additionally, PL-4 produced more *DH100P* than either IvP101 or IvP35. PL-4 produced the most *DH100F* (69.8) while, both IvP101 and IvP35 produced fewer (44 and 39.4, respectively). Overall, PL-4 displayed a higher *HIR* (11.6%) compared to IvP101 and IvP35 (6.8% and 4.3%, respectively, Table 2.1).

After sowing the spotless seeds, some developing seedlings were found to be false positive, i.e., not dihaploids, upon chloroplast counting and flow cytometry. On average 4.8% of the total plantlets from each HI displayed the anthocyanin marker in stems and were therefore discarded. From the remaining plantlets, confirmed dihaploids were 78.1%, 68.0% and 57.9% for PL-4, IvP101 and IvP35, respectively. The rest of the plantlets were triploids or tetraploids.

PL-4 showed a high positive correlation between *Spotless100F* and *DH100F* ($r = 0.91$, $p < 0.001$) whereas that relationship was not as robust for IvP101 ($r = 0.61$, $p < 0.01$) or IvP35 ($r = 0.64$, $p < 0.001$). In contrast, *SS* and *Spotless100F* were moderately correlated for PL-4 ($r = 0.61$, $p < 0.001$) and IvP101 ($r = 0.60$, $p < 0.01$). Notably, IvP101, but neither IvP35 nor PL-4, displayed a significant correlation between *FSP* and *DH100P* ($r = 0.81$, $p < 0.001$).

Dead and abnormal seedlings of undetermined ploidy occurred in the HI cross progeny (6.7% for PL-4, 2.3% and 5.6% for IvP101 and IvP35, respectively). Abnormal dihaploids were also noted (1.4 for PL-4, 10.1 and 6.3 for IvP101 and IvP35, respectively). These could represent extreme aneuploidy cases (Tan et al. 2015; Amundson et al. 2021).

The values for efficiency traits varied among the pistillate parents as well as the HIs. Of the 40 pistillate parents used in this study, 10 showed *DH100F* higher than 69.4, which was PL-4 average. These pistillate parents were: CIP392820.1, CIP300056.33, CIP313051.7, CIP390637.1, CIP391180.6, CIP397077.16, CIP398208.219, CIP388615.22, CIP388676.1 and CIP300093.14. The pistillate parent CIP392820.1 yielded the highest *DH100F* (282) followed by CIP300056.33 with 220. In contrast, CIP313050.21 and Serranita, a popular Peruvian variety, did not produce any dihaploid with any HI (Supplemental Table S.2.2).

Performance of HIs across the Cytoplasm Types

The cytoplasm type of the pistillate parent is correlated with the incidence of male sterility in their descendants, an important trait for breeding (Hosaka and Sanetomo 2012; Provan et al. 1999). Therefore, we examined the influence of cytoplasm of the pistillate parents on the efficiency traits i.e., *HIR*, *DH100F* and *DH100P*.

Pistillate parents were grouped by their cytoplasm types, which were previously determined by Mihovilovich et al. (2015) using the method and nomenclature by Hosaka and Sanetomo (2012): 19 had the D-type cytoplasm, 13 had the T-type, 7 had the W-type and 1 had the A-type. For the analysis, only dihaploids belonging to the T (n = 738), W (n = 469) and D (n = 402) cytoplasm were considered as observations.

Pistillate parents with W-type cytoplasm showed higher *HIR* and *DH100F* for each HI, followed by parents with T- type and D- type. Pistillate parents harboring D-type cytoplasm, which is usually associated with male sterility, displayed the lowest values for the following traits: *FSP, Spotless100F, DH100P, DH100F* and *HIR* (Data not shown). Nonetheless, we found that PL-4 displayed a more homogeneous response across the different cytoplasm types for the efficiency

traits — *HIR* (*p*-value = 0.870) and *DH100F* (*p*-value = 0.335) (Fig. 2.3a and Fig. 2.3b, respectively).

Discussion

A HI that yields more dihaploids regardless of the pistillate parent, would greatly benefit potato breeding by reducing dihaploid production costs and speeding-up the development of diploid parental lines. Nevertheless, since the release of the IvPs (Hermsen and Verdenius 1973), no new HI has become available. Here, we describe a new HI, PL-4, which displays desirable features. PL-4 has been used for multiple years by CIP breeders. For example, during production of a dihaploid mapping population for PLRV resistance from the tetraploid landrace LOP-868, Velásquez (2005) observed that PL-4 generated a higher number of dihaploids than IvP101. Subsequently, Mihovilovich et al. (2013) only used PL-4, finding a *HIR* of 16.7%, which is higher than that expected from IvP101.

Although the CIP clones used for this study are different from the typical North American and European clones, they nonetheless represent a broad genetic range of potato variation and provide an interesting test of haploid induction efficiency. Our findings provide evidence for PL-4's high *HIR* and broad pistillate parent compatibility.

Consistent production and pollen fertility are the first requirements for dihaploid production. In addition to profuse flowering and pollen shedding capacity, in our study the three HIs displayed a moderate pollen viability. Environmental conditions may affect viability as Dongyu et al. (1995) observed high and low pollen viability rates in IvP35 and IvP101 across environments, respectively. Previously, Liu and Douches (1993) chose not to work with IvP35 due to poor pollen

production. Taken together, our observations suggest that PL-4 carries favorable reproductive traits compared to the IvPs.

The availability of dihaploid identification systems is critical for efficient dihaploid production. Visual differentiation is based on the dominant anthocyanin marker observed in seed and stems (Hermsen and Verdenius 1973). By using both the seed spot and the nodal band on seedling, we observed a false positive rate of 21.9% in PL-4 compared to 32.0% and 42.1% for IvP101 and IvP35, respectively. These results indicate that potato HIs need a better dihaploid identification approach as suggested by Liu and Douches (1993). Despite the moderate rates of false positives, our study suggests that PL-4 can be useful in a large-scale dihaploid production scheme.

Our study is one of the very few that investigates the potential of new HIs. Often, these studies on haploid induction only used limited numbers of pistillate parents. Nonetheless, the traits evaluated here were consistent across multiple studies. For example, *DH100F* values for *phu* 1.22 were 13.9 (Montelongo-Escobedo and Rowe 1969), 13.4 (Hanneman and Ruhde 1978) and 3.9 (Liu and Douches 1993). Conversely, IvP48 and IvP35 had 255 and 276 *DH100F,* respectively (Hermsen and Verdenius 1973). Later, Hutten et al. (1993) reported that *DH100F* values for IvP35, IvP48 and IvP101 were 152, 170 and 255, respectively and, although they lacked replication, they noted a significant interaction of the pistillate parent with the HIs. Nonetheless, IvP101 has been the prevalent HI used to generate dihaploid lines (Manrique-Carpintero et al. 2018; Pham et al. 2019; Yermishin and Voronkova 2017). Our results show that PL-4's *DH100F* value (69) was significantly higher than IvP101 (44) and IvP35 (39) (Table 2.1).

The Haploid Induction Rate (*HIR*) seems to be the most adequate trait to compare HIs across different crops. The *HIR* of PL-4 (~11% dihaploids/well-developed seed) compares favorably to that of elite RWS-derived maize HIs, which displayed values of 8 to 13% (Chaikam et al. 2016). In wheat, some HIs *TaMTL*-edited plants reach up to 15.7% (Liu et al. 2020). In rice, HI *Osmatl*-edited plants display 2 - 6% (Yao et al. 2018). In contrast, in sorghum, HIs yield up to 2% haploids (Hussain and Franks 2019).

The selection of the spotless seeds during the haploid induction process can be time consuming, thus a reduced amount of *Spotted100F* is convenient for fast screening. Our results showed that the *Spotted100F* value was significantly lower for PL-4 and IvP101, than for IvP35, which was nearly twofold the PL-4 value (Table 2.1). We evaluated the ratio of spotted/spotless seeds of the HIs. PL-4 displayed 2.5:1, while IvP101 and IvP35 exhibited 4.1:1 and 5.6:1, respectively. Following Hermsen and Verdenius (1973) classification of high (6:1) versus low (3:1) seed setters, we assigned IvP35 as high- and PL-4 and IvP101 as low-seed setters. Hermsen and Verdenius (1973) also stressed that a high-seed set is an unfavorable trait while a low-seed set can be beneficial when it does not compromise the *HIR*. Same authors also noted a high correlation ($r = 0.93$) between *SS* and the haploids generated by low-seed setters. Our findings indicate a significant but low correlation between *SS* and *DH100F* for the low-seed setters: PL-4 and IvP101 ($r = 0.34$ and $r = 0.49$, respectively, $p < 0.05$).

Currently, D- and T- type cytoplasm are the most prevalent in modern cultivars and they are related to male sterility. The cytoplasmic diversity of breeding stocks has prompted a call for incorporating different cytoplasmic types in breeding schemes (Hosaka and Sanetomo 2012; Provan et al. 1999;

Sanetomo and Gebhardt 2015). We evaluated the performance of the HIs across the cytoplasmic type of pistillate parents. Our results indicate that PL-4 had the most homogeneous behavior across cytoplasm types and the highest mean for the most important efficiency traits—*DH100F* and *HIR* (Fig. 2.3).

Abnormal or lethal phenotypes among the progeny from a haploid induction cross are common, reflecting the genetic load of deleterious or lethal alleles from their tetraploid pistillate parents (Hermsen et al. 1978; Van Breukelen et al. 1977; Hutten et al. 1993; Pham et al. 2019). These compromised plantlets cannot survive further rounds of multiplications and agronomical analysis. For example, Pham et al. (2019) found that 20% of dihaploids derived from cv. Superior and IvP101 could not be evaluated for agronomic traits under field conditions due to their poor vigor. By comparison, in our screenhouse study less than 10% of the spotless plants were lost.

We have demonstrated the use of a combination of HIs, cytoplasm type and genetic background to boost haploid induction within a breeding program. The extensive haploid induction crosses performed in this study were aimed at incorporating several traits of interest from the tetraploid pool into a hybrid diploid breeding pipeline.

PL-4 is available at the CIP Genebank and has been deposited in the US potato germplasm repository and therefore available to the potato community to accelerate breeding and particularly the conversion of cultivated potato to diploidy.

Availability

In vitro plantlets of PL-4 are available and can be requested from CIP Lima, Peru by email at CIP-Germplasm@cgiar.org. In addition, PL-4 has been deposited in the US Potato Genebank in Sturgeon Bay, Wisconsin (PI695419). If use of PL-4 contributes to development of new variety(s), or scientific discovery(s), it is requested to recognize CIP as the breeder.

Acknowledgments

This research was undertaken and funded as part of the CGIAR Research Program on Roots, Tubers and Bananas (RTB) and the National Science Foundation Plant Genome Integrative Organismal Systems (IOS) Grant 1444612 (Rapid and Targeted Introgression of Traits via Genome Elimination).

We acknowledge the contributions of the late CIP scientists Rolando Cabello and Dr. Mahesh Upadhya, who pioneered haploid induction research at CIP and developed PL-4; Dr. Awais Khan and Elisa Mihovilovich for their assistance in various aspects of the development of this work; Juan Huaccachi, Flor Osorio and Rene Asto provided technical support for the project.

Author contributions

B.O, I.M.H, LC, and M.B conceived the research. B.O, I.M.H, L.C and M.B designed experiments. B.O and M.S performed experiments. M.S, B.O, M.A and R.E analyzed data. B.O, M.S and M.A interpreted the data. H.L.K supervised later stages of the research. B.O, M.S, I.M.H, L.C, and M.B wrote the manuscript with input from all authors.

Literature cited

Amundson, K.R., B. Ordoñez, M. Santayana, M.L. Nganga, I.M. Henry, M. Bonierbale, A. Khan, E.H. Tan, and L. Comai. 2021. Rare instances of haploid inducer DNA in potato dihaploids and ploidy-dependent genome instability. *The Plant Cell.* doi:10.1093/plcell/koab100.

Amundson, K.R., B. Ordoñez, M. Santayana, E.H. Tan, I.M. Henry, E. Mihovilovich, M. Bonierbale, and L. Comai. 2020. Genomic Outcomes of Haploid Induction Crosses in Potato (*Solanum tuberosum* L.). *Genetics* 214: 369–380.

Bradshaw, J.E. 2007. Breeding potato as a major staple crop. In Breeding major food staples, ed. M.S. Kang and P.M. Priyadarshan, 277-332. Oxford: Blackwell Scientific Publishing.

Brien, C.J. 2020. asremlPlus: augments Asreml-R in Fitting Mixed Models and Packages Generally in Exploring Prediction Differences. R Package Version 4.1-28. Available online: https://cran.at.r-project.org/package=asremlPlus. Accessed on 15 November 2020.

Butler, D.G., B.R. Cullis, A.R. Gilmour, B.G. Gogel, and R. Thompson. 2017. ASReml-R Reference Manual Version 4. VSN International Ltd, Hemel Hempstead, HP1 1ES, UK.

Chaikam, V., L. Martinez, A.E. Melchinger, W. Schipprack, and P.M. Boddupalli. 2016. Development and validation of red root marker-based haploid inducers in maize. *Crop Science* 56: 1678–1688.

Clulow, S.A., M.J. Wilkinson, R. Waugh, E. Baird, M.J. Demaine, and W. Powell. 1991. Cytological and molecular observations on *Solanum phureja*-induced dihaploid potatoes. *Theoretical and Applied Genetics* 82: 545–551.

Dongyu, Q., Z. Dewei, M.S. Ramanna, and E. Jacobsen. 1995. A comparison of progeny from diallel crosses of diploid potato with regard to the frequencies of 2n-pollen grains. *Euphytica* 92: 313–320.

Gomez 2006. Guía para las caracterizaciones morfológicas básicas en colecciones de papas nativas. En Manual para caracterización In situ de cultivos nativos, ed. R. Estrada, T. Medina, A. Roldan, 26-50. Instituto Nacional de Investigación y Extensión Agraria-INIEA.

Hanneman, R.E., and R.W. Ruhde. 1978. Haploid extraction in *Solanum tuberosum* group Andigena. *American Potato Journal* 55: 259–263.

Hermsen, J.G.T., L.M. Taylor, E.W.M. Van Breukelen, and A. Lipski. 1978. Inheritance of genetic markers from two potato dihaploids and their respective parent cultivars. *Euphytica* 27: 681–688.

Hermsen, J.G.Th., and J. Verdenius. 1973. Selection from *Solanum tuberosum* group phureja of genotypes combining high-frequency haploid induction with homozygosity for embryo-spot. *Euphytica* 22: 244–259.

Hosaka, K., and R. Sanetomo. 2012. Development of a rapid identification method for potato cytoplasm and its use for evaluating Japanese collections. *Theoretical and Applied Genetics* 125: 1237–1251.

Hussain, T., and C. Franks. 2019. Discovery of Sorghum Haploid Induction System. *Methods in Molecular Biology* 1931: 49–59.

Hutten, R.C.B., E.J.M.M. Scholberg, D.J. Huigen, J.G.T. Hermsen, and E. Jacobsen. 1993. Analysis of dihaploid induction and production ability and seed parent x pollinator interaction in potato. *Euphytica* 72: 61–64.

Jansky, S.H., A.O. Charkowski, D.S. Douches, G. Gusmini, C. Richael, P.C. Bethke, D.M. Spooner, R.G. Novy, H. De Jong, W.S. De Jong and others. 2016. Reinventing potato as a diploid inbred line--based crop. *Crop Science* 56: 1412–1422.

Lindhout, P., D. Meijer, T. Schotte, R.C.B. Hutten, R.G.F. Visser, and H.J. van Eck. 2011. Towards F1 Hybrid Seed Potato Breeding. *Potato Research* 54: 301–312.

Liu, C.-A., and D.S. Douches. 1993. Production of haploids of potato (*Solanum tuberosum subsp. tuberosum*) and their identification with electrophoretic analysis. *Euphytica* 70: 113–126.

Liu, C., Y. Zhong, X. Qi, M. Chen, Z. Liu, C. Chen, X. Tian, J. Li, Y. Jiao, D. Wang, Y. Wang, M. Li, M. Xin, W. Liu, W. Jin, and S. Chen. 2020. Extension of the *in vivo* haploid induction system from diploid maize to hexaploid wheat. *Plant Biotechnology Journal* 18: 316–318.

Manrique-Carpintero, N.C., J.J. Coombs, G.M. Pham, F.P.E. Laimbeer, G.T. Braz, J. Jiang, R.E. Veilleux, C.R. Buell, and D.S. Douches. 2018. Genome Reduction in Tetraploid Potato Reveals Genetic Load, Haplotype Variation, and Loci Associated with Agronomic Traits. *Frontiers in Plant Science* 9: 944.doi: 10.3389/fpls.2018.00944.

Mihovilovich, E., M. Aponte, H. Lindqvist-Kreuze, and M. Bonierbale. 2013. An RGA-Derived SCAR Marker Linked to PLRV Resistance from *Solanum tuberosum* ssp. andigena. *Plant Molecular Biology Reporter* 32: 117–128.

Mihovilovich, E., R. Sanetomo, K. Hosaka, B. Ordoñez, M. Aponte, and M. Bonierbale. 2015. Cytoplasmic diversity in potato breeding: case study from the International Potato Center. *Molecular Breeding* 35: 137-146.

Montelongo-Escobedo, H., and P.R. Rowe. 1969. Haploid induction in potato: Cytological basis for the pollinator effect. *Euphytica* 18: 116–123.

Ordoñez, B., M. Orrillo, and M.W. Bonierbale. 2017. Technical manual potato reproductive and cytological biology. International Potato Center (CIP). ISBN 978-92-9060-480-8. 65 p.

Ortiz, R., E.L. Camadro, and M. Iwanaga. 1993. Utilización potencial de clones de papa obtenidos por autofecundación como inductores de haploidia en cruzamientos 4x x 2x. *Revista Latinoamericana de la Papa* 5: 46–53.

Ortiz, R. and E. Mihovilovich. 2020. Genetics and cytogenetics of the potato. In: The Potato Crop. Its agricultural, nutritional and social contribution to humankind. ed. H. Campos H., O. Ortiz. Cham (Switzerland). Springer, Cham.

Peloquin, S.J., A.C. Gabert, and R. Ortiz. 1996. "Nature of 'Pollinator' Effect in Potato (*Solanum tuberosum* L.) Haploid Production. *Annals of Botany* 77: 539–42.

Pham, G.M., G.T. Braz, M. Conway, E. Crisovan, J.P. Hamilton, F.P.E. Laimbeer, N. Manrique-Carpintero, L. Newton, D.S. Douches, J. Jiang, R.E. Veilleux, and C.R. Buell. 2019. Genome-wide inference of somatic translocation events during potato dihaploid production. The Plant Genome 12: 180079. doi: 10.3835/plantgenome2018.10.0079.

Provan, J., W. Powell, H. Dewar, G. Bryan, G.C. Machray, and R. Waugh. 1999. An extreme cytoplasmic bottleneck in the modern European cultivated potato (*Solanum tuberosum*) is not reflected in decreased levels of nuclear diversity. *Proceedings of the Royal Society of London. Series B: Biological Sciences* 266: 633–639.

R Core Team. 2020. Core R: A Language and Environment for Statistical Computing, Version 3.5. 3. Vienna: R Foundation for Statistical Computing.

Rokka, V.-M., L. Pietilä, and E. Pehu. 1996. Enhanced production of dihaploid lines via anther culture of tetraploid potato (*Solanum tuberosum L. ssp. tuberosum*) clones. *American Potato Journal* 73: 1–12.

Sanetomo, R., and C. Gebhardt. 2015. Cytoplasmic genome types of European potatoes and their effects on complex agronomic traits. *BMC Plant Biology* 15: 162. doi: 10.1186/s12870-015-0545-y.

Tan, E.H., I.M. Henry, M. Ravi, K.R. Bradnam, T. Mandakova, M.P. Marimuthu, I. Korf, M.A. Lysak, L. Comai, and S.W. Chan. 2015. Catastrophic chromosomal restructuring during genome elimination in plants. *eLife* 4: e06516. doi:10.7554/eLife.06516.

Van Breukelen, E.W.M., M.S. Ramanna, and J.G.Th. Hermsen. 1977. Parthenogenetic monohaploids (2n=x=12) from *Solanum tuberosum* L. and *S. verrucosum* Schlechtd. and the production of homozygous potato diploids. *Euphytica*26: 263–271.

Velásquez, A.C. 2005. Caracterización genética de la resistencia al virus del enrollamiento de la hoja de papa (PLRV) en un cultivo de *Solanum tuberosum ssp. andigena* asistida por marcadores moleculares. B.Sc. Thesis. Universidad Nacional Agraria La Molina, Lima, Peru.

Wangenheim, K.H.v., S.J. Peloquin and R.W. Hougas. 1960. Embryological investigations on the formation of haploids in the potato (*Solanum tuberosum*). *Zeitschrift fur Vererbungslehre* 91: 391–399.

Yao, L., Y. Zhang, C. Liu, Y. Liu, Y. Wang, D. Liang, J. Liu, G. Sahoo, and T. Kelliher. 2018. *OsMATL* mutation induces haploid seed formation in indica rice. *Nature Plants* 4: 530–533.

Yermishin, A.P., and E.V. Voronkova. 2017. Development of initial material for marker assisted potato (*Solanum tuberosum* L.) parental line breeding at the diploid level. *Agricultural and Biological Chemistry*. 52: 50–62.

Tables

Table 2.1. Pooled data per HI on seven haploid induction traits. Data is averaged across three years (2015-2017).

Characters	**Abbreviation**	**PL-4**	**IvP101**	**IvP35**
Fruit set percentage (%)	*FSP*	30.0 a	26.8 a	34.0 a
Seed set rate	*SS*	6.73 b	7.31 ab	9.67 a
Spotted seeds per 100 fruits	*Spotted100F*	476.9 b	579.9 b	820.7 a
Spotless seeds per 100 fruits	*Spotless100F*	193.9 a	140.3 a	147.7 a
Dihaploids per 100 pollinations	*DH100P*	21.2 a	13.2 ab	12.0 b
Dihaploids per 100 fruits	*DH100F*	69.8 a	44.0 b	39.4 b
Haploid Induction Rate (%)	*HIR*	11.6 a	6.8 b	4.3 b

Values followed by the same lowercase letter are not significantly different at $p < 0.05$.

Figures

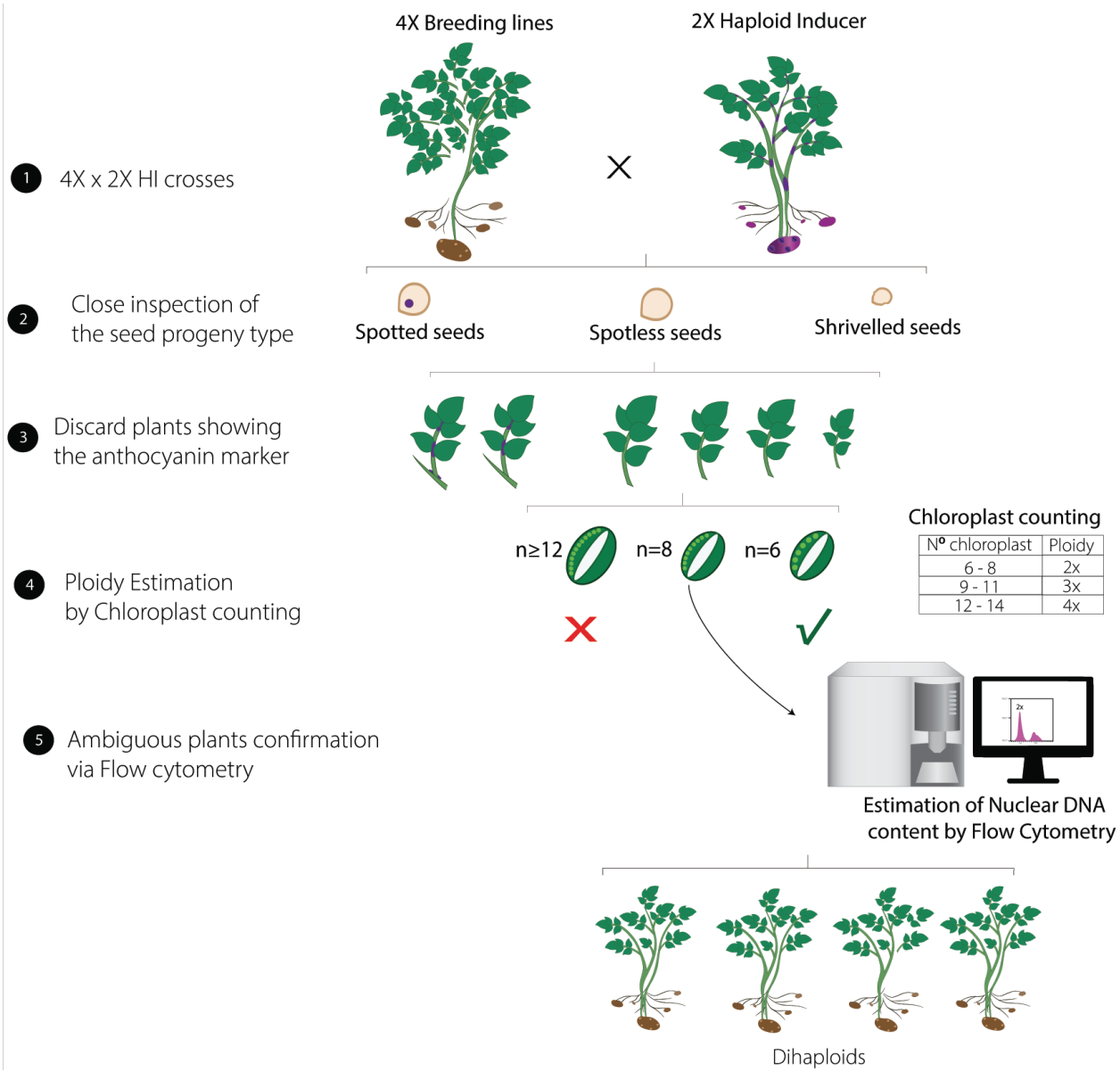

Fig. 2.1. Workflow for identifying dihaploids as a multi-step process. Observation of the anthocyanin marker in embryos and stems, followed by chloroplast counts allowed the rapid discarding of tetraploid or triploid hybrids from the putative dihaploids in early development stages. Ambiguous plants were confirmed by flow cytometry.

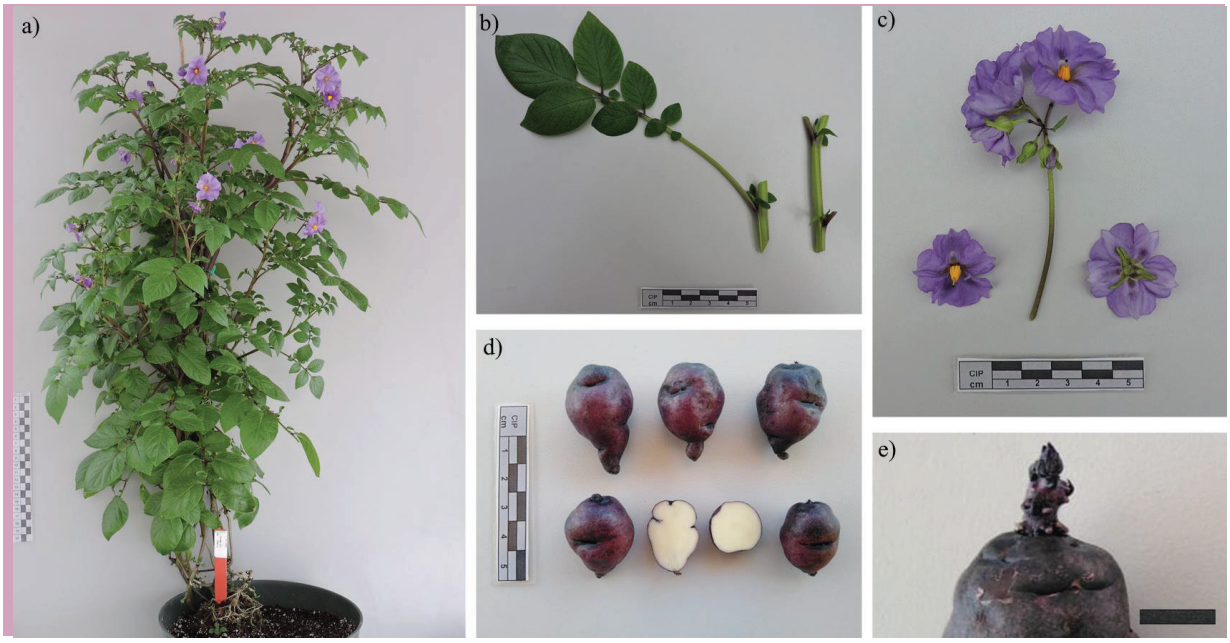

Fig. 2.2. Representative photographs of PL-4. A) Whole plant at the flowering stage. PL-4 displayed a semi-erect growth habit. **B)** Adaxial side of leaf. Stems were purple with extended green pigments on the surface and intense dark purple nodal bands. **C)** Inflorescence and flowers. Flowers had a rotated form. The stigma shape was capitated with a purple color. Anthers had a yellow-orange color. **D)** Tubers. The tuber shape was obovate and had slightly deep eyes. Tuber skin was predominantly purplish-red with dark purple spots. The tuber flesh color was cream and there was no secondary flesh color., and **E)** Sprout. Mainly apical sprouts of predominantly purple color. Gray bar indicates 1 cm.

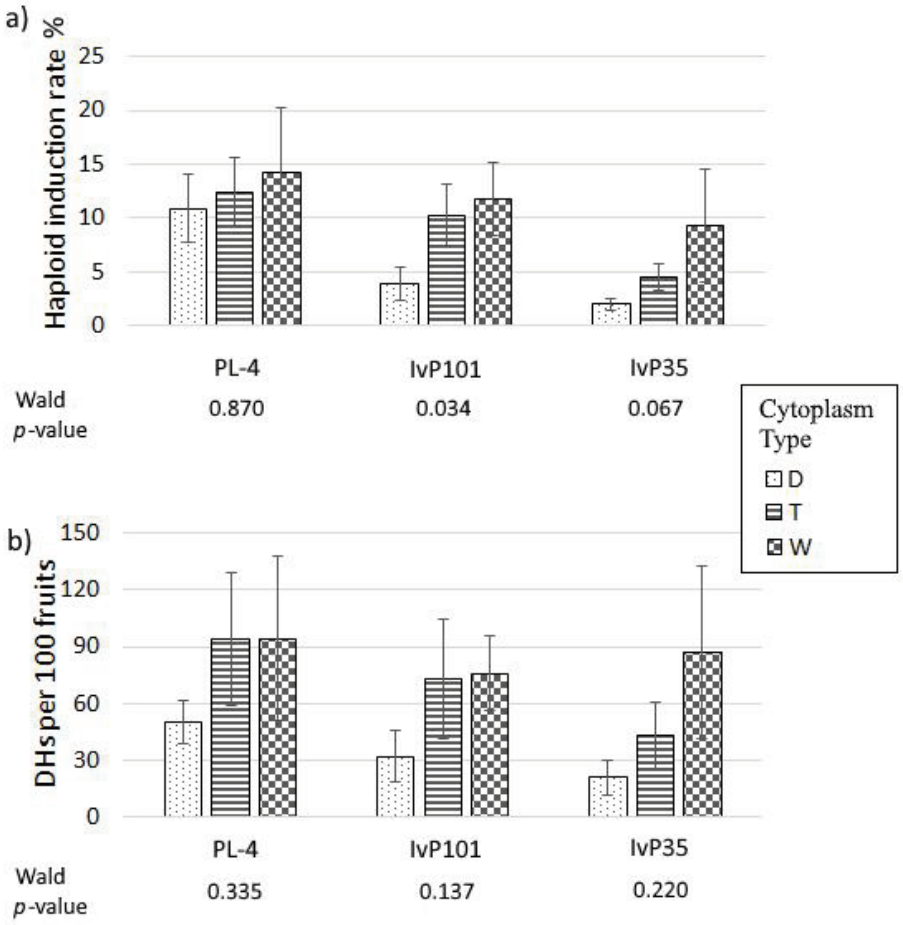

Fig. 2.3. Performance of the three HIs considering cytoplasm type as a factor. a) Haploid Induction Rate (*HIR*). b) Dihaploids per 100 fruits (*DH100F*). p-values of Wald test are shown below each bar group.

Supplemental Material

All supplemental figures and datasets are available from Dataverse at https://data.cipotato.org/dataset.xhtml?persistentId=doi:10.21223/SP9MFB

Supplemental Tables

Suppl. Table S.2.1. List of pistillate parents used in this study.

CIP Number	Breeder code	Pedigree	Cytoplasm type[a]
CIP300048.12	LR00.006	CIP392973.48 × BARI Alu-73	D
CIP300056.33	LR00.014	95.071 × CIP387170.9	W
CIP300072.1	LR00.022	95.139 × BARI Alu-73	T
CIP300093.14	LR00.026	95.206 × BARI Alu-73	W
CIP301023.15	C01.020	CIP391180.6 × CIP387170.9	T
CIP302428.20	LD-54.20	MARIELA × CIP392745.7	D
CIP304345.102	LD-28.102	CIP388615.22 × CIP676008	W
CIP304349.25	LD-32.25	CHIEFTAIN × CIP392745.7	T
CIP304371.67	LD-57.67	MONALISA × CIP392745.7	T
CIP304387.39	LD-73.39	REINHORT × CIP392745.7	T
CIP313047.57	LRY-3.57	CIP396311.1 × Alca Tarma	T
CIP313050.21	LRY-6.21	CIP391180.6 × Alca Tarma	D
CIP313051.7	LRY-7.7	CIP397099.4 × Alca Tarma	D
CIP313067.88	LRY-23.88	SERKHOSIL × ROSITA	D
CIP387164.4	LBr-40	CIP382171.10 × CARIBAY	D
CIP388615.22	C91.640	B-71-240.2 × CIP386614.16	T
CIP388676.1	Maria Bonita-INIA	CIP378015.18 × PVY-BK	T
CIP390478.9	Tacna/Pskom	SERRANA INTA × CIP386287.1	W
CIP390637.1	93.003	PW-31 × CIP385305.1	W
CIP391180.6	C90.266	CIP385305.1 × CIP378017.2	D
CIP391533.1	LR-93.060	G-7445 × CIP385280.1	D

CIP Number	Breeder code	Pedigree	Cytoplasm type[a]
CIP391691.96	Serranita	RUKINZO × LB-CUZ.1	D
CIP391931.1	458	SR-17.50 × SELF	D
CIP392780.1	Basadre	SEDAFIN × YY.3	D
CIP392820.1	BARI Alu-73	MONALISA × CIP388216.1	T
CIP392822.3	LR-93.073	MARIELA × YY.1	D
CIP392973.48	95.048	KRASA × CIP385280.1	D
CIP393228.67		CIP386209.1 × CIP387170.9	D
CIP394881.8	95.118	B84-606.5 × CIP386287.1	W
CIP397039.53	C97.182	CIP388615.22 × CIP388972.22	W
CIP397073.16	Serkhosil	CIP392823.4 × BARI Alu-73	D
CIP397077.16	Alliance	CIP392025.7 × BARI Alu-73	D
CIP397099.4	WA.073	CIP392822.3 × CIP391207.2	D
CIP398180.292		CIP392657.171 × CIP392633.64	D
CIP398190.89		WAKAYA × CIP392639.2	D
CIP398203.244		CIP393280.82 × CIP392633.64	T
CIP398208.219		CHUCMARINA × CIP392633.64	T
CIP702853	Alca Tarma	Landrace × Landrace	A
CIP800048	Desiree	URGENTA × DEPESCHE	T
CIP800827	Atlantic	WAUSEON × Lenape	T

[a] Designated scales for cytoplasm type were previously described by Mihovilovich et al. 2015.

Suppl. Table S. 2.2. Summary of haploid induction traits grouped by pistillate parents.

Pistillate Parent	Breeder code/Variety	HI used	*DH100P*	*DH100F*	*HIR* (%)
CIP300048.12	LR00.006	3	12.1 ± 5.6	34.4 ± 3.2	5.6 ± 2
CIP300056.33	LR00.014	3	15.5 ± 5.6	220.5 ± 97.7	30.1 ± 13.7
CIP300072.1	LR00.022	3	26 ± 11	66.8 ± 39.7	10.1 ± 6.4
CIP300093.14	LR00.026	3	20.4 ± 5.5	72.1 ± 31.2	9.4 ± 7.3
CIP301023.15	C01.020	3	12.6 ± 6.7	39.6 ± 26.6	6.8 ± 4.2
CIP302428.20	LD-54.20	1	10.5	22.2	10.5
CIP304345.102	LD-28.102	1	41.2	53.8	9.2
CIP304349.25	LD-32.25	1	0	0	0
CIP304371.67	LD-57.67	1	na	0	0
CIP304387.39	LD-73.39	2	9.7 ± 13.8	24.2 ± 34.2	5.3 ± 7.5
CIP313047.57	LRY-3.57	3	2.1 ± 3.6	3.3 ± 5.8	2 ± 3.4
CIP313050.21	LRY-6.21	3	0	0	0
CIP313051.7	LRY-7.7	1	1.4	200	20
CIP313067.88	LRY-23.88	1	10	33.3	33.3
CIP387164.4	LBr-40	2	0	0	0
CIP388615.22	C91.640	3	42.5 ± 31.8	75.3 ± 53.6	14.2 ± 8.2
CIP388676.1	Maria Bonita-INIA	3	8.1 ± 2.7	74 ± 29.4	7.2 ± 4.2
CIP390478.9	Tacna/Pskom	3	1.6 ± 2.4	7.7 ± 11.4	0.7 ± 1.2
CIP390637.1	93.003	3	36.8 ± 16.1	123.5 ± 73.8	14.6 ± 2.3
CIP391180.6	C90.266	1	18.9	100	11.7
CIP391533.1	LR-93.060	1	6.7	16.7	3.7

Pistillate Parent	Breeder code/Variety	HI used	*DH100P*	*DH100F*	*HIR* (%)
CIP391691.96	Serranita	3	0	0	0
CIP391931.1	458	3	2 ± 2	10.4 ± 6.9	1.7 ± 0.9
CIP392780.1	Basadre	2	4.9 ± 0.6	13.4 ± 4.7	3.3 ± 0.4
CIP392820.1	BARI Alu-73	3	140.6 ± 40.1	282 ± 151.3	21.2 ± 14.8
CIP392822.3	LR-93.073	3	33.4 ± 33.1	58.1 ± 45.2	8.1 ± 4.8
CIP392973.48	95.048	3	1.8 ± 1.6	22.7 ± 25.3	18 ± 27.8
CIP393228.67		2	8 ± 11.3	29.7 ± 41.9	5 ± 7.1
CIP394881.8	95.118	1	0	0	0
CIP397039.53	C97.182	2	19.9 ± 5.6	34 ± 12.7	7.3 ± 6.4
CIP397073.16	Serkhosil	3	5.1 ± 2.3	23.4 ± 4.5	1.9 ± 0.6
CIP397077.16	Alliance	3	27.9 ± 12.8	89.7 ± 11.9	6.3 ± 2.8
CIP397099.4	WA.073	1	23.8	62.5	5.1
CIP398180.292		1	8.3	66.7	7.7
CIP398190.89		1	6.5	16	2
CIP398203.244		1	4.1	10	2.4
CIP398208.219		1	32	88.9	20
CIP702853	Alca Tarma	1	2.8	4.8	1.6
CIP800048	Desiree	2	19.9 ± 19	51.5 ± 12.1	5.9 ± 2.3
CIP800827	Atlantic	2	20.7 ± 17.9	40.7 ± 33.4	4 ± 2.8

n.a: not available.
Values indicate mean ± standard deviation.

Suppl. Table S.2.3. Pearson's correlation among the haploid induction traits.

Trait 1	Trait 2	PL-4	IVP101	IVP35
FSP	*DH100P*	0.38*	0.81***	0.33 ns
SS	*Spotless100F*	0.61***	0.60**	0.48*
SS	*DH100F*	0.34*	0.49*	0.26 ns
Spotless100F	*DH100F*	0.91***	0.61**	0.64***
Spotless100F	*HIR*	0.43**	0.25ns	0.47*
DH100P	*HIR*	0.39*	0.42ns	0.46*

Significance: n.s, non-significant, or significant at * $p < 0.05$; ** $p < 0.01$; *** $p < 0.001$.

Chapter 3

Landscape of novel genomic rearrangements in a dihaploid cross progeny of potato

[Unpublished]

Benny Ordoñez[1,2], Isabelle M. Henry[1] and Luca Comai[1*]

1 Plant Biology and Genome Center University of California, Davis, 1 Shields Avenue, Davis, CA, 95616,USA

2 Integrative Genetics and Genomics Graduate Group, University of California, Davis, CA 95616, USA.

*Corresponding author: lcomai@ucdavis.edu

Abstract

In potato breeding, ploidy barriers hamper the introgression of desirable traits from wild relatives into the cultivated background. The haploid induction system facilitates gene flow by enabling a reduction from tetraploidy to diploidy. Haploid induction is achieved through a cross between a tetraploid cultivar and a specific line named Haploid Inducer (HI). In addition to dihaploids, this cross can generate progeny carrying novel and complex chromosome reorganizations. These are usually either undiscovered or not extensively studied. To optimally use HI crosses, it is crucial to understand the parental origin, frequency, and phenotypic impact of these rearrangements. They may also offer alternative strategies for accelerating breeding and enhancing genetic diversity.

In this study, we present the complete spectrum of karyotypic variations that arise from potato haploid induction crosses. We introduced a new category —shriveled seeds—that had never been studied before and is enriched with aneuploid types. Validating previous studies, we demonstrated the consistent production of dihaploids harboring whole or partial HI chromosomes. Moreover, we identified a potential chromothriptic case among the dihaploids. Finally, we examined the tuber characteristics from the progeny under greenhouse conditions, highlighting that some lines, despite their additional HI chromosomes, exhibit favorable tuber appearance. This study sheds light on the potential utilization of lines harboring novel rearrangements as chromosome vectors in potato breeding pipelines.

Introduction

Solanum tuberosum L (potato) is the third most important crop for human consumption worldwide (Kearney, 2010). Its high nutritional content and adaptability make potato a critical crop for food security. However, progress in potato breeding has been relatively slow compared to other crops,

primarily due to factors such as polyploidy, tetrasomic inheritance, and high heterozygosity (Halterman et al. 2016; Jansky, 2009). For instance, the main cultivar in the US, Russet Burbank, was introduced in 1876 and remains in use. To ensure optimal potato variety performance, there is a need to accelerate the introduction of novel traits at a faster rate.

Many of these 'novel' traits can be found within the gene pool of diploid wild relatives. Nevertheless, accessing these characteristics using traditional techniques can be cumbersome. This ongoing challenge for potato breeders underscores the importance of developing innovative approaches to facilitate faster potato improvement. One flexible alternative for harnessing and utilizing the extensive diversity of wild potato relatives is diploid potato breeding. This is part of a promising approach for speeding up the fixation of favorable alleles.

In potatoes, as in other crops, dihaploids, aneuploids, and hybrids arise from haploid induction—a process achieved through interploidy (4x-2x) crosses involving a tetraploid variety of interest and a specific *S. phureja* diploid line known as the haploid inducer (HI). Breeders have employed haploid induction for years to generate dihaploids from 4x varieties (De Maine' & Jervis, 1989; Iwona Wasilewicz-Flis, 2005; Velásquez et al. 2007), and numerous studies have reported the successful use of HI lines to efficiently generate dihaploids (Ordoñez et al. 2021). Nevertheless, only a few studies have focused on the fate of HI DNA in the dihaploids. Although the HI DNA is expected to be absent from maternal dihaploids, this has not been strictly determined. HI DNA may persist in the dihaploids after recombination with the maternal chromosomes (introgression) or as entire or rearranged chromosomes (addition).

Studies using limited molecular markers suggested that dihaploids generated with HI IvP48 have more residual HI DNA than dihaploids produced using other HIs (Clulow et al. 1991; Straadt and

Rasmussen 2003; Ercolano et al. 2004; Wilkinson et al. 1995; Clulow et al. 1993). For instance, Straadt and Rasmussen (2003) using a limited number of markers reported the absence of HI DNA into 30 dihaploids generated using IvP101, suggesting that IvP101 is a superior HI compared to IvP48. Bartkiewicz et al. (2018) conducted single nucleotide polymorphisms (SNPs) genotyping on 218 potato dihaploids obtained from crosses using haploid inducers IvP35 and IvP101, while Pham et al. (2019) performed a whole genome sequencing (WGS) on 95 dihaploids from IvP101. Both studies reported widespread and ubiquitous introgressions of short HI DNA regions in the dihaploids. This conclusion was questioned by a recent study conducted by Amundson et al. (2020, 2021) that addressed chromosomal instability resulting from potato haploid induction crosses using WGS. This study characterized diverse haploid induction progeny, and revealed that, overall, only 0.7% of dihaploids carried whole or partial HI chromosomes. Regardless of the frequency and extent of HI DNA remaining in the dihaploid progeny, the structure of the HI DNA has been incompletely characterized.

One significant limitation in the aforementioned studies is their failure to cover all progeny types and to provide a comprehensive phenotypic characterization. In the case of Amundson et al, this limitation stemmed from the separation of the plant material produced at the International Potato Center (CIP) based in Lima, Peru, from the genotyping laboratory in Davis, California, US.

In the present study, we focused on inducing and sequencing dihaploid lines derived from the tetraploid variety Red Polenta (Amundson et al. 2023) and the HI IvP48, with the aim of investigating the complete spectrum of karyotypic variation that can arise from potato haploid induction crosses. Specifically, we wanted to test whether the HI chromosomal instability noted by the Amundson study could be reproduced. The lines generated here also provide ideal materials for subsequent research in the role of the HI DNA in potato improvement.

Materials and Methods

Plant material and Induction crosses

The *Solanum tuberosum* line PI 310467, hereafter referred to as 'Red Polenta' (Amundson et al. 2023), was pollinated with the haploid inducer (HI) IvP48. Haploid induction crosses were conducted in a greenhouse with supplementary lighting at Davis, CA in 2016 and 2017. The resulting seeds were sown *in vitro* on Gamborg medium (Gamborg et al. 1968). All plantlets, both progeny and parentals, were maintained in a culture room at a temperature of 20 ± 2ºC under fluorescent lighting with 16-hour photoperiod. Cuttings of all lines were harvested to grow each clone on soil in the greenhouse as well.

Flow cytometry

The ploidy of each progeny was determined by estimating nuclear DNA content using flow cytometry. Approximately ~ 2 cm^2 of leaf tissue was chopped using a new razor blade for 2 minutes in 1.5 ml Chopping Buffer (15 mM Tris, 2 mM Na2EDTA, 0.5 mM spermine tetrahydrochloride, 80 mM KCl, 20 mM NaCl, 0.1% Triton X-100, 15 mM -mercaptoethanol, pH 7.5, filter through a 0.22 mm filter). The homogenate was filtered through the 40-µm nylon filter followed by centrifugation (1200× rpm, 10 min) to collect the nuclei. The supernatant was discarded, and the pellet was resuspended with 650 µL of fresh Chopping Buffer, then 25 µl of 1 mg/ml propidium iodide (PI, Sigma P4170) and 25 µl of 1 mg/ml DNase-free RNase A (Sigma V900498) were added to stain the DNA. The stained samples were incubated in darkness for 15 minutes prior to analysis. The samples were analyzed using a standard FAC Scan flow cytometer, with the laser illumination at 538 nm and 617 nm filter. Parental lines, Red Polenta and IvP48 were

used as 4x and 2x controls, respectively. At least 7000-10000 events were used to determine ploidy.

Genomic DNA sequencing, variant calling and Dosage analysis

The genomic DNA extraction was performed as previously described by Ghislain et al. (2004) and Illumina library preparation was done using 400bp sheared input DNA with KAPA Hyper Prep kit (cat. No KK8504). Sequencing was performed at the University of California, Davis DNA Technologies Core on the Illumina Novaseq™6000, using paired-end dual index 150bp reads. A full description of the DNA extraction, library prep, and sequencing, and demultiplexing is described in Amundson et al. (2021). Variant calling and dosage analysis were conducted as described in Amundson et al. (2021).

Phenotypic characterization under greenhouse conditions

Each progeny was phenotypically characterized at the seedling stage under *in vitro* conditions and at the harvest stage under greenhouse conditions. For the latter, plantlets were transplanted into 7" pots and cultivated in a greenhouse for four months. During this period, flowering was recorded, and pollen viability was assessed using Acetocarmine glycerol jelly, as described by Ordonez et al. (2017).

To further investigate the genetic influence of additional chromosomes on the dihaploids phenotype, we conducted assessments of tuber characteristics, focusing on tuber flesh color and tuber skin color. These traits were assessed using previously described descriptors (Gomez, 2006).

Results

Haploid induction crosses produce three types of seeds

From the 1,162 Red Polenta flowers pollinated with HI IvP48 pollen, we obtained 712 berries, yielding a total of 3,995 seeds. Traditionally, seed progeny from haploid induction crosses have been categorized based on the presence or absence of the 'embryo spot marker' inherited from the HI, distinguishing between spotted seeds (resulting from normal fertilization) and spotless seeds (representing mostly the desired maternal dihaploids).

In this study, we introduced an additional category: shriveled seeds, which encompass both 'completely collapsed seeds' (seeds lacking endosperm) and 'partially collapsed seeds' (seeds lacking a fully functional endosperm). This new category of progeny has not been described previously and allows for the exploration of the entire phenotypic spectrum resulting from this type of cross (Fig. 3.1). Out of the total seeds, 763 were spotless, 959 were spotted, and 2273 were shriveled. This diverse set of progeny seeds will be referred to as the 'BB' population.

To ensure germination and survival of as many of the shriveled seeds as possible, these seeds were treated with gibberellic acid (1500 ppm) for 24 hours and then germinated in Petri dishes containing Gamborg medium in a culture room. After 15 days, incisions were made in the partially collapsed seeds to facilitate their germination. This process resulted in a successful germination rate of approximately 2.8% (N = 65) of the shriveled seeds. These seeds could carry novel genomic combinations that are not normally observed without actively rescuing the seeds. Additionally, 43% (N=331) of the spotless seeds successfully germinated, and 30 spotted seeds were included in the experiment as well, bringing the overall number of successfully germinated seeds to 426.

The overall lower germination percentage may be attributed to the lack of the typical dormancy-breaking treatment, which involves reducing the relative humidity of the seeds to 10% before initiating any germination assay.

Importantly, 145 of the tetraploids identified and withheld from the analysis because they were identified as maternal selfed progeny based on SNP analysis (see below). These tetraploids can be explained by the development of non-reduced eggs or selfing from the Red Polenta cultivar, as observed in the study by Amundson et al. (2021). These individuals did not arise from the 4x-2x HI crosses and could potentially distort the frequency of progeny types. Overall, the BB hybrid progeny studied here encompasses a total of 281 seeds, of which could be categorized as follows: 66.2% spotless seeds, 23.1% partially collapsed seeds and 10.7% spotted seeds.

Comprehensive seed sowing unearth novel phenotypes

In conventional potato breeding pipelines, aberrant phenotypes are neither documented nor retained when seedlings from haploid induction crosses are sown. Consequently, unique phenotypes arising from this type of cross have typically not been observed.

Throughout the vegetative period, we evaluated *in vitro* plantlets to identify atypical phenotypes, which included, for example, the absence of a typical shoot apical meristem, narrow leaves, albinism or bushy appearance. Among all the plantlets, 49% exhibited a 'regular' phenotype, while 32% were phenotypically aberrant in one way or another. Notably, 19% of the plantlets completely lacked a shoot apical meristem, resulting in the development of roots only, as illustrated in Fig. 3.2. These particular plantlets (47) were deemed unsuitable for further analysis, bringing down the BB progeny to 234 (Table 3.1). The absence of an apical meristem in potato plants has been documented in progenies resulting from interspecific crosses with strong crossing barriers, as

reported by Ordoñez et al. (2023), so it is possible that this abnormality is not derived from the haploid induction mechanism.

Ploidy is not strictly associated with seed type

A month and a half after germination, when the plantlets reached an appropriate stage for analysis, we determined their ploidy level using flow cytometry (Fig. 3.3 and Table 3.1). Overall, 73.9% of the plantlets were diploid, 18.8% were triploid, and 7.3% were tetraploid.

Interestingly, we observed incomplete penetrance of the purple nodal marker among the seeds. For instance, some of the plantlets that had been initially classified as spotless during the seedling stage were later reclassified as spotted when they exhibited adequate growth stem characteristics such as the purple nodal bands in the stem—a typical characteristic of *S. phureja*. Considering the proposed IvP48 homozygosity for the dominant seed purple marker, the anticipated baseline ploidy for plantlets displaying the seed spot marker as well as the purple nodal bands is 3x or 4x. However, plantlets resulting from the spotted seeds consisted of 50% triploid, 36.7% tetraploids, and 13.3% diploids.

The ploidy of plantlets germinated from spotless seeds was predominantly diploid (96.8%), followed by 3.2% triploids. In contrast, plantlets from the shriveled seeds, exhibiting abnormal endosperm development, displayed a composition of 48% triploid, 40% diploids, and 12% tetraploids. The higher prevalence of triploids could be attributed to the deleterious effect on endosperm of the triploid block, preventing interploidy hybridization and linked to the Endosperm Balance number (EBN) hypothesis (Johnston et al. 1980; Johnston & Hanneman, 1980).

Furthermore, the successful rescue of a portion of these seeds suggests that the rescue process played a crucial role in shaping this outcome. The presence of other ploidies among these seeds also underscores the possibility of additional factors contributing to poor endosperm growth.

Aneuploidy is common in the BB progeny and enriched in the progeny of the shriveled seeds

We conducted chromosome dosage analysis using low-coverage whole-genome sequencing (0.5x coverage), as described in Amundson et al. (2020), for all viable BB progeny, while Red Polenta and IvP48 were sequenced to 64x and 32x coverage, respectively. To determine the frequency of HI aneuploidy among the dihaploids, we identified homozygous SNP between the two parents to determine the parental origin of the additional chromosomes. These SNPs were then used to calculate the percentage of HI DNA across the genome of each line. For instance, in a diploid, an observed percentage of 33% indicates that the additional chromosome belongs to the HI, while 0% HI SNPs indicates that the additional chromosome originated from Red Polenta. Representative SNP dosage plots are shown in Fig. 3.4.

Skim Illumina sequencing of all the BB progeny revealed widespread maternal aneuploidy in the offspring. Specifically, 15% of the dihaploid lines exhibited maternal aneuploidy (Table 3.2), with chromosome 8 being most often variable in dosage. We attribute this phenomenon to the presence of a previously identified translocation between chr 7 and chr 8 in Red Polenta (Comai et al. 2021), potentially leading to multivalent pairing and abnormal chromosome segregation at meiosis. Maternal aneuploidy involved most of the chromosomes, with the exception of chr1, chr9 and chr10. In most cases, a single additional copy of a chromosome was present, but cases with several additional chromosomes were observed as well (Table 3.3).

In total, we identified seven instances of additional HI chromosomes among the 173 dihaploids lines assayed (Table 3.2). Specifically, among the 20 dihaploid plantlets originating from shriveled seeds, we observed four instances with an additional copy of HI chr11, and three instances of an additional HI chr7. Additionally, two aneuploid plantlets carried multiple additional HI chromosomes among the 149 dihaploids arising from spotless seeds.

In contrast, the four plantlets arising from spotted seeds, each exhibiting a diploid genome, were categorized as 'clean' dihaploids. This observation is significant as it suggests that the seed spot marker in IvP48 may not be fully dominant. However, as these plantlets grew, they lost any purple spot marker attributed to HI (see below).

Next, we explored the frequency of aneuploids among the 3x and 4x hybrids. Our findings revealed that aneuploids constituted a slightly higher proportion in triploid hybrids (59.1%) compared to 47.1% in tetraploid hybrids. This observation contrasts with the results of Amundson et al. (2021), who reported higher proportions of aneuploids in tetraploids vs triploids (70% vs 22%). This difference can be explained because most of the 3x hybrids arose from shriveled seeds, a category that was not included in Amundson's study.

Amundson et al. (2021) also observed more occurrences of HI chromosomal breaks in dihaploid and tetraploid progenies resulting from haploid induction crosses, but not in the triploid progenies. Their findings suggested a correlation between instability, sperm ploidy, and haploid induction.

Among the 61 triploid and tetraploid hybrid lines collectively derived from all progeny, we consistently observed an additional chr8, along with variations involving losses and gains of other chromosomes. Notably, when analyzing the 145 tetraploid selfs, this distinctive pattern remained,

highlighting a consistent presence of an additional chr 8. This observation can be attributed to the pre-existing structural variation in Red Polenta (Comai et al. 2021).

Surprisingly, among the triploid hybrids originating from spotted seeds, we identified a particular case (BB-383) that exhibited a loss of HI chr1, a gain of HI chr5, and an additional maternal chr8. Additionally, an albino triploid plant showed partial loss of the HI in chr3 and chr4.

To validate our findings of aneuploidy in the triploid hybrids, we sequenced two technical replicates of two triploid lines (BB-155, and BB-172) displaying a 'regular' phenotype and a naturally occurring 'albino' triploid (BB-115) at a ~25x coverage.

The patterns obtained using deep-sequencing coverage were consistent with their low-sequencing coverage. Specifically, one of the triploid lines, BB-155 exhibited a tetrasomic copy of chr7 while the other triploid line, BB-172 displayed a loss of chr10. Meanwhile, the albino triploid plant (BB-115) exhibited triploidy with an apparent fragmentation of chr1, chr3, chr4, chr9 and chr12. (Fig. 3.5).

Two BB dihaploid line show extreme chromosome rearrangements

To further characterize the cases of whole and partial HI chromosome additions among the dihaploid lines, we performed sequencing at 20x coverage on two aneuploid plants. These instances represent the two cases of compound aneuploidy, a phenomenon not previously reported in any potato dihaploid population. Our findings indicate that the dihaploid lines, BB-266 and BB-329, possessed six and four additional HI chromosomes, respectively (Fig. 3.6 and Fig. 3.7). The patterns obtained through deep-sequencing coverage were consistent with the results obtained at low-sequencing coverage depth.

In the case of BB-266, which exhibited an aberrant phenotype and demonstrated poor growth under *in vitro* and greenhouse conditions, we observed additional HI chr1, chr2, chr4, and chr6, along with a shattered HI chr9 and a segment of the top arm of chr12. This shattered chromosome may be attributed to a potential chromoanagenesis event, a phenomenon that, although rare, has been reported in other crops and specifically in the progeny of haploid induction crosses in *A. thaliana* (Tan et al. 2015). Contrastingly, the line BB-329, which exhibited a 'regular' phenotype and was able to form tubers under greenhouse conditions, showed intact additional HI chr8, chr9, chr11, and chr12.

Taken together, these results suggest that the partial retention of HI DNA can be associated with chromosomal damage and remodeling, potentially suggesting chromoanagenesis. However, further investigation is required to validate this finding.

Variability in pollen and tuber characteristics within the BB progeny

Given the high heterozygosity in Red Polenta cv. (Amundson et al. 2023), its dihaploids are expected to exhibit variability in many morphological traits such as tuber characteristics (Sharma et al. 2009). Thus, the BB dihaploid lines could provide valuable material for conducting genetic studies on different traits. Specifically, the cases of single trisomies can be attractive for cytogenetic studies for the localization of genes on chromosomes as reported by Wagenvoort and Ramanna (1979).

To further investigate whether the presence of additional HI chromosomes influences the phenotype of the lines, we evaluated two key traits. First, we assessed flowering and pollen viability—crucial steps in appraising the feasibility of employing them further in potato

improvement pipelines, as selected dihaploids can be used in crosses with other diploids wild relatives or tetraploid lines, if unreduced pollen is present. Second, we examined their tuber characteristics, anticipating the identification of instances exhibiting favorable tuber appearance under greenhouse conditions. We followed Hutten et al.'s (1995) classification system for flowering and pollen grain development in dihaploid populations, which consists of six classes: 1) no flower buds, 2) deciduous flower buds, 3) flowers but no pollen, 4) stainable pollen 0-20%, stainable pollen 21-60% and 6) stainable pollen 61-100%. Regarding tuberization, we designated plantlets that produced at least one tuber—facilitating clonal propagation of the lines—as lines capable of 'forming tubers'.

Although it was expected that not all the dihaploid lines would produce flowers and viable pollen, we found that only two (BB-291 and BB-312) out of the 173 dihaploid lines exhibited stainable pollen, both in the range of 21-60%. It is worth noting that both dihaploids were euploid. Interestingly, 41 out of 44 triploids formed flower buds, but only six produced pollen, ranging from 0-20% (Fig. 3.8). While all the 4x hybrids produced pollen with a viability ranging from 60-100%.

Out of the 173 dihaploid lines, which included both aneuploids and euploids, only 24.8% formed tubers (Fig. 3.9, Top panel). The tuber skin color of the dihaploids that formed tubers varied from cream to blackish, and the tuber flesh exhibited a spectrum from cream to yellow (Fig. 3.10). The frequencies of different skin color types observed in the dihaploids are detailed in Supl.Table S.3.1. However, a large sample of dihaploids is required for a comprehensive assessment of this characteristic, as some distinctive features might have been interconnected, especially in the cases of aneuploidy.

Our specific focus was on the dihaploid lines. Interestingly, however, the ability to form tubers was higher in triploid and tetraploids with 68.2% and 88.2%, respectively. This indicated that the inbreeding associated with HI uncovered deleterious alleles affecting tuberization, an important trait in this species. For comparison, the tetraploid progeny of selfed Red Polenta, also, exhibited a higher percentage (60%) of tuber formers, as illustrated in Fig. 3.9, Bottom panel. Consistent with the hypothesis of masked deleterious alleles, the 40 dihaploids displaying aneuploidy, displayed 18 tuber producers, a distinctly higher frequency than pure dihaploids (Fig. 3.9, Top panel). Notably, the dihaploid line trisomic for chromosome 8 (BB-216) produced a red tuber, and its creamy flesh had a red narrow vascular ring. This distinctive feature was not observed in tubers from other dihaploid lines but was present in tubers from some of the triploid lines (Data not shown). Consistent with the observation of material aneuploids, three of the seven lines that exhibited additional HI chromosomes were also able to produce tubers. Specifically, the BB-329 line displayed a blackish skin color and yellow flesh color, while both the BB-344 and BB-415 lines produced tubers with yellow skin color and cream flesh color (Table 3.4).

Interestingly, the four dihaploids that arose from spotted seeds did not exhibit any purple or red phenotype in the tubers that could be attributed to the HI genome. It is possible that they arose from a misclassification of the spotted marker, or that these plants were chimeric and had HI chromosomes in the spot forming tissue, but not in the axillary buds that form tubers. Frequent chimerism of embryos from HI has been documented in Arabidopsis (Marimuthu et al. 2021).

Discussion

As the relevance of diploid potato breeding continues to grow, understanding the full spectrum of karyotypic variations resulting from a 4x by 2x haploid induction cross has become crucial. If novel rearrangements are revealed, understanding their parental origin, frequency, and their phenotypic impact becomes essential to explore alternative strategies for their use in the incorporation of desirable genes and for enhancing genetic diversity. The additional and/or remodeled chromosomes arising from this system could serve as tools for chromosome engineering and, furthermore, they could speed-up the incorporation of new traits in potato.

The characterization of the novel category of seed —shriveled seeds—adds a unique dimension to our understanding of seed phenotypes arising from haploid induction crosses. This category has been overlooked in traditional breeding pipelines, which typically prioritize the examination of well-developed seeds directly sown into pots with soil to rapidly identify desired dihaploids with the best characteristics from the parental tetraploid cultivar. The two subcategories of shriveled seeds, which are completely ‘collapsed seeds' and 'partially collapsed seeds' can be explained by hybrid seed lethality, as observed in other crops following interploidy hybridizations. This lethality manifests as embryo arrest and/ or endosperm defects, resulting in seed abortion (He et al. 2023). Importantly, the prevalence of triploids in the plantlets germinated from the shriveled seeds underscores the influence of the triploid block in the endosperm.

Here, we confirmed that the potato haploid induction system produces dihaploids harboring whole or partial haploid inducer (HI) chromosomes, consistent with our previous research (Amundson et al. 2021). However, it is important to note that the lines harboring chromosomal rearrangements, as discovered in this study, were diverse, infrequent, and often associated with phenotypic

abnormalities that prevent their further utilization from the breeding standpoint, such as the lack of flower production and / or tuber formation.

The frequency of additional chromosomes originating from the tetraploid maternal parent was slightly higher at 19.07%, compared to reported frequencies in other dihaploid potato populations. For instance, Wagenvoort & Lange (1975) reported frequencies ranging from 3.5 to 11%. Amundson et al. (2020) found an 11% frequency in a curated dataset of spotless seeds from a 4x variety in the Andigenum Group. Similarly, our recent study, Amundson et al. (2021) reported a frequency of 9.6% among a diverse group of 4x lines from the Tuberosum Group. The higher frequency of maternal aneuploids in the BB population can be attributed to the lack of selection against weaker forms, pre-existing structural variation in Red Polenta and the inherent proneness of potato to errors during meiosis, as observed by Pham et al. (2019) using the variety Superior. Notably, certain trisomies occur more frequently than others. For example, in our population, we observed a high number of trisomy for chromosome 8. In contrast, the study by Wagenvoort and Ramanna (1979) used the variety Gineke and other approaches to produce trisomics, the more prevalent trisomies were observed in chromosome 4, while the rarest were found in chr8 and chr10.

In our study, a phenotypically distinct dihaploid line (BB-266) exhibited a likely chromothriptic event, revealing a shattered HI chromosome 8 whose copy number fluctuates between 2 and 1. This is consistent with the occurrence of chromoanagenesis documented in haploid induction progeny of Arabidopsis (Tan et al. 2015). In Arabidopsis, the haploid induction system is CENH3-based, involving the crossing of a haploid inducer carrying a mutated form of the centromeric histone 3 (CENH3) with a wild-type (WT). Chromothripis, a manifestation of chromoanagenesis, occurs when a chromosome missegregates, is captured in a micronucleus, and undergoes frequent

dsDNA breaks. The resulting fragments are either lost or reassembled at random (Guo et al. 2021, 2023). Our findings document this type of instability in potato. Interestingly, the outcomes of chromothripsis include the formation of minichromosomes when a chromosomal fragment spanning the centromere circularizes and becomes a persistent element (Tan et al. 2023). Because of the repetitive nature of pericentromeric regions and centromeres such elements would be challenging to identify in a genomically complex plant such as potato. However, knowledge of their potential existence should inform future studies on genomic instability during potato Haploid Induction.

Phenotypic variation was observed at all plant growth stages in the BB progeny, consistent with the findings by Sharma et al. (2009) in their study of androgenic dihaploids. Notably, only two dihaploids showed the capacity to produce moderately fertile pollen. This is in stark contrast to the dihaploids derived from the Tuberosum variety Atzimba, which exhibited profuse flowering and the ability to hybridize with other diploids (Iwanaga 1984). Conversely, dihaploids from the tetraploid *S.acaule*, as reported by Camadro et al. (1992), exhibited low blooming and produced no pollen.

Chávez and Sosa (2009) emphasized that the degree of homozygosity in the dihaploids is comparable to about three generations of inbreeding. Hence, the relatively low percentage (24.8%) of tuber formation among the dihaploids was not unexpected. However, it is noteworthy that up to 68% of the 3x and 4x hybrids formed tubers, along with 60% of the tetraploid self-plants. This can be explained because higher ploidies can tolerate aneuploidy better than their diploid counterparts (Kush 1973). For example, there is precedent for the utilization of potato aneuploids with chromosome numbers ranging from 48 to 53 chromosomes, showcasing high fertility, tuber formation and resistance to important pests. These traits allowed them to be successfully

incorporated into further breeding schemes (Iovene et al. 2004; Andino et al. 2022; Caruso et al. 2008). However, to date, there is limited information regarding the influence of aneuploidy on dihaploids and their morpho-agronomic traits.

In summary, this study has presented novel phenotypes resulting from haploid induction crosses in potato. Additionally, a high frequency of maternal aneuploids has been observed as well, originating from errors in tetraploid meiosis. The material generated here will serve as a valuable experimental tool for studying the role of additional chromosomes in the potato phenotype. Our findings also provide new insights in terms of the exploitation of potatoes showing unusual chromosome numbers by crossing with standard potato cultivars.

Funding

This work was supported by the National Science Foundation Plant Genome Integrative Organismal Systems (IOS) Grant 1444612 (Rapid and Targeted Introgression of Traits via Genome Elimination) to L.C, and a grant from the Innovative Genome Institute at UC Berkeley awarded to LC.

Acknowledgements

We wish to thank Sara Jovanovich, Kevin Morimoto, and Victoria Stewart for their assistance with flow cytometry and DNA extraction. Additionally, Dr. Amundson for his bioinformatics support.

Author contributions

B.O and L.C conceived the research and designed the experiments. B.O performed experiments, analyzed and interpreted data. B.O, I.M.H and L.C wrote the manuscript.

Literature cited

Amundson, K. R., Henry, I. M., & Comai, L. (2023). The United States Potato Genebank Holding of cv. Desiree is a Somatic Mutant of cv. Urgenta. American Journal of Potato Research: An Official Publication of the Potato Association of America, 100(1), 27–38.

Amundson, K. R., Ordoñez, B., Santayana, M., Nganga, M. L., Henry, I. M., Bonierbale, M., Khan, A., Tan, E. H., & Comai, L. (2021). Rare instances of haploid inducer DNA in potato dihaploids and ploidy-dependent genome instability. The Plant Cell.

Amundson, K. R., Ordoñez, B., Santayana, M., Tan, E. H., Henry, I. M., Mihovilovich, E., Bonierbale, M., & Comai, L. (2020). Genomic Outcomes of Haploid Induction Crosses in Potato (Solanum tuberosum L.). Genetics, 214(2), 369–380.

Andino, M., Gaiero, P., González-Barrios, P., Galván, G., Vilaró, F., & Speranza, P. (2022). Potato Introgressive Hybridisation Breeding for Bacterial Wilt Resistance Using Solanum commersonii Dun. as Donor: Genetic and Agronomic Characterisation of a Backcross 3 Progeny. Potato Research, 65(1), 119–136.

Bartkiewicz, A. M., Chilla, F., Terefe-Ayana, D., Lübeck, J., Strahwald, J., Tacke, E., Hofferbert, H.-R., Linde, M., & Debener, T. (2018). Maximization of Markers Linked in Coupling for Tetraploid Potatoes via Monoparental Haploids. Frontiers in Plant Science, 9, 620.

Camadro, E. L., Masuelli, R. W., & Cortes, M. C. (1992). Haploids of the wild tetraploid potato Solanum acaule ssp. acaule: generation, meiotic behavior, and electrophoretic pattern for the aspartate aminotransferase system. Genome, 35.

Caruso, I., Castaldi, L., Caruso, G., Frusciante, L., & Carputo, D. (2008). Breeding potential of Solanum tuberosum–S. commersonii pentaploid hybrids: fertility studies and tuber evaluation. Euphytica/ Netherlands Journal of Plant Breeding, 164(2), 357–363.

Chávez, R. S., & Sosa, M. H. (2009). Use of dihaploids in the breeding of Solanum tuberosum L. Hereditas, 70(1), 135–152.

Clulow, S. A., Wilkinson, M. J., & Burch, L. R. (1993). Solanum phureja genes are expressed in the leaves and tubers of aneusomatic potato dihaploids. Euphytica/ Netherlands Journal of Plant Breeding, 69(1-2), 1–6.

Clulow, S. A., Wilkinson, M. J., Waugh, R., Baird, E., Demaine, M. J., & Powell, W. (1991). Cytological and molecular observations on Solanum phureja-induced dihaploid potatoes. TAG. Theoretical and Applied Genetics. Theoretische Und Angewandte Genetik, 82(5), 545–551.

Comai, L., Amundson, K. R., Ordoñez, B., Zhao, X., Braz, G. T., Jiang, J., & Henry, I. M. (2021). LD-CNV: rapid and simple discovery of chromosomal translocations using linkage disequilibrium between copy number variable loci. Genetics

De Maine', M. J., & Jervis, L. (1989). The use of dihaploids in increasing the homozygosity of tetraploid potatoes. Euphytica/ Netherlands Journal of Plant Breeding, 44, 37.

Ercolano, M. R., Carputo, D., Li, J., Monti, L., Barone, A., & Frusciante, L. (2004). Assessment of genetic variability of haploids extracted from tetraploid (2n = 4x = 48) Solanum tuberosum. Genome / National Research Council Canada = Genome / Conseil National de Recherches Canada, 47(4), 633–638.

Gamborg, O. L., Miller, R. A., & Ojima, K. (1968). Nutrient requirements of suspension cultures of soybean root cells. Experimental Cell Research, 50(1), 151–158.

Ghislain, M., Spooner, D. M., Rodríguez, F., Villamón, F., Núñez, J., Vásquez, C., Waugh, R., & Bonierbale, M. (2004). Selection of highly informative and user-friendly microsatellites (SSRs) for genotyping of cultivated potato. TAG. Theoretical and Applied Genetics, 108(5), 881–890.

Gomez 2006. Guía para las caracterizaciones morfológicas básicas en colecciones de papas nativas. En Manual para caracterización In situ de cultivos nativos, ed. R. Estrada, T. Medina, A. Roldan, 26–50. Instituto Nacional de Investigación y Extensión Agraria-INIEA

Guo, W., Comai, L., & Henry, I. M. (2023). Chromoanagenesis in plants: triggers, mechanisms, and potential impact. Trends in Genetics: TIG, 39(1), 34–45.

Guo, W., Comai, L., & Henry, I. M. (2021). Chromoanagenesis from radiation-induced genome damage in Populus. PLoS Genetics, 17(8), e1009735.

Halterman, D., Guenthner, J., Collinge, S., Butler, N., & Douches, D. (2016). Biotech Potatoes in the 21st Century: 20 Years Since the First Biotech Potato. American Journal of Potato Research: An Official Publication of the Potato Association of America, 93(1), 1–20.

He, H., Shiragaki, K., & Tezuka, T. (2023). Understanding and overcoming hybrid lethality in seed and seedling stages as barriers to hybridization and gene flow. Frontiers in Plant Science, 14, 1219417.

Hutten R. C. B., Soppe W. J. J., Hermsen J. G. T., Jacobsen E. (1995). Evaluation of dihaploid populations from potato varieties and breeding lines. Potato Research, 38, 77–86.

Iovene, M., Barone, A., Frusciante, L., Monti, L., & Carputo, D. (2004). Selection for aneuploid potato hybrids combining a low wild genome content and resistance traits from Solanum commersonii. TAG. Theoretical and Applied Genetics. Theoretische Und Angewandte Genetik, 109(6), 1139–1146.

Iwanaga, M. (1984). Discovery of a synaptic mutant in potato haploids and its usefulness for potato breeding. TAG. Theoretical and Applied Genetics. Theoretische Und Angewandte Genetik, 68(1-2), 87–93.

Iwona Wasilewicz-Flis, H. J. (2005). Induction and application of dihaploids of potato Solanum tuberosum L. Plant Breeding and Seed Science, 52.

Jansky, S. (2009). Chapter 2 - Breeding, Genetics, and Cultivar Development. In J. Singh & L. Kaur (Eds.), Advances in Potato Chemistry and Technology (pp. 27–62). Academic Press.

Johnston, S. A., den Nijs, T. P., Peloquin, S. J., & Hanneman, R. E., Jr. (1980). The significance of genic balance to endosperm development in interspecific crosses. TAG. Theoretical and Applied Genetics. Theoretische Und Angewandte Genetik, 57(1), 5–9.

Johnston, S. A., & Hanneman, R. E. (1980). Support of the endosperm balance number hypothesis utilizing some tuber-bearingSolanum species. American Potato Journal, 57(1), 7–14.

Kearney, J. (2010). Food consumption trends and drivers. Philosophical Transactions of the Royal Society of London. Series B, Biological Sciences, 365(1554), 2793–2807.

Khush GS (1973) Cytogenetics of aneuploids. Academy, New York, p 301

Marimuthu, M. P. A., Maruthachalam, R., Bondada, R., & Kuppu, S. (2021). Epigenetically mismatched parental centromeres trigger genome elimination in hybrids. Science Advances, 7(47).

Ordoñez, B., Aponte, M., Lindqvist-Kreuze, H., & Bonierbale, M. (2023). A case study of potato germplasm enhancement using distant late blight resistant wild relatives. Crop Science. https://doi.org/10.1002/csc2.21038

Ordoñez, B., Santayana, M., Aponte, M., Henry, I. M., Comai, L., Eyzaguirre, R., Lindqvist-Kreuze, H., & Bonierbale, M. (2021). PL-4 (CIP596131.4): an Improved Potato Haploid Inducer.

American Journal of Potato Research: An Official Publication of the Potato Association of America. https://doi.org/10.1007/s12230-021-09839-y

Pham, G. M., Braz, G. T., Conway, M., Crisovan, E., Hamilton, J. P., Laimbeer, F. P. E., Manrique-Carpintero, N., Newton, L., Douches, D. S., Jiang, J., & Others. (2019). Genome-wide inference of somatic translocation events during potato dihaploid production. The Plant Genome.

Sharma, S., Sarkar, D., & Pandey, S. K. (2009). Phenotypic characterization and nuclear microsatellite analysis reveal genomic changes and rearrangements underlying androgenesis in tetraploid potatoes (Solanum tuberosum L.). Euphytica/ Netherlands Journal of Plant Breeding, 171(3), 313.

Straadt, I. K., & Rasmussen, O. S. (2003). AFLP analysis of Solanum phureja DNA introgressed into potato dihaploids. Plant Breeding = Zeitschrift Fur Pflanzenzuchtung, 122(4), 352–356.

Tan, E. H., Henry, I. M., Ravi, M., Bradnam, K. R., Mandakova, T., Marimuthu, M. P., Korf, I., Lysak, M. A., Comai, L., & Chan, S. W. (2015). Catastrophic chromosomal restructuring during genome elimination in plants. eLife, 4. https://doi.org/10.7554/eLife.06516

Tan, E. H., Ordoñez, B., Thondehaalmath, T., Seymour, D. K., Maloof, J. N., Maruthachalam, R., & Comai, L. (2023). Establishment and inheritance of minichromosomes from Arabidopsis haploid induction. Chromosoma. https://doi.org/10.1007/s00412-023-00788-5

Velásquez, A. C., Mihovilovich, E., & Bonierbale, M. (2007). Genetic characterization and mapping of major gene resistance to potato leafroll virus in Solanumtuberosum ssp. andigena. TAG. Theoretical and Applied Genetics. Theoretische Und Angewandte Genetik, 114(6), 1051–1058.

Wagenvoort, M., & Lange, W. (1975). The production of aneudihaploids in Solanum tuberosum L. group Tuberosum (the common potato). Euphytica/ Netherlands Journal of Plant Breeding, 24(3), 731–741.

Wagenvoort, M., & Ramanna, M. S. (1979). Identification of the trisomic series in diploid Solanum tuberosum L. group Tuberosum. II. Trivalent configurations at pachytene stage. Euphytica/ Netherlands Journal of Plant Breeding, 28(3), 633–642.

Wilkinson, M. J., Bennett, S. T., Clulow, S. A., Allainguillaume, J., Harding, K., & Bennett, M. D. (1995). Evidence for somatic translocation during potato dihaploid induction. Heredity, 74 (Pt 2), 146–151.

Tables

Table 3.1. Ploidy level estimation in 281 lines from 4x-2x haploid induction crosses grouped by seed type.

Ploidy	**Progeny seed type**		
	Well-developed		**Shriveled**
	Spotless	**Spotted**	**Partially collapsed**
2x	149	4	20
3x	5	15	24
4x	0	11	6
ND*	32	-	15
Total	**186**	**30**	**65**

*ND=Not determined due to lack of apical meristem

Table 3.2. Chromosome dosage analysis of the 173 dihaploid lines.

Nº dihaploids tested	Origin of the additional chromosome	Nº lines detected	% Aneuploidy
173	HI	7	4.05
	non-HI (tetraploid parent)	33	19.07

Table 3.3. Additional chromosomes identified in the dihaploid lines, depending on their parental origin (non-HI vs HI).

Additional Chromosome	Lines carrying chromosomes from the Red Polenta (non-HI)	Lines carrying chromosomes from IvP48 (HI)
chr1	none	BB-266
chr2	BB-338	BB-266
chr3	BB-338	none
chr4	BB-245, BB-335	BB-266
chr5	BB-1, BB-249, BB-367	none
chr6	BB-96	BB-266
chr7	BB-10, BB-36, BB-110, BB-375	BB-415, BB-344 (partial arm), BB-335
chr8	BB-38, BB-85, BB-88, BB-97(partial arm), BB-99, BB-102(partial arm), BB-192, BB-216, BB-236, BB-268, BB-302, BB-308; BB-317, BB-332, BB-337, BB-338, BB-350, BB-368, BB-376 (partial arm), BB-403, BB-411, BB-415, BB-420, BB-422, BB-424	BB-329
chr 9	none	BB-329, BB-266 (shattered)
chr10	none	none
chr11	BB- 221, BB-332, BB-422	BB-422, BB-411, BB-329
chr12	BB-242	BB-329, BB-266

Table 3.4. Tuber characteristics of dihaploid lines carrying additional HI chromosomes.

		Tuber characteristic		
Line code	Additional HI chromosome	Formation^	Skin	Flesh
BB-335	chr7	N	-	-
BB-344	Partial chr7	Y	Yellow	Cream
BB-411	chr11	N	-	-
BB-415	chr7	Y	Yellow	Cream
BB-422	chr11	N	-	-
BB-266	chr1; chr2; chr4; chr6; chr9; chr12	N	-	-
BB-329	chr8; chr9; chr11; chr12	Y	Blackish	Yellow

^ N=no; Y=yes

Figures

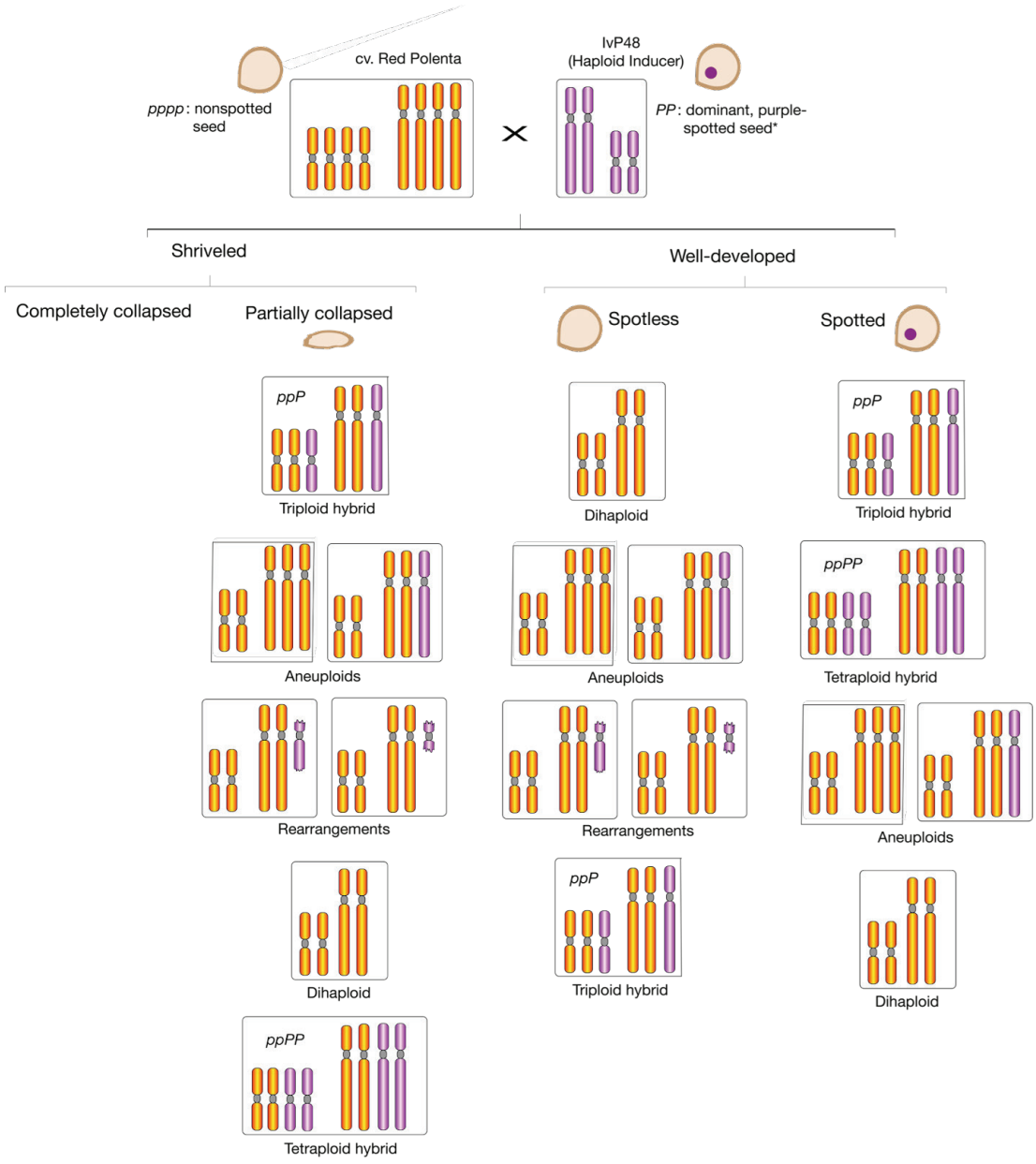

Fig. 3.1. Outcomes of potato haploid induction crosses. For simplicity, the potato genome is represented with two chromosome types. Progeny types are arranged based on frequency in the BB population.

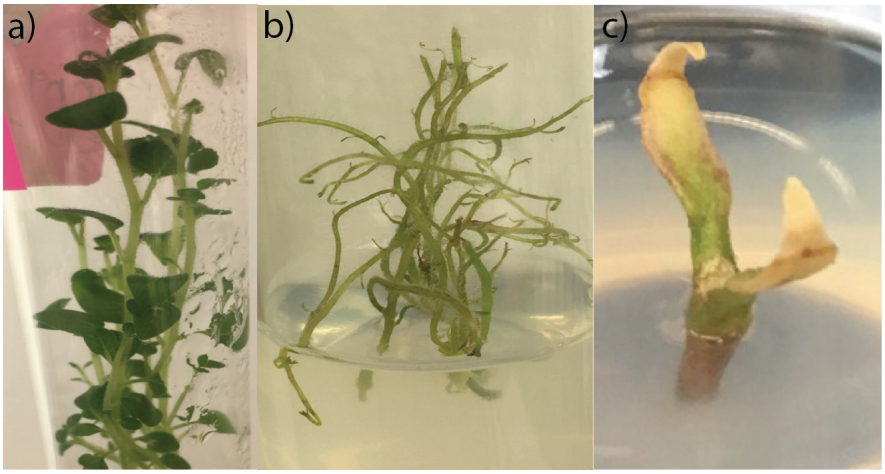

Fig. 3.2. A-C) *In vitro* plantlets were divided into three categories a) regular phenotype (BB-172), b) aberrant phenotype (BB-94), and c) complete lack of shoot apical meristem (BB-168).

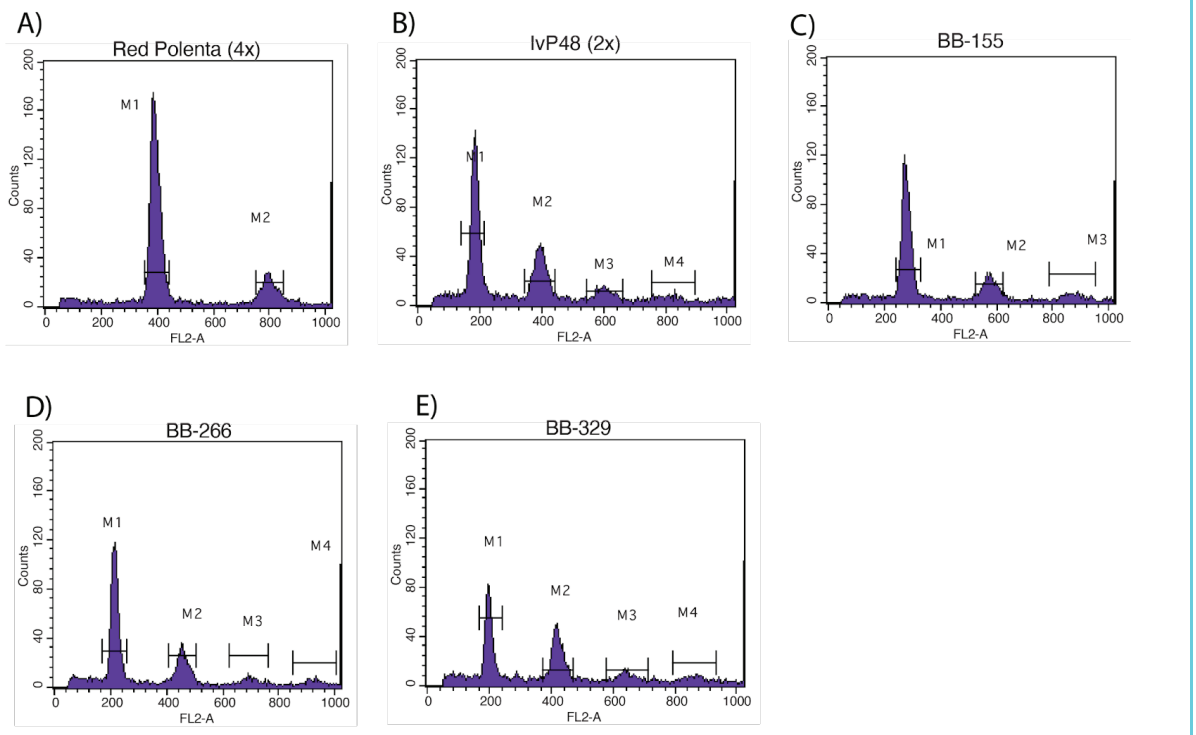

Fig. 3.3. Histograms depicting relative fluorescence intensity for lines of various ploidy levels derived from haploid induction crosses. The lines in the panel are a) Red Polenta (4x), b) IvP48 (2x), c) BB-155 (3x), d) BB-266 (2x + 6) and e) BB-329 (2x + 4).

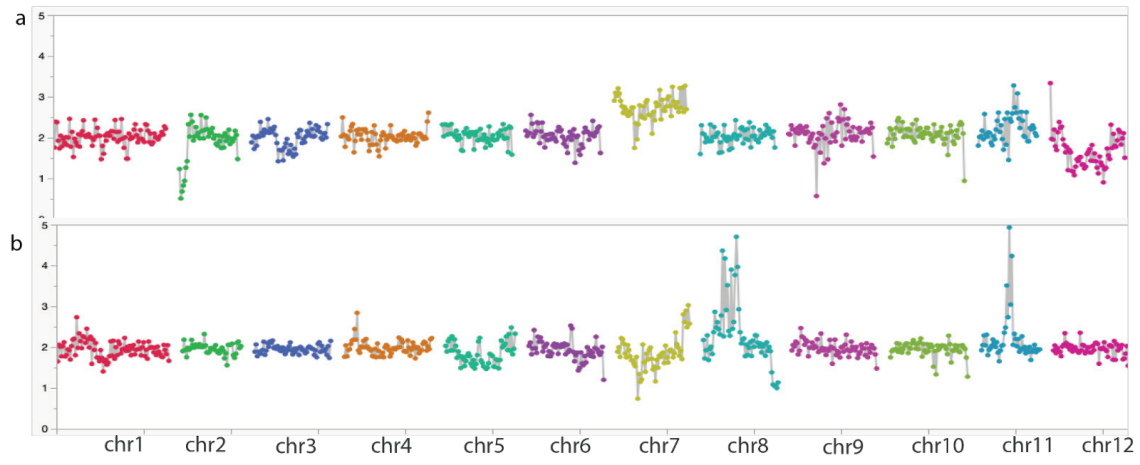

Fig. 3.4. Dosage plot in non-overlapping 1Mb bins to identify aneuploidy in dihaploids. Values close to 2 indicate the expected diploid state. a**)** Maternal trisomy of chromosome 7, b) Maternal trisomy of the pericentromeric region of chromosomes 8 and 11. Trisomy of the end of chromosome 7 and monosomy of the end of chromosome 8 originates from a pre-existing translocation in the maternal parent Red Polenta (Comai et al. 2021).

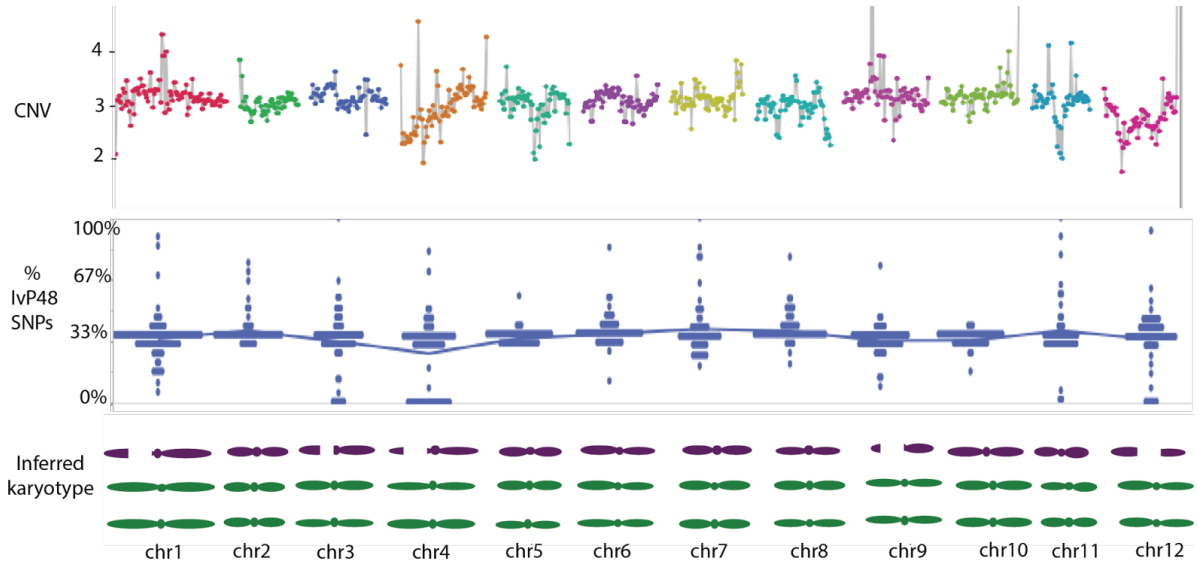

Fig. 3.5. Dosage plot in non-overlapping 1Mb bins to identify the aneuploidy in the albino triploid line BB-115. Top panel: Copy number plot representing read depth in non-overlapping 1MB bins, with a value of 3 indicating the expected triploid state. Standardized coverage shows that BB-115 has fragmented chr1, chr3, chr4, chr9 and chr12. Center Panel: Parental SNP allele plot. The percentage of alleles originating from the haploid inducer (HI) was expected to be approximately 33%, while it was anticipated to be close to 0% if all copies originated from the 4x maternal parent. **Bottom Panel:** Inferred karyotype of the line.

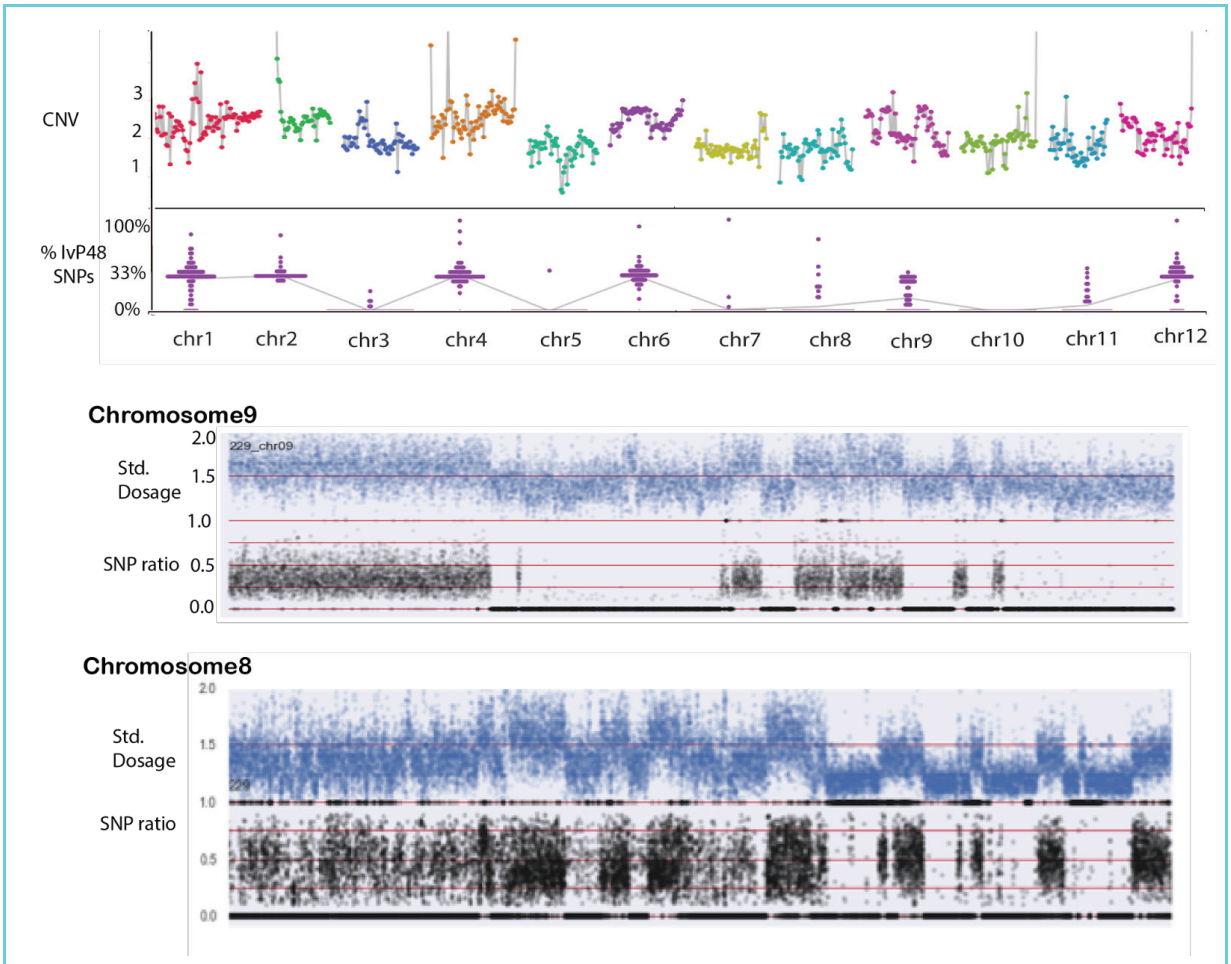

Fig. 3.6. A BB dihaploid line exhibiting extreme chromosome rearrangement (BB-266). Top Panel: Copy number plot representing read depth in non-overlapping 1MB bins, with a value of 2 indicating the expected diploid state. Standardized coverage shows that BB-266 carries three copies of chromosomes chr1, chr2, chr4, chr6, and chr12, along with an additional fragmented copy of chr9. **Center Panel**: Parental SNP allele plot. The percentage of alleles originating from the haploid inducer (HI) was expected to be approximately 33%, while it was anticipated to be close to 0% if all copies originated from the 4x maternal parent. **Bottom Panel:** zoomed in on the shattered region of chromosome 8 and chromosome 9.

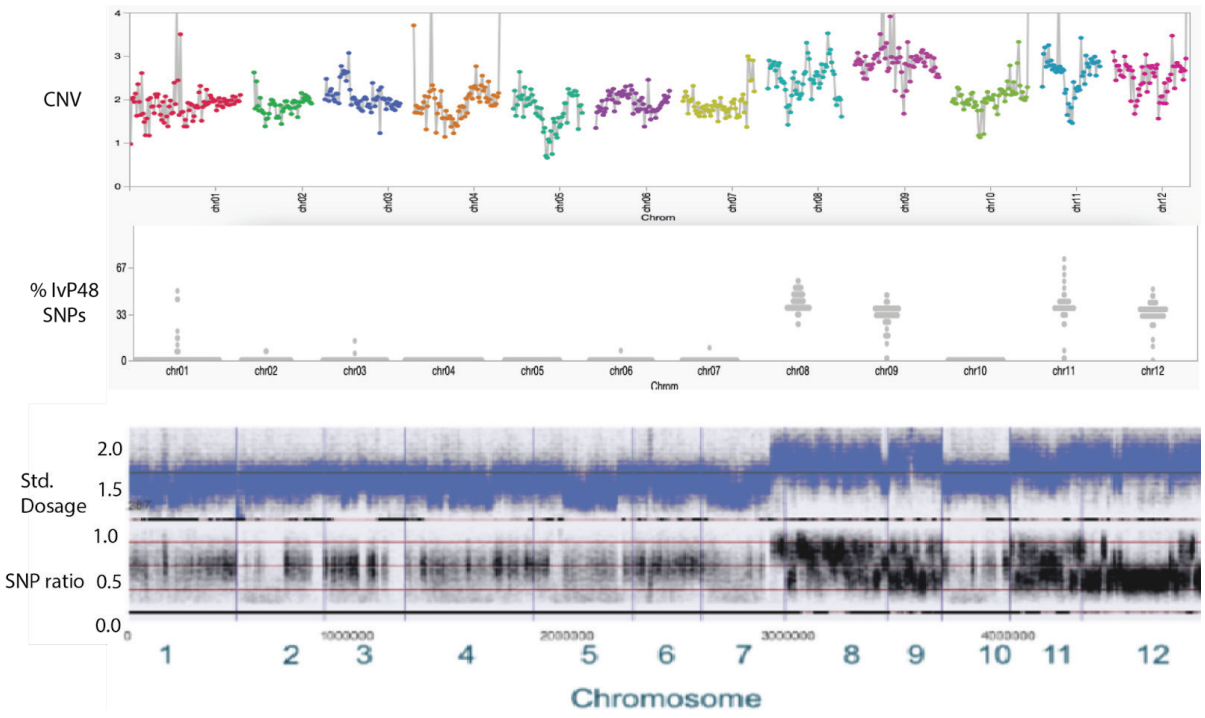

Fig. 3.7 A BB dihaploid line exhibiting four additional HI chromosomes (BB-329). Top Panel: Copy number plot representing read depth in non-overlapping 1MB bins, with a value of 2 indicating the expected diploid state. Standardized coverage shows that BB-329 carries three copies of chromosomes chr8, chr9, chr11, and chr12. **Center Panel:** Parental SNP allele plot. The percentage of alleles originating from the haploid inducer (HI) was expected to be approximately 33%, while it was anticipated to be close to 0% if all copies originated from the 4x maternal parent. **Bottom Panel:** SNP ratio of all the 12 chromosomes.

Fig. 3.8 Phenotypic characteristics of triploid line BB-155 in greenhouse conditions. a) Flower buds, b) Mature flowers, and c) Predominantly dead pollen under Acetocarmine Glycerol Jelly.

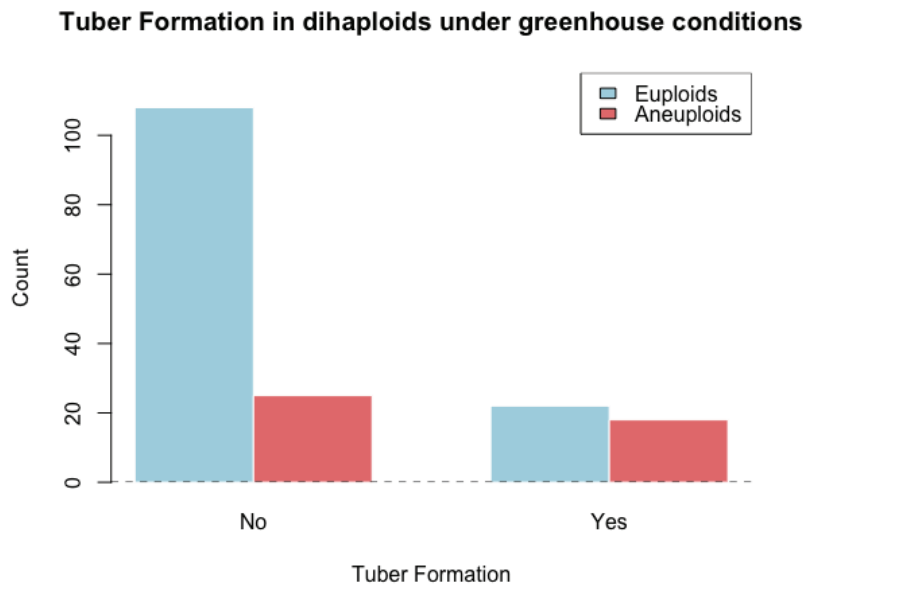

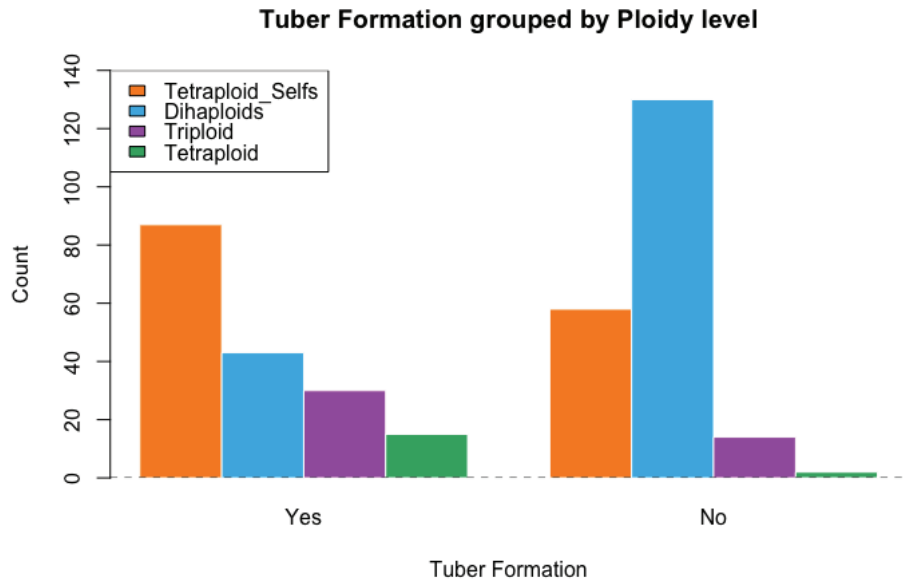

Fig. 3.9 Tuber characteristics of the BB progeny grouped by ploidy types. Top panel) Tuber formation among dihaploids grouped by different ploidies. Bottom panel) Tuber formation within the BB progeny.

Fig. 3.10. Examples of variability in tuber characteristics within the dihaploid BB lines. Each picture represents a different dihaploid line.

Supplemental material

Supplemental Table

Suppl. Table S.3.1. Forty-three dihaploids that formed tubers under greenhouse conditions in Davis, CA.

Lines code	Ploidy	Predominant tuber skin color	Tuber flesh predominant color	Notes
BB-3	euploid	yellow	yellow	
BB-4	euploid	yellow	yellow	
BB-34	euploid	yellow	yellow	
BB-50	euploid	red	cream	
BB-70	euploid	yellow	yellow	
BB-71	euploid	yellow	yellow	
BB-87	euploid	white-cream	white	
BB-88	aneuploid	yellow	cream	
BB-89	euploid	red	cream	
BB-93	euploid	yellow	yellow	
BB-96	aneuploid	yellow	yellow	
BB-100	euploid	white-cream	yellow	
BB-102	aneuploid	yellow	yellow	
BB-123	euploid	yellow	cream	
BB-216	aneuploid	red	cream	yellow around eyes, and a flesh secondary red color with narrow vascular ring
BB-217	euploid	yellow	white	
BB-222	euploid	white-cream	cream	
BB-257	euploid	white-cream	white	
BB-263	euploid	white-cream	white	
BB-274	euploid	yellow	white	
BB-279	euploid	white-cream	white	
BB-280	euploid	yellow	white	

Lines code	Ploidy	Predominant tuber skin color	Tuber flesh predominant color	Notes
BB-292	euploid	white-cream	white	
BB-306	euploid	yellow	cream	
BB-308	aneuploid	yellow	yellow	
BB-312	euploid	yellow	white	
BB-317	aneuploid	yellow	cream	
BB-327	euploid	yellow	yellow	
BB-329	aneuploid	blackish	yellow	
BB-332	aneuploid	red	cream	
BB-337	aneuploid	yellow	yellow	
BB-344	aneuploid	yellow	cream	
BB-350	aneuploid	yellow	cream	
BB-368	aneuploid	yellow	yellow	
BB-373	euploid	white-cream	cream	
BB-375	aneuploid	yellow	yellow	
BB-376	aneuploid	yellow	yellow	
BB-395	euploid	yellow	yellow	
BB-402	euploid	yellow	yellow	
BB-403	aneuploid	yellow	yellow	
BB-415	aneuploid	yellow	cream	
BB-420	aneuploid	yellow	cream	
BB-424	aneuploid	yellow	yellow	

Chapter 4

Characterization and Inheritance patterns of minichromosomes in Arabidopsis

Benny Ordoñez[1,2], Isabelle M. Henry[1] and Luca Comai[1*]
1 Plant Biology and Genome Center University of California, Davis, 1 Shields Avenue, Davis, CA, 95616,USA
2 Integrative Genetics and Genomics Graduate Group, University of California, Davis, CA 95616, USA.

*Corresponding author: lcomai@ucdavis.edu

Note - Some of the information in this chapter was published in 2023 with the following reference: Tan, E.H., Ordoñez, B., Thondehaalmath, T. et al. Establishment and inheritance of minichromosomes from Arabidopsis haploid induction. Chromosoma (2023). https://doi.org/10.1007/s00412-023-00788-5. The remaining parts of this chapter are unpublished.

Abstract

Minichromosomes are small, rearranged chromosomes that include a centromere but lack most of both chromosome arms. They hold the potential to serve as chromosome vectors, enabling the stacking of valuable genes but reducing the likelihood of trait segregation in important crops. To realize this potential, minichromosomes must be reliably generated and stably inherited across generations.

In this study, we characterize a previously identified line derived from a haploid induction cross in *Arabidopsis thaliana*, which contains a single-copy minichromosome known as *mini1a. Mini1a*, originated from the centromeric region of chromosome 1 of the haploid inducer (HI) genome. Our findings indicate that *mini1a* has a ~28% transmission rate through selfing. Notably, *mini1a* exhibits a ring structure, consistent cytological behavior across generations, and does not pair at meiosis. However, sequencing results demonstrate structural variations affecting the centromeric regions. Moreover, our observations suggest that the presence of *mini1a* can have detrimental effects on plant fertility. Finally, we noted that the presence of a wild-type (WT) allele of ch1 on the minichromosome exhibited poor ability to complement the mutant phenotype associated with a homozygous knock-out mutation. Overall, our findings suggest that the use of minichromosomes as vectors for bioengineering, while promising, will not be straightforward.

Introduction

Minichromosomes (minis), which are typically one-third the size of regular chromosomes, include a centromere, at least one origin of replication (ORI), and a feature suitable to preserve the chromosomal end integrity. To this end, linear minichromosomes feature telomeres, while circular minichromosomes form a ring-shaped structure (Murata, 2014). Both linear or circularized minis

are capable of germline transmission and maintenance as extrachromosomal entities (Tan et al. 2023).

The occurrence of minis has been documented in various species, including Arabidopsis, maize, tobacco, barley, potato and others (Yin et al. 2021; Murata 2014; Yan et al. 2017; Murata et al. 2006). They emerge spontaneously from chromosome breaks during genome instability (Fig. 4.1), facilitated by processes such as X-ray mutagenesis, biobalistic, a recombination system such as Cre/LoxP, Agrobacterium-mediated transformation, wide hybridization, or genome elimination (Kapusi et al. 2012; Liu et al. 2022). Despite their prominence, the molecular mechanisms underlying their formation remain relatively understudied. These mechanisms might encompass non-homologous end-joining (NEHJ), homology-directed repair (HDR) along with chromosome missegregation, breakage-fusion-bridge (BFB) cycles and chromoanagenesis (McClintock 1931; Guo et al. 2023; Birchler and Han 2013; Comai and Tan 2019).

In the model organism Arabidopsis, Murata et al. (2006, 2008, 2014) and Yokota et al. (2011) provided a comprehensive overview of the generation and characterization of naturally occurring and experimentally induced linear and circular minis. Notably, their minis are generally smaller than those found in other plants. For instance, a mini known as mini-4S originated from a centromere breakage of chromosome 4, yet it displayed stable transmission. The authors observed that genetic factors influenced the stability of these minis, with variations among different ecotypes. Another mini, mini-δ, derived from the short arm of chromosome 2, was transmitted through male gametes and remained functional despite its smaller size, suggesting a 500 kb minimum for a functional kinetochore. While a lower size limit of around 5% of genome size was

suggested for meiotic stability (Schubert 2001), factors such as centromere size and mini structure (linear vs. circular) may also impact mini stability.

In crop research, maize serves as a prominent model organism. McClintock (1931; 1938; 1942; 1941) initiated this field by discovering and describing a mini with unique cytological behavior. This mini assumed a ring shape due to the instability of maize chromosome ends, triggered by a break-fusion-break (BFB) cycle caused by eroded telomeres. Decades later, supernumerary and dispensable chromosomes, known as 'B chromosomes' have become key materials for generating minis in maize. B chromosomes have been extensively studied for insights into centromere functions and transmission rate (Birchler et al. 2010; Masonbrink and Birchler 2012; Birchler and Yang 2021; Kato et al. 2005; Chen et al. 2022; Liu et al. 2020). B-minichromosomes are formed when A-B fusion forms a dicentric chromosome and triggers BFB cycles that lead to progressive whittling of the mini (Han et al. 2007). Characterization of 22 resulting mini's indicated that some, depending on undetermined structural features, can pair. At the same time, these mini's underwent frequent sister chromatid disjunction at anaphase I. A recent study has provided evidence of transcriptional activity in B chromosomes (Hong et al. 2020) sparking an exciting debate about their potential use in combination with haploids to accelerate breeding. Inheritance and stability of minis, however, will play an important role in determining their potential utility.

While investigating the byproducts of haploid induction in Arabidopsis, instances of genome instability have come to light. For example, Seymour et al. (2012) observed three lines carrying minis in the progeny of a CENH3-based genome elimination cross. Additionally, Tan et al. (2015) extensively described genome instability leading to chromosomal restructuring in similar CENH3-

based genome elimination crosses. In their study, the authors discovered shattered chromosomes from the haploid inducer (HI) among the expected haploid offspring, highlighting the role of the phenomenon known as chromoanagenesis in the formation of these small rearranged chromosomes. Kuppu et al. (2015) reported two minis within the haploid progeny of a genome elimination cross. Taken together, these findings demonstrate that approximately 1% of phenotypically normal Arabidopsis haploids resulting from crosses with the CENH3-based GFP-tailswap haploid inducer (HI) carry rearranged small chromosomes or minis originating from centromeric and adjacent pericentromeric regions.

Utilizing the minis that have arisen from haploid induction crosses, as natural plant chromosome vectors (NPCVs) to incorporate desirable genes, holds great potential. An in-depth understanding of their formation, including any possible patterns among chromosomes that develop into minis, is essential. Furthermore, the investigation of their transgenerational stability is crucial for the harnessing of this technology. This importance is particularly due to their unique structures, such as telocentric or ring-shaped, which may impact mitosis through sister chromatid exchange (SCE) (Fig. 4.2), leading to tissue-specific mosaicism or affecting their meiotic behavior.

This study examines a mini derived from haploid induction crosses in Arabidopsis, with a primary research focus on assessing the transgenerational transfer ability of the Arabidopsis mini. A combination of cytological observations and genomic analysis was employed to describe the dynamics of these minis. Three mini lines were identified in the progeny of a CENH3-based genome elimination cross (Seymour et al. 2012). Specifically, the F1 hybrid of Sq-8 (CS22601)/NFA-8 (CS22598)) ecotypes was crossed to the GFP-tailswap strain in the Columbia

(Col-0) ecotype background, as outlined in Ravi et al. (2011) and Ravi & Chan (2010). Genotyping by sequencing analysis within the resulting doubled haploids revealed the presence of short segments of the haploid inducer (Col-0) DNA spanning the centromere on chromosomes 1 and 3, as reported in Seymour et al. (2012). The focus of this study centers on the line DHR194, hereafter referred to as *mini1a*. *Mini1a* was selected for further studies due to the preliminary observation that it could be transmitted at ~40% frequency in the S1 to S4 generations. An earlier study by Tan et al. (2015) identified the junction that circularized chromosome 1 using a modified breakpoint assembly method that leverages read pairs. This *mini1a*-specific junction provided convenient genotyping through PCR markers (Fig. 4.3). An analysis of the amplified junction region structure revealed a 17bp duplication near the major breakpoint at position 17,824,627 on chromosome 1. According to the TAIR10 reference, *mini1a* is 4MB in size. However, based on the full centromere assembly reported by Naish et al. (2021), its predicted size increases to 6MB.

Materials and Methods

Plant Material and Growth conditions

The *mini1a* lines were grown in a growth chamber at 22°C for 5–6 weeks, exposed to conditions of 16 hours of light and 8 hours of darkness.

The chlorophyll b-less mutants used in this study were obtained from the Arabidopsis Biological Resource Center at Ohio State University (ABRC) (Table S.4.1). The seeds were surface sterilized using 20% (v/v) bleach, vernalized for 3 days at 4°C, and then grown on Murashige and Skoog medium with 1% (w/v) agar at pH 5.6. When they reached the five-day-old seedling stage, they were transferred to a growth chamber with the same conditions as the *mini1a* lines.

In contrast, the *mini1a* lines followed the same vernalization procedure but were directly grown in mixed soil.

Generational and meiotic stability of mini1a

The meiotic behavior of *mini1a* was analyzed by conducting selfing and crosses in six consecutive generations using *mini1a* lines (Fig. 4.4). Each individual carrying *mini1a* was allowed to self, and the selfed seeds were subsequently genotyped for the presence of *mini1a*. SNP analyses for *mini1a* were performed using CAPS markers, as well as the *mini1a*-specific junction PCR to assay for the presence of *mini1a,* as previously described by Tan et al. (2015, 2023). Oligonucleotide sequences used are in Table S.4.2.

Reciprocal crosses were performed between wild-type (WT) Landsberg *erecta* (L*er*) and individuals carrying *mini1a*. When the siliques matured, all F1 seeds from dehiscing siliques were collected. The segregation of *mini1a* in the F1 progenies was determined using the *mini1a*-specific junction PCR as well. Based on the observed transmission rate of *mini1a* in outcrosses, i.e., 12.5% through ovules and 10.7% through pollen, we calculated the expected transmission rate through selfing as 100*(1 - (1 - 0.125) * (1 - 0.107)) = 21.8%.

Mini1a structure variation across generations assessment

The analysis of structural variation in *mini1a* between different generations (S5 to S10) was performed using whole-genome sequencing on a total of 46 individuals. This included both

individuals carrying *mini1a* and individuals who did not inherit *mini1a*: S5 (n=3), S6 (n=8), S7 (n=11), S8 (n=11) and S9 (n= 10) and S10 (n=3) (Fig. 4.5).

For each selected individual, genomic DNA (gDNA) extraction was performed as previously described (Ghislain et al. 2004), and library preparation was conducted using 400bp sheared input DNA with KAPA Hyper Prep kit (cat. No KK8504). Sequencing was carried out by Novogene (Novogene Inc).

Paired-end raw reads were trimmed using Trim_galore (version 0.6.7, https://github.com/FelixKrueger/TrimGalore) with Cutadapt (version 3.4). BWA (version 0.7.17) was employed to align the short reads to the Col-CEN reference genome (Naish et al. 2021) with default parameters (Li 2013). Dosage variation analysis was carried out along non-overlapping consecutive bins spanning the entire genome, following the method outlined in Henry et al. (2015). Briefly, bin coverage was normalized using a customized script (https://github.com/Comai-Lab/bin-by-sam) to one of the individuals from the same pedigree who had failed to carry *mini1a*. The expected relative read coverage for a diploid individual was set to 2, whereas values of 1 or 3 indicate deletion or duplication, respectively.

Cytological characterization of mini1a

To investigate the behavior of *mini1a* during meiosis, young flower buds were collected at various development stages from different generations (S6, S7 and S8), and fixed in Carnoy's fixative, composed of 60% ethanol, 30% chloroform, and 10% glacial acetic acid. Meiotic spreads were

prepared following the procedure described by Ravi et al. (2011), and male meiocyte stages were visualized using DAPI staining.

For the pollen viability assays, six anthers from lines representing generations S5 to S8 and carrying *mini1a* were selected. Flower buds from different branches were collected. These anthers were stained in Alexander dye and observed under a light microscopy, following the method described by (Alexander, 1969).

Mitotic mini1a stability assessment

A complementation experiment was conducted to assess mitotic stability and dosage changes of *mini1a*. Crosses were made between lines with the mutation in the CAO gene (Table S.4.2) and *mini1a* lines from generation S7, S9 and S10. Lines carrying this mutation exhibited a light green (LG) phenotype, while lines carrying *mini1a* displayed a regular green (G) phenotype. The segregation of the G:LG phenotype ratio was examined in the F1, F2 and F3 progeny, along with the presence of *mini1a*.

Results

Mini1a transmission rate varies across generations

An accurate evaluation of the transmission efficiency of the first four selfing generations of *mini1a* was not conducted. However, starting from generation S5 to S12, the meiotic transmission of *mini1a* and its stability over multiple generations were determined after selfing the line carrying *mini1a* or after hybridization with Landsberg *erecta* (L*er*). Transmission efficiency during selfing ranged from 22 to 47% (Table 4.1). Interestingly, in generations S7, S8, and S10, three progeny families did not inherit *mini1a* (Table 4.1 and Fig. 4.5), suggesting occasional instability and loss

from the germline. Using reciprocal crosses to wild-type (WT) L*er gl-1*, the transmission rates of *mini1a* through the female and male were 12.5 and 10.7%, respectively (Table 4.2). The observed transmission rate upon selfing is therefore consistent with the combined probability of male and female transmission (0.218; see Methods). Taken together, these results indicated that minichromosomes produced by haploid induction can be transmitted at a rate consistent with those of trisomic chromosomes (Koornneef & Van der Veen, 1983).

Detrimental effect of mini1a on plant fertility

To explore the role of *mini1a* in plant fertility, we collected flower buds from four generations (S5 to S8). Three flower buds were sampled from two branches of each individual carrying *mini1a* in generations S5 (n=4), S6 (n=1), S7 (n=3), and S8 (n=5). Additionally, flower buds were collected from individuals who had not inherited *mini1a* in generations S5 (n=1), S6 (n=4), S7 (n=1), and S8 (n=2).

Among the anthers analyzed, an unusual phenotype was detected. Normally, anthers will display uniformly red and, occasionally, green pollen grains, based on whether they are live or dead, respectively (Fig. 4.6A and 4.6B). With partial sterility, one expects a varying ratio of mixed grain types. Different from these expectations, anthers either contained mostly viable pollen or mostly unviable. In fact, some anthers were divided in completely sterile and fully fertile sectors (Fig. 4.6C). Variations in fertility were observed in individuals from generation S5, S7 and S8. Surprisingly, in generation S6 individuals were either 100% fertile or had 0% fertility (Fig. 4.6D). Collectively, these results suggest that the presence of *mini1a* is compatible with full fertility but can also lead to catastrophic events that affect pollen fertility.

Next, the meiotic behavior of *mini1a* was assessed in generations S6 to S9. *Mini1a* exhibited consistent cytological behavior across all generations. During meiosis I, *mini1a* undergoes random segregation to one of the poles instead of sister chromatid separation as observed in some maize minichromosome lines (Han et al. 2007). In the S6 generation, *mini1a* appeared either as a disomic or a monosomic particle (Fig. 4.7), similarly to that observed in the F2 generation of *mini1a* (Han et al. 2023). The disomic state could possibly be due to early sister chromatid separation. However, when monosomic, normal behavior of sister chromatid separation at anaphase II was observed. To further determine the structure and copy state of *mini1a*, we sequenced several individuals of *mini1a* lines representing the variation between different generations.

Mini1a structure and copy number is variable across generations

The structure of *mini1a* was characterized in selected individuals from each generation by Illumina sequencing at ~10X coverage. Given that the ring-shaped *mini1a* had been defined in the region spanning 13Mb to 19Mb, a closer inspection of the sequence read coverage in the areas surrounding that region was conducted. If *mini1a* has remained unchanged transgenerationally, the same structure should be consistently observed across generations. However, if *mini1a's* undergo breakage-fusion-bridge (BFB) cycles, structures different from the initial *mini1a* should arise in one or more of the generations.

Forty six individuals representing generations S5 to S10 were sequenced, reads were mapped on Col-CEN and used to derive coverage per 100,000 bp bins (Fig. S.4.1). Using the coverage data, a pattern-based cluster dendrogram was created for *mini1a* lines. It revealed five distinct patterns: the presence of one full copy of *mini1a*, the presence of two full copies of *mini1a*, the presence of

a deleted version of *mini1a*, the presence of two copies of the same deleted version of *mini1a,* and, finally, complete loss of *mini1a* (Fig. 4.8). These patterns served as the foundation for a detailed illustration of the structural variations in *mini1a* across generations (Fig. 4.9).

In Generation S5, among the 3 individuals assessed, one had a full copy of *mini1a*, one had a deleted version of one copy of *mini1a*, and one did not harbor any *mini1a*. The deletion pattern observed in the S5 *mini1a*, referred to as *mini1a*Δ, remained largely consistent in subsequent generations, suggesting a single deletion event. In each generation, individuals with and without minis were identified. Importantly, individuals that were negative by the PCR assay, were also negative for all *mini1a* sequences providing no evidence for loss of sequences sampled by the PCR assay. Among the individuals positive for *mini1a* or *mini1a*Δ, at least 4 lines displayed additional smaller rearrangements. Further classification of the breakpoints can be performed to identify these additional rearrangements. Separation in the pedigree of *mini1a* from *mini1a*Δ is evident in generation S7. Taken together, these findings imply that breakage and a major deletion affecting ~1Mb of *mini1a* occurred in the early generations, possibly as a result of a breakage-fusion-bridge (BFB) process. In addition, the dosage pattern clearly indicated that two copies of *mini1a,* as well as *mini1a*Δ, could exist stably, at least during an individual's life span. It is also plausible that two copies would be inherited through selfing (see Discussion).

Complementation of the chlorophyll b-less mutant gene with mini1a

To further elucidate mechanisms of transgenerational mitotic instability, we undertook a complementation experiment that could provide a visual assay for assessing *mini1a* stability and potential dosage changes. In this assay, *mini1a* was expected to complement a homozygous mutant

(*ch1*) in the *CHLOROPHYLLIDE A OXYGENASE* (*CAO*) gene, responsible for Ch1b synthesis. The *CAO* (AT1G44446.1) gene is essential for normal photosynthesis, and its deficiency in Arabidopsis leads to a light green phenotype (LG) known as 'chlorina' (Espineda et al. 1999) (Fig. 4.10). According to the TAIR10 genome assembly, AT1G44446.1 is positioned on chromosome 1 at 16MB. However, in the Col-PEK genome assembly (Wang et al. 2021), it is situated at 19MB, while the latest Col-Cen genome assembly assigns it to 18MB. Notably, this gene is closely linked to the centromere of chr.1 and included in both *mini1a* and *mini1a*Δ.

We expected that a single allele contributed by *mini1a* should complement mutation of the chromosomal copies. Loss or instability may become evident through variegation, which could suggest either the absence of inherited *mini1a* or the presence of a rearranged *mini1a* lacking the CH1 gene. For this purpose we crossed a ch1 -/- plant to a *mini1a* line (+/+/mini+ for the CH1 gene) and the resulting progeny was self-fertilized (Fig. 4.11).

The chlorophyll b-less mutants used in this study displayed reduced size and poor growth and exhibited a light green phenotype. Consequently, Petri dishes containing agar medium with 1% sucrose were employed for seed germination and seedling growth before transfer to soil in a growth chamber. Following this treatment, plants grew sufficiently well to be crossed.

The same green phenotype as the *mini1a* parent lines was observed in all of the F1 progeny generated. The percentage of *mini1a* transmission to this F1 progeny was recorded using PCR of the *mini1a* junction. It varied depending on cross (Table 4.3). However, this variation did not correlate with the mutant line used. With the exception of cross *mini1a* × *ch1-3,* the transmission

rate observed on these crosses was typically lower than previously observed in WT crosses (Table 4.2), suggesting an effect of environment and / or genetic context on transmission rates. Following that, selfing was performed on F1 individuals carrying *mini1a*, with the expectation that both genotype and phenotype would display the ratios provided in Fig. 4.11.

We screened the F2 families using the same PCR assay for the presence of *mini1a*, while scoring the green (G) and light green (LG) phenotypes. Assuming a transmission rate of 0.2 for *mini1a* in the selfing cross (as previously observed), a green-to-light green ratio of 4:1 is expected when *mini1a* is present, and 3:1 when it is absent. In other words, a percentage of green progeny significantly higher than 75% suggests the presence of the minichromosome and complementation. A chi-square test was conducted to ascertain whether there was a significant difference between observed and expected ratios of chlorophyll phenotypes. Deviations from the expected 3:1 ratio were observed in three families: MCHR642 and MCHR641, which resulted from crosses involving the *ch1-3* (CS3121) mutant line, and MCHR653, originating from a cross using *ch1-1*(CS3119), as detailed in Table 4.4.

The F2 family MCHR653, displayed a 5:1 ratio of green to light-green progeny (400 green : 79 light green), suggesting complementation of a subset of the -/- progeny by *mini1a*. The presence of *mini1a* was assayed in this population. Only 11% of the total F2 individuals analyzed had inherited *mini1a*. This rate was lower than expected from selfing, but consistent with the transmission rate observed in previous crosses where *mini1a* was the female parent (12.5%, Table 4.2).

Given this transmission rate, the expected frequency of *ch1* -/-/mini+ individuals is expected to be 0.025 (0.125 x 0.2), predicting that 11 individuals relied on the *mini1a CH1* allele for chlorophyll synthesis. Unfortunately, it was not possible to determine which individuals fell in this category because there was no sequence difference between the WT copy of CH1 present on the minichromosome and the one present in chromosome 1. Therefore, *ch1* -/-/mini+ and *ch1* +/-/mini+ individuals could not be distinguished.

Assuming that some of the individuals carrying *mini1a* were mutants of the CH1 genes, we observed these individuals in detail. Somatic loss of *mini1a* in these individuals, should result in a variegated phenotype. Surprisingly, we did not observe clearly delineated light-green patches in any of the individuals. Some exhibited diffused variegation, which could be explained by epigenetic silencing of the CH1 gene (Hynes and Todd 2003).

To determine whether some of the *mini1a* carrying individuals were indeed homozygous mutants for the CH1 gene, we next observed the inheritance patterns in the F3 generation. The F2 lines carrying *mini1a* were selfed, and the seeds were germinated and the phenotypic ratio (G:LG) and presence of *mini1a* was recorded. In total, 25 distinct F3 families, either *ch1* -/-/mini+ or *ch1* +/-/mini+, were assessed. This revealed a spectrum of phenotypic ratios, ranging from 1:1 to 7:1 green to light-green (Table 4.5). A -/- mutant that is complemented by the minichromosome should produce progeny that is mostly light green because transmission of the mini is typically only observed in a minority of the progeny. These results indicated that none of the F2 individuals that carried *mini1a* were homozygous for the Ch1 mutation.

Within these families, diffuse patches were observed in multiple individuals, with nearly 70 individuals in a particular family displaying these patches (Fig. 4.12). Notably, the 5:1 green to light-green ratio expected from a *ch1* heterozygote with a *mini1a*-linked *CH1+* allele, was displayed by two of these families. Strikingly, a darker green coloration was exhibited by few individuals with a +/+/mini+ genotype. This variation could potentially be explained by the accumulation of multiple copies of *mini1a*, if expression of CH1 is dosage-dependent. Unfortunately, these lines were not subjected to sequencing, making it impossible to draw firm conclusions at this point.

In summary, the analysis of *ch1* complementation yielded inconclusive results. In the absence of *mini1a*, all *ch1* mutant alleles displayed the expected 3:1 (green:light green) ratio. However, in *mini1a* F2 families, we observed the expected depletion of the light green types as 5:1 instead of 3:1. Subsequently, in F3 families, however, we did not observe 1:4 green:light green segregation (0.2 *mini1a* transmission in a -/- background). We thus failed to retrieve ch1 -/- individuals that were green because of *mini1a*- mediated complementation and were unable to investigate the stability of *mini1*a using this visual system.

Discussion

The primary objective of this study was to investigate a mini chromosome derived from a haploid induction cross in Arabidopsis. Our research mainly focused on the inheritance pattern of the mini though both crosses and selfing. While minis have been previously generated and studied in Arabidopsis, few studies have explored their transgenerational inheritance.

We carried out an extensive characterization of the Arabidopsis line harboring *mini1a*. Cytologically, the major finding was that *mini1a* has a circular structure with junction sites flanking the centromere of chr1. Most of the examined cells carried *mini1a* as a single unpaired circle with a distinct DAPI-stained knob, as observed during prophase and metaphase (Fig. 4.5). Occasionally, two unpaired circles per cell were visible, suggesting the presence of two copies of *mini1a*. We could not determine from the cytological analysis if the two copies of the mini were a persistent state present in all cells of an individual, or if they were caused by accidental and rare premature disjunction of sister chromatids.

When a ring-shaped mini undergoes breakage-bridge fusion (BFB) cycles, significant structure rearrangement occurs. These changes encompass deficiencies, deletions, inversions and alterations in the amount of constitutive heterochromatin. Cytological changes like these are likely to be accompanied by transfers of segments from one chromosome arm to another, as noted by Lukaszewski (1995) or they can change their size, become lost or increase their copy number, as observed by McClintock (1931;1938) and depicted in Fig. 4.2. In cancer studies, recent research suggests that the immediate genomic consequences of BFB are simple patterns of copy alterations localized near the site of the breakage on bridge chromosomes (Umbreit et al. 2020). Instability could happen progressively within individuals and across generations, creating a mosaic population in which some cells, either carrying an altered minis or did not carry one at all having failed to carry minis. These cells may undergo competition and selection. In our case, we expected that rearrangements in *mini1a* would occur if a crossover took place between sister chromatids. The resulting dicentric would result in bridges, breaks, and fusion to repair the broken ends.

Detailed cytological analysis of *mini1a* across multiple generations did not reveal any obvious structural variations.

In self-crosses, *mini1a* was transmitted to approximately 28% of the progeny, consistent with the observed transmission rate of approximately 0.12 through both male and female gametes. For certain lines, a very low transmission rate was observed, which may be explained by mitotic instability and loss of the *mini1*a. Until now, comprehensive characterization and tracking over multiple generations have been reported for Brassica minis. In contrast, Arabidopsis has seen only limited examination. Our study offers direct evidence regarding the behavior of ring-shaped mini lines at a high level of resolution. Previous reports have predominantly relied on cytology, FISH (Fluorescence In Situ Hybridization), and techniques like pulsed-field gel electrophoresis (PFGE), which can be laborious and have limited resolution. More recently, skim sequencing has been used for mini identification. However, to confirm structural changes, a deeper coverage of multiple individuals carrying minis is necessary. In this study, we employed whole-genome sequencing (WGS) at a minimum coverage of 10x, enabling a more thorough analysis and characterization of the structural changes in mini lines across various generations.

The molecular characterization of the mini revealed several key findings. At the S5 generation, two mini structures were identified: one ancestral and the other harboring a 12 kb deletion affecting a highly repeated centromeric region. This region, as determined by CENH3 binding, flanks the core centromere, in accordance with Naish et al. (2021). While a few other rearrangements occurred over the following four generations, they were limited to single lines (Data analysis is ongoing). This suggests that either these minis are either relatively stable or that the other

rearrangements are incompatible with their maintenance. Additionally, it was observed that the one-versus two-copy states are stable and distinct characteristics of both individuals and pedigrees.

We attempted to characterize mitotic stability using two approaches. The first was to characterize fertility in *mini 1a*-carrying individuals. We expected to see no effect because BFB and loss of the mini should not be deleterious. We were surprised to find that plants often formed sectors of fertile and sterile anthers. Sterile sectors only formed on *mini1a* positive plants. We conclude that *mini1a*-containing cells in the shoot apical meristem undergo a catastrophic event that causes sterility. The nature of this event is unknown. One possibility is that instability in the mini causes rearrangements in the regular chromosomes resulting in gametophytic lethality. The second approach entailed leveraging the visual trait provided by the *ch1* mutation. *Mini1a* and *mini1a*Δ, being derived from Col-0, carry a wild-type *CH1* allele. In the *ch1* -/- chromosomal background, loss of the mini should result in light green cells.

The mitotic inheritance of *mini1a* remains a subject of ongoing investigation. The complementation assay with chlorophyll b-less mutants was expected to provide insights but the results were inconclusive. Instead of observing the anticipated regular patches, as reported in the fate map of the meristem by Irish and Sussex (1992), irregular variegation was detected in several instances (Fig. 4.12). These irregularities may be attributed to somatic mosaicism resulting from occasional loss of the ring structure or gene silencing due to position effect variegation. Intriguingly, an increase in the number of irregular patches was observed in the F3 compared to the F2 lines. Therefore, a more detailed characterization of the rearrangement's effect on *CH1* gene expression is still needed. In a study conducted by Masonbrink and Birchler (2012) on maize

plants, the accumulation of up to 21 copies of B minichromosomes was found to be associated with some sterility, but contrary to what observed with regular B chromosomes, no other deleterious effect was observed. Maize plants with a low copy of B minichromosomes were fertile and exhibited a wild-type appearance. In contrast, our Arabidopsis plants with 1 or 2 copies of minis could be fully fertile and did not display deleterious effects. They did, however, have the potential to become fully sterile, sometimes by forming sterile sectors. We infer that *mini1a* can interact with the host genome to produce a catastrophic outcome.

In plants, mitotic inheritance of minis has not been extensively studied, despite their significant impact on the expression of crucial genes. Birchler et al. (2010) recommended avoiding ring minis as natural plant chromosome vectors (NPCVs), drawing from McClintock's observation that they tend to be highly unstable and prone to rearrangement during somatic mitosis in development. In their 2015 study, Tan et al. suggested the use of the minis generated from genome elimination in Arabidopsis as an ideal system for investigating mitotic genome instability and its associated consequences.

Our study has provided several insights into mini behavior. We found that, although rearranged forms of this mini arose over time, a conformation of *mini1a* consistent with the original one described by Tan in the early generations of the *mini1a* lineage, was still relatively common in the advanced generations. One deleted form (*mini1a*Δ) was also frequent in the advanced generations: interestingly this form lost a region rich in centromeric repeats, but preserved the CENH3-interacting core of the centromere (Naish et al. 2021). Surprisingly, in two consecutive generations, we could detect one or two copies of both the original and the deleted version of *mini1a* indicating

that *mini1a* could exist stably in one or two copies. Additionally, if copy number changes were common, we should have found intermediate dosages because plant tissues should contain cells with both dosage types. As predicted by McClintock pioneering studies, a ring chromosome such as *mini1a* is subject to instability that leads to rearranged forms. These are likely to result from BFB-cycles (Fig. 4.2).

The presence of rearrangements in the centromeric regions of minis derived from B chromosomes has been reported before by Kato et al. (2005). The authors proposed that these structural changes likely result from a process involving misdivision of the centromere during meiosis I, followed by fission of the centromere during meiosis II. They highlighted that this misdivision phenomenon can lead to structural changes in small chromosomes across multiple generations.

The sudden and catastrophic sterility could be explained if the broken ends of *mini1a* recombine with normal chromosomes. These fusion products could be unstable, resulting in genomes that cannot result in complete and balanced meiotic products. An unresolved problem is the unclear complementation of *ch1* -/- by the mini + allele. The observation of altered green:light green ratios in *mini1a* lineages is consistent with complementation. However, we failed to retrieve clear cases where a -/- chromosomal genotype was complemented by the + allele on the mini. The expression of the minichromosome alleles could be unstable, perhaps because of lack of meiotic pairing (Hynes and Todd 2003). Elucidation of this problem was deemed beyond the scope of this research.

In addition to providing concrete information on mitotic stability of minis, our work is important because it demonstrates that a circular minichromosome can be sufficiently stable to enable maintenance of useful genes in an extrachromosomal state. Further, mini provides useful tools to probe genomic stability and elucidate genomic rearrangements in a genetically tractable eukaryote. Further studies could elucidate the somatic and meiotic behavior of minis. This knowledge can have practical applications in human research, especially in relationship to cancer genomic instability (Pristyazhnyuk and Menzorov 2018; Gaubatz 1990). Mini formation and the loss of the induced ring minis have been proposed as a potential chromosome therapy strategy to selectively eliminate an undesired chromosome while also providing a mechanism for dosage compensation and replacement of the lost chromosome (Kim et al. 2017).

In humans, the phenotypes associated with ring chromosomes are highly variable. The most influential factors that determined the expressed phenotype include the specific chromosome involved, the size and configuration of the ring, and the extent of the deleted segment containing essential genes (Guilherme et al. 2011, 2016). In contrast, dynamic mosaicism, in which the structure and number of rings varies in the somatic cells of an individual is a frequent finding (Speevak et al. 2003). There is also variation in the stability of ring chromosomes among different tissues (Sodré et al. 2010).

In crop research, polyploid crops like potato and wheat are considered ideal candidates for carrying natural plant chromosome vectors (NPCVs) due to their heterozygosity and their greater tolerance to chromosomal losses and gains, in comparison to diploid plants. Historically, the incorporation of foreign or 'alien' genes from other crops involved the use of 'addition lines'(Chang and de Jong

2005). These lines could be monosomic or disomic and might exhibit 'desirable' phenotypes, such as increased resistance to Fusarium in wheat (Garvin et al. 2015), nematode resistance in oil-seed rape (Peterka et al. 2004), or morphological abnormalities (Muehlbauer et al. 2000). However, the generation and selection of these lines frequently proved unreliable, time-consuming, and, on the whole, cumbersome. In terms of transmission rates, the transmission of alien chromosomes displayed substantial variability, similarly to *mini1a* line. For instance, Ali et al. (2001) found that the transmission rate of monosomic additions of tomatoes in a potato background varied greatly (0- 32% in chromosome 9 and 14-88% in chromosome 6) between the different families. As a result, additions of potato, onion and beet background were often retained through vegetative propagation.

In summary, minis offer intriguing possibilities as natural plant chromosome vectors (NPCVs), despite being reported in crops resulting from haploid inducer crosses, such as in potato, only once by Amundson et al. (2021). While comprehensive karyotypic characterization is still in progress, mini lines hold great promise as valuable tools for targeted introgression from wild relatives, effectively mitigating the associated genetic drag (Birchler, 2014; Houben et al. 2008). Moreover, the inherent instability in minis can also be advantageous. For instance, the eventual loss of CRISPR-associated (Cas) gene is typically advantageous during genome editing.

Funding

This work was supported by National Science Foundation Plant Genome Integrative Organismal Systems (IOS) Grant PGRP IOS-2055260 "RESEARCH-PGR: Mechanisms of haploid induction

in potato" awarded to Luca Comai, and by NSF-PRG-P1956429: "RESEARCH-PGR: Variants and Recombinants without Meiosis", also awarded to Luca Comai.

Acknowledgements

We wish to thank Christine Chen, Tram Ngo, Laila Canosa and Winky Wong for their help with genotyping. Vienna Elmgreen, Fangchen Liu and Cecilia Yung for their help with DNA extraction.

Author contributions

Ravi Maruthachalam, Danelle Seymour, and Julin Maloof discovered and documented the appearance of minichromosomes in haploids produced by CENH3-based genome elimination. Ek Han Tan characterized the structure of *mini1a* in earlier generations. Ek Han Tan and Benny Ordoñez created the pedigrees. Benny Ordoñez characterized *mini1a* meiotic and mitotic inheritance and stability, performed the complementation assay and assessed the *mini1a* structure and copy number across generations. Tejas Thondehaalmath and Ravi Maruthachalam performed the cytological analysis of *mini1a*. Ek Han Tan, Ravi Maruthachalam, Julin Maloof, Isabelle Henry and Luca Comai supervised the research. Benny Ordoñez, Ek Han Tan, and Luca Comai wrote the Tan et al. 2023 manuscript with input and feedback from all authors.

Literature cited

Alexander, M. P. (1969). Differential staining of aborted and nonaborted pollen. Stain Technology, 44(3), 117–122.

Amundson, K. R., Ordoñez, B., Santayana, M., Nganga, M. L., Henry, I. M., Bonierbale, M., Khan, A., Tan, E. H., & Comai, L. (2021). Rare instances of haploid inducer DNA in potato dihaploids and ploidy-dependent genome instability. The Plant Cell. https://doi.org/10.1093/plcell/koab100

Birchler, J. A. (2014). Engineered minichromosomes in plants. Current Opinion in Plant Biology, 19, 76–80.

Birchler, J. A., & Han, F. (2013). Meiotic behavior of small chromosomes in maize. Frontiers in Plant Science, 4, 505.

Birchler, J. A., Krishnaswamy, L., Gaeta, R. T., Masonbrink, R. E., & Zhao, C. (2010). Engineered Minichromosomes in Plants. Critical Reviews in Plant Sciences, 29(3), 135–147.

Birchler, J. A., & Yang, H. (2021). The supernumerary B chromosome of maize: drive and genomic conflict. Open Biology, 11(11), 210197.

Chang, S.-B., & de Jong, H. (2005). Production of alien chromosome additions and their utility in plant genetics. Cytogenetic and Genome Research, 109(1-3), 335–343.

Chen, J., Birchler, J. A., & Houben, A. (2022). The non-Mendelian behavior of plant B chromosomes. Chromosome Research: An International Journal on the Molecular, Supramolecular and Evolutionary Aspects of Chromosome Biology, 30(2-3), 229–239.

Comai, L., & Tan, E. H. (2019). Haploid Induction and Genome Instability. Trends in Genetics: TIG, 35(11), 791–803.

Espineda, C. E., Linford, A. S., Devine, D., & Brusslan, J. A. (1999). The AtCAO gene, encoding chlorophyll a oxygenase, is required for chlorophyll b synthesis in Arabidopsis thaliana. Proceedings of the National Academy of Sciences of the United States of America, 96(18), 10507–10511.

Garvin, D. F., Porter, H., Blankenheim, Z. J., Chao, S., & Dill-Macky, R. (2015). A spontaneous segmental deletion from chromosome arm 3DL enhances Fusarium head blight resistance in wheat. Genome / National Research Council Canada = Genome / Conseil National de Recherches Canada, 58(11), 479–488.

Gaubatz, J. W. (1990). Extrachromosomal circular DNAs and genomic sequence plasticity in eukaryotic cells. Mutation Research/DNAging, 237(5), 271–292.

Ghislain, M., Spooner, D. M., Rodríguez, F., Villamón, F., Núñez, J., Vásquez, C., Waugh, R., & Bonierbale, M. (2004). Selection of highly informative and user-friendly microsatellites (SSRs) for genotyping of cultivated potato. TAG. Theoretical and Applied Genetics. Theoretische Und Angewandte Genetik, 108(5), 881–890.

Guilherme, R. S., Meloni, V. F. A., Kim, C. A., Pellegrino, R., Takeno, S. S., Spinner, N. B., Conlin, L. K., Christofolini, D. M., Kulikowski, L. D., & Melaragno, M. I. (2011). Mechanisms of ring chromosome formation, ring instability and clinical consequences. BMC Medical Genetics, 12, 171.

Guilherme, R. S., Moysés-Oliveira, M., Dantas, A. G., Meloni, V. A., Colovati, M. E., Kulikowski, L. D., & Melaragno, M. I. (2016). Position effect modifying gene expression in a patient with ring chromosome 14. Journal of Applied Genetics, 57(2), 183–187.

Guo, W., Comai, L., & Henry, I. M. (2023). Chromoanagenesis in plants: triggers, mechanisms, and potential impact. Trends in Genetics: TIG, 39(1), 34–45.

Haider Ali, S. N., Ramanna, M. S., & Visser, E. J. R. G. (2001). Establishment of a complete series of a monosomic tomato chromosome addition lines in the cultivated potato using RFLP and GISH analyses. Theoretical and Applied Genetics.

Han, F., Gao, Z., Yu, W., & Birchler, J. A. (2007). Minichromosome analysis of chromosome pairing, disjunction, and sister chromatid cohesion in maize. The Plant Cell, 19(12), 3853–3863.

Henry, I. M., Zinkgraf, M. S., Groover, A. T., & Comai, L. (2015). A System for Dosage-Based Functional Genomics in Poplar. The Plant Cell, 27(9), 2370–2383.

Hong, Z.-J., Xiao, J.-X., Peng, S.-F., Lin, Y.-P., & Cheng, Y.-M. (2020). Novel B-chromosome-specific transcriptionally active sequences are present throughout the maize B chromosome. Molecular Genetics and Genomics: MGG, 295(2), 313–325.

Houben, A., Dawe, R. K., Jiang, J., & Schubert, I. (2008). Engineered plant minichromosomes: a bottom-up success? The Plant Cell, 20(1), 8–10.

Hynes, M. J., & Todd, R. B. (2003). Detection of unpaired DNA at meiosis results in RNA-mediated silencing. BioEssays: News and Reviews in Molecular, Cellular and Developmental Biology, 25(2), 99–103.

Irish, V. F., & Sussex, I. M. (1992). A fate map of the Arabidopsis embryonic shoot apical meristem. Development , 745–753.

Kapusi, E., Ma, L., Teo, C. H., Hensel, G., Himmelbach, A., Schubert, I., Mette, M. F., Kumlehn, J., & Houben, A. (2012). Telomere-mediated truncation of barley chromosomes. Chromosoma, 121(2), 181–190.

Kato, A., Zheng, Y.-Z., Auger, D. L., Phelps-Durr, T., Bauer, M. J., Lamb, J. C., & Birchler, J. A. (2005). Minichromosomes derived from the B chromosome of maize. Cytogenetic and Genome Research, 109(1-3), 156–165.

Kim, T., Plona, K., & Wynshaw-Boris, A. (2017). A novel system for correcting large-scale chromosomal aberrations: ring chromosome correction via reprogramming into induced pluripotent stem cell (iPSC). Chromosoma, 126(4), 457–463.

Koornneef, M., & Van der Veen, J. H. (1983). Trisomics in Arabidopsis thaliana and the location of linkage groups. Genetica, 61, 41–46.

Kuppu, S., Tan, E. H., Nguyen, H., Rodgers, A., Comai, L., Chan, S. W. L., & Britt, A. B. (2015). Point Mutations in Centromeric Histone Induce Post-zygotic Incompatibility and Uniparental Inheritance. PLoS Genetics, 11(9), e1005494.

Li, H. (2013). Aligning sequence reads, clone sequences and assembly contigs with BWA-MEM. In arXiv [q-bio.GN]. arXiv. http://github.com/lh3/bwa

Liu, C., Wang, J., Fu, S., Wang, L., Li, H., Wang, M., Huang, Y., Shi, Q., Zhou, Y., Guo, X., Zhu, C., Zhang, J., & Han, F. (2022). Establishment of a set of wheat-rye addition lines with resistance to stem rust. TAG. Theoretical and Applied Genetics. Theoretische Und Angewandte Genetik, 135(7), 2469–2480.

Liu, Y., Su, H., Zhang, J., Shi, L., Liu, Y., Zhang, B., Bai, H., Liang, S., Gao, Z., Birchler, J. A., & Han, F. (2020). Rapid Birth or Death of Centromeres on Fragmented Chromosomes in Maize. The Plant Cell, 32(10), 3113–3123.

Lukaszewski, A. J. (1995). Chromatid and chromosome type breakage-fusion-bridge cycles in wheat (Triticum aestivum L.). Genetics, 140(3), 1069–1085.

Masonbrink, R. E., & Birchler, J. A. (2012). Accumulation of multiple copies of maize minichromosomes. Cytogenetic and Genome Research, 137(1), 50–59.

McClintock, B. (1931). Cytological observations of deficiencies involving known genes, translocations and an inversion in Zea mays. University of Missouri, College of Agriculture, Agricultural Experiment Station.

McClintock, B. (1938). The Production of Homozygous Deficient Tissues with Mutant Characteristics by Means of the Aberrant Mitotic Behavior of Ring-Shaped Chromosomes. Genetics, 23(4), 315–376.

McClintock, B. (1941). SPONTANEOUS ALTERATIONS IN CHROMOSOME SIZE AND FORM IN ZEA MAYS. In Cold Spring Harbor Symposia on Quantitative Biology (Vol. 9, Issue 0, pp. 72–81). https://doi.org/10.1101/sqb.1941.009.01.010

McClintock, B. (1942). The Fusion of Broken Ends of Chromosomes Following Nuclear Fusion. Proceedings of the National Academy of Sciences of the United States of America, 28(11), 458–463.

Muehlbauer, G. J., Riera-Lizarazu, O., Kynast, R. G., Martin, D., Phillips, R. L., & Rines, H. W. (2000). A maize chromosome 3 addition line of oat exhibits expression of the maize homeobox gene liguleless3 and alteration of cell fates. Genome / National Research Council Canada = Genome / Conseil National de Recherches Canada, 43(6), 1055–1064.

Murata, M. (2014). Minichromosomes and artificial chromosomes in Arabidopsis. Chromosome Research: An International Journal on the Molecular, Supramolecular and Evolutionary Aspects of Chromosome Biology, 22(2), 167–178.

Murata, M., Shibata, F., & Yokota, E. (2006). The origin, meiotic behavior, and transmission of a novel minichromosome in Arabidopsis thaliana. Chromosoma, 115(4), 311–319.

Murata, M., Yokota, E., Shibata, F., & Kashihara, K. (2008). Functional analysis of the Arabidopsis centromere by T-DNA insertion-induced centromere breakage. Proceedings of the National Academy of Sciences of the United States of America, 105(21), 7511–7516.

Naish, M., Alonge, M., Wlodzimierz, P., Tock, A. J., Abramson, B. W., Schmücker, A., Mandáková, T., Jamge, B., Lambing, C., Kuo, P., Yelina, N., Hartwick, N., Colt, K., Smith, L. M., Ton, J., Kakutani, T., Martienssen, R. A., Schneeberger, K., Lysak, M. A., … Henderson, I. R. (2021). The genetic and epigenetic landscape of the Arabidopsis centromeres. Science, 374(6569), eabi7489.

Peterka, H., Budahn, H., Schrader, O., Ahne, R., & Schütze, W. (2004). Transfer of resistance against the beet cyst nematode from radish (Raphanus sativus) to rape (Brassica napus) by monosomic chromosome addition. Theoretical and Applied Genetics, 109(1), 30–41.

Pristyazhnyuk, I. E., & Menzorov, A. G. (2018). Ring chromosomes: from formation to clinical potential. Protoplasma, 255(2), 439–449.

Ravi, M., & Chan, S. W. L. (2010). Haploid plants produced by centromere-mediated genome elimination. Nature, 464(7288), 615–618.

Ravi, M., Shibata, F., Ramahi, J. S., Nagaki, K., Chen, C., Murata, M., & Chan, S. W. L. (2011). Meiosis-specific loading of the centromere-specific histone CENH3 in Arabidopsis thaliana. PLoS Genetics, 7(6), e1002121.

Schubert, I. (2001). Alteration of chromosome numbers by generation of minichromosomes – Is there a lower limit of chromosome size for stable segregation? In Cytogenetic and Genome Research (Vol. 93, Issues 3-4, pp. 175–181). https://doi.org/10.1159/000056981

Seymour, D. K., Filiault, D. L., Henry, I. M., Monson-Miller, J., Ravi, M., Pang, A., Comai, L., Chan, S. W. L., & Maloof, J. N. (2012). Rapid creation of Arabidopsis doubled haploid lines for quantitative trait locus mapping. Proceedings of the National Academy of Sciences of the United States of America, 109(11), 4227–4232.

Sodré, C. P., Guilherme, R. S., Meloni, V. F. A., Brunoni, D., Juliano, Y., Andrade, J. A. D., Belangero, S. I. N., Christofolini, D. M., Kulikowski, L. D., & Melaragno, M. I. (2010). Ring chromosome instability evaluation in six patients with autosomal rings. Genetics and Molecular Research: GMR, 9(1), 134–143.

Speevak, M. D., Smart, C., Unwin, L., Bell, M., & Farrell, S. A. (2003). Molecular characterization of an inherited ring (19) demonstrating ring opening. American Journal of Medical Genetics. Part A, 121A(2), 141–145.

Tan, E. H., Henry, I. M., Ravi, M., Bradnam, K. R., Mandakova, T., Marimuthu, M. P., Korf, I., Lysak, M. A., Comai, L., & Chan, S. W. (2015). Catastrophic chromosomal restructuring during genome elimination in plants. eLife, 4. https://doi.org/10.7554/eLife.06516

Tan, E. H., Ordoñez, B., Thondehaalmath, T., Seymour, D. K., Maloof, J. N., Maruthachalam, R., & Comai, L. (2023). Establishment and inheritance of minichromosomes from Arabidopsis haploid induction. Chromosoma. https://doi.org/10.1007/s00412-023-00788-5

Umbreit, N. T., Zhang, C.-Z., Lynch, L. D., Blaine, L. J., Cheng, A. M., Tourdot, R., Sun, L., Almubarak, H. F., Judge, K., Mitchell, T. J., Spektor, A., & Pellman, D. (2020). Mechanisms generating cancer genome complexity from a single cell division error. Science, 368(6488). https://doi.org/10.1126/science.aba0712

Wang, B., Yang, X., Jia, Y., Xu, Y., Jia, P., Dang, N., Wang, S., Xu, T., Zhao, X., Gao, S., Dong, Q., & Ye, K. (2021). High-quality Arabidopsis thaliana Genome Assembly with Nanopore and HiFi Long Reads. Genomics, Proteomics & Bioinformatics. https://doi.org/10.1016/j.gpb.2021.08.003

Yan, X., Li, C., Yang, J., Wang, L., Jiang, C., & Wei, W. (2017). Induction of telomere-mediated chromosomal truncation and behavior of truncated chromosomes in Brassica napus. The Plant Journal: For Cell and Molecular Biology, 91(4), 700–713.

Yin, X., Zhang, Y., Chen, Y., Wang, J., Wang, R. R.-C., Fan, C., & Hu, Z. (2021). Precise Characterization and Tracking of Stably Inherited Artificial Minichromosomes Made by Telomere-Mediated Chromosome Truncation in Brassica napus. Frontiers in Plant Science, 12, 743792.

Yokota, E., Shibata, F., Nagaki, K., & Murata, M. (2011). Stability of monocentric and dicentric ring minichromosomes in Arabidopsis. Chromosome Research: An International Journal

on the Molecular, Supramolecular and Evolutionary Aspects of Chromosome Biology, 19(8), 999–1012.

Tables

Table 4.1. Transmission rates of *mini1a* in selfed progenies over eleven generations.

Generation *mini1a**	Nºfamilies (Individuals) assayed	Nº individuals carrying minis	Transmission rate average, %	Transmission rate range, %
F2	1 (17)	8	47	na
S1	1 (10)	6	60	na
S2	1 (10)	3	30	na
S3	1 (7)	3	42.8	na
S4	1 (15)	6	40	na
S5	2 (162)	76	47	46 – 48
S6	5 (299)	128	43	31.4 – 52.2
S7	11 (664)	173	23	0 – 55.3
S8	8 (408)	122	29.1	0 – 55.6
S9	16 (789)	213	25.8	5.6 – 47.7
S10	4 (250)	28	19.2	0 – 38.9

*Pool data per combination

na: not applicable

Table 4.2. Parental transmission rate of the *mini1a*

Parental combination*	**N° individuals scored**	**N° individuals carrying *mini1a***	***Mini1a* transmission rate %**
mini1a × WT	320	40	12.5
WT × *mini1a*	168	18	10.7

WT: *Landsberg erecta* glabra

*Pool data per combination

Table 4.3. Transmission rate of *mini1a* in crosses using different chlorophyll b-less mutants.

Cross Combination[^]	**N^{o} cross combinations**	**% *mini1a* transmission rate**
mini1a$^{S7,S9\ \&S10}$ × *ch1-1* (CS3119)	23	4.3%
mini1a^{S10} × *ch1-2* (CS3120)	3	0%
mini1a$^{S7,S9\&S10}$ × *ch1-3* (CS3121)	9	11.6%
mini1a$^{S9\ \&S10}$ × *ch1-1*, *gi-1* (CS3354)	6	1.4%
mini1a^{S9} × *ch1*, *gi-1* (CS3362)	1	10%
mini1a$^{S7\&S10}$ × *ch1*-1 (CS41)	10	0%

[^] Symbols represented the generations of *mini1a* lines used in the respective cross combinations.

Table 4.4. Chi-square goodness-of-fit analysis of the F2 progeny of crosses complementing chlorophyll b-less mutant with *mini1a*.

F2 Family code	Pedigree^	Phenotypic ratio observed (G:LG)	X^2	p-value
MCHR642	[MCHR343 #68 × *ch1-3* CS 3121](×)	251:143	26.81	**<0.001** ***
MCHR643	[MCHR343 #55 × *ch1-3* CS 3121](×)	333:105	0.25	0.616 ns
MCHR644	[MCHR343 #64 × *ch1-3* CS 3121](×)	245:91	0.78	0.378 ns
MCHR646	[MCHR343 #68 × *ch1-3* CS 3121](×)	36:7	1.74	0.188 ns
MCHR647	[MCHR343 #55 × *ch1-3* CS 3121](×)	397:120	0.88	0.349 ns
MCHR648	[MCHR343 #49 × *ch1-3* CS 3121](×)	60:11	3.42	0.064 ns
MCHR649	[MCHR343 #55 × *ch1-3* CS 3121](×)	809:232	4.09	0.043 *
MCHR650	[MCHR343 #64 × *ch1-3* CS 3121](×)	213:69	0.04	0.841 ns
MCHR651	[MCHR343 #64 × *ch1-3* CS 3121](×)	236:50	8.62	**0.003** **
MCHR652	[MCHR290 #84 × *ch1*, *gi-1* CS 3362](×)	40:15	0.15	0.703 ns
MCHR653	[MCHR343 #59 × *ch1-1* CS 3119](×)	400:79	18.49	**<0.001** ***

^ MCHR343 correspond to a *mini1a* line from generation S10, and MCHR290 corresponds to a *mini1a* line from generation S9.

*** significant at p<0.001, ** significant at p<0.05, ns: not significant.

Table 4.5. Phenotypic ratio of different F3 families and their corresponding genotypes.

Genotype	Nº of families assayed^	Phenotypic ratio observed (G:LG)	Range of individuals displaying irregular patches
-/-	1	0:1	-
+/-	1	3:1	-
+/+/mini+	1	1:0	-
	1(***)	1:1	11
	3 (2**)	2:1	0 - 5
	12 (ns)	3:1	0 -70
+/-/*mini*+ or -/-/mini+	5 (1***)	4:1	0 -16
	2 (1**)	5:1	-
	1 (**)	6:1	-
	1 (ns)	7:1	-

^The number of families exhibiting a green to light-green ration significantly different from the 3:1 expected ratio is indicated within brackets, with the following notations:
*** for $p < 0.001$, ** for $p < 0.05$, and 'ns' for no significant difference.

Figures

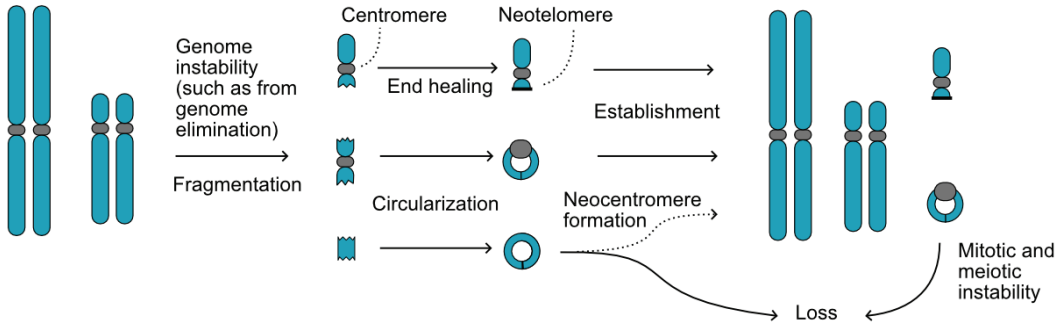

Fig. 4.1. Formation of minichromosomes as a result of genome instability. It is proposed that minichromosomes arise from genome instability, leading to fragmentation. Chromosomal fragments that contain a centromere, or form a neocentromere, can be stabilized by either formation of telomeres or by circularization. The resulting chromosomes are typically characterized by instability, primarily due to their small size or circular nature.

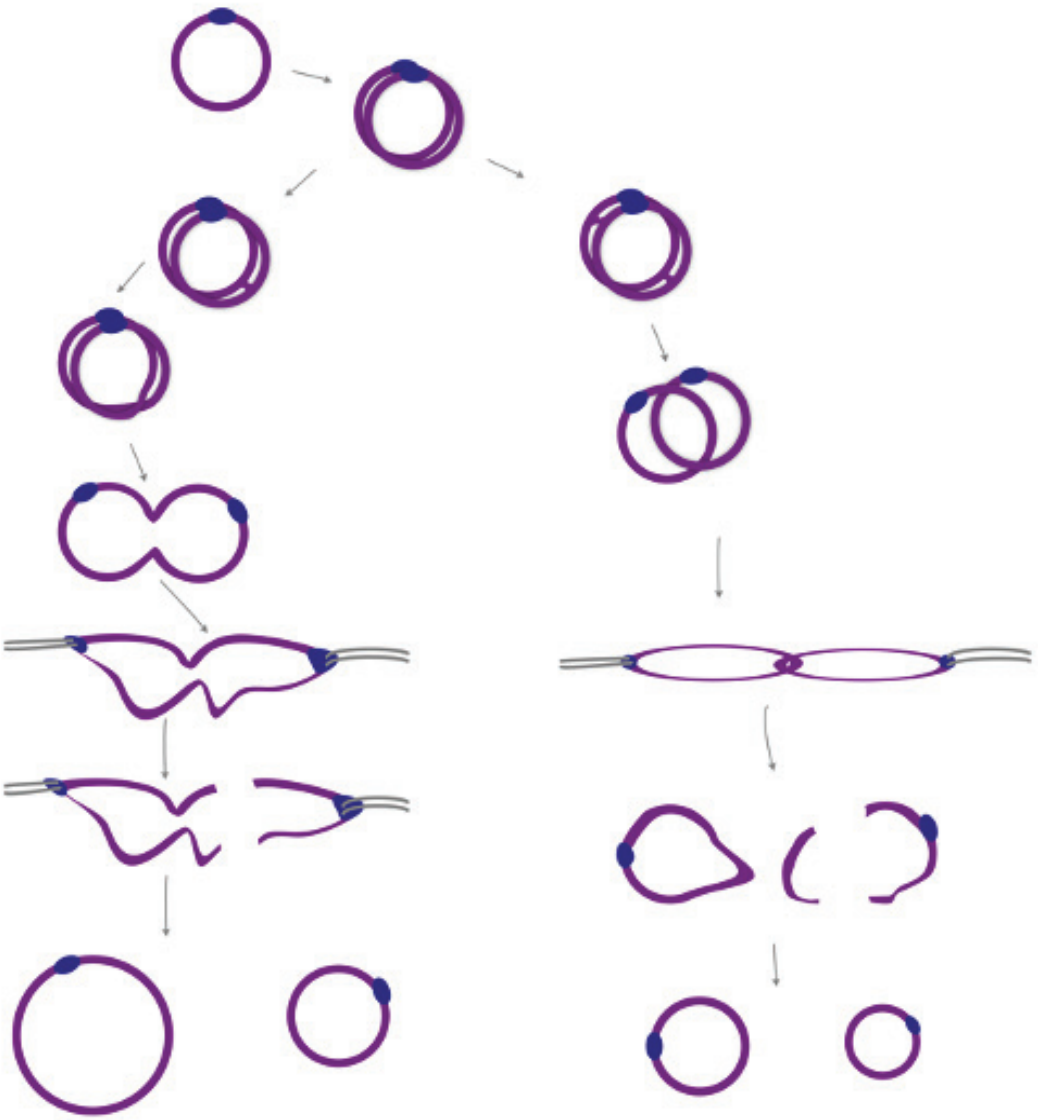

Fig. 4.2. Ring minichromosome (mini) instability in the cell cycle. The fate of a ring mini in the cell cycle depends on sister chromatid exchange (SCE) during S phase and G2 phase. Ring minis remain intact in the absence of SCE. When there is an odd number of SCEs, ring chromosomes double in size and form dicentric chromosomes. In the case of an even number of SCEs, chromosomes either separate normally or form interlocked rings, which break during the metaphase-anaphase transition, producing rings or fragments of different sizes. This illustration is based on Pristyazhnyuk and Menzorov (2018).

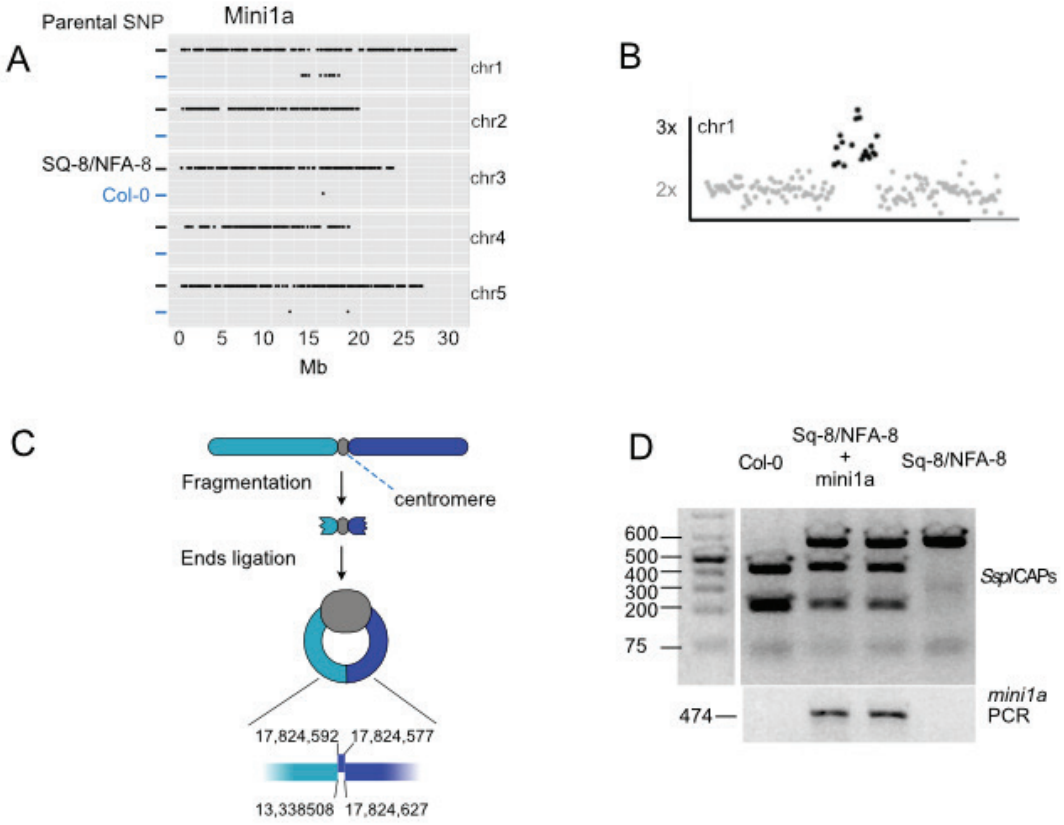

Fig. 4.3. Detection and analysis of *mini1a*. The presence of a *mini1a* minichromosome derived from the GFP-tailswap haploid inducer (Col-0 Ecotype) in haploid induced Sq-8/NFA-8 F1 hybrids was confirmed by genomic analysis. A) Detection of Col-0 SNPs on chromosome 1 (chr1) of a haploid individual, B) Dosage plot of F2 doubled haploid line *mini1a*, C) Origin, inferred structure, and breakpoint junction of *mini1a* at circularization site, and D) Cleaved amplified polymorphic sequence (CAPS) assay using the restriction enzyme SspI to distinguish Sq-8/NFQ-8 lines containing *mini1a* using a SNP at position 13,405,811of chr1, as well as corresponding *mini1a* junction PCR of *mini1a* at the expected breakpoint junction site.

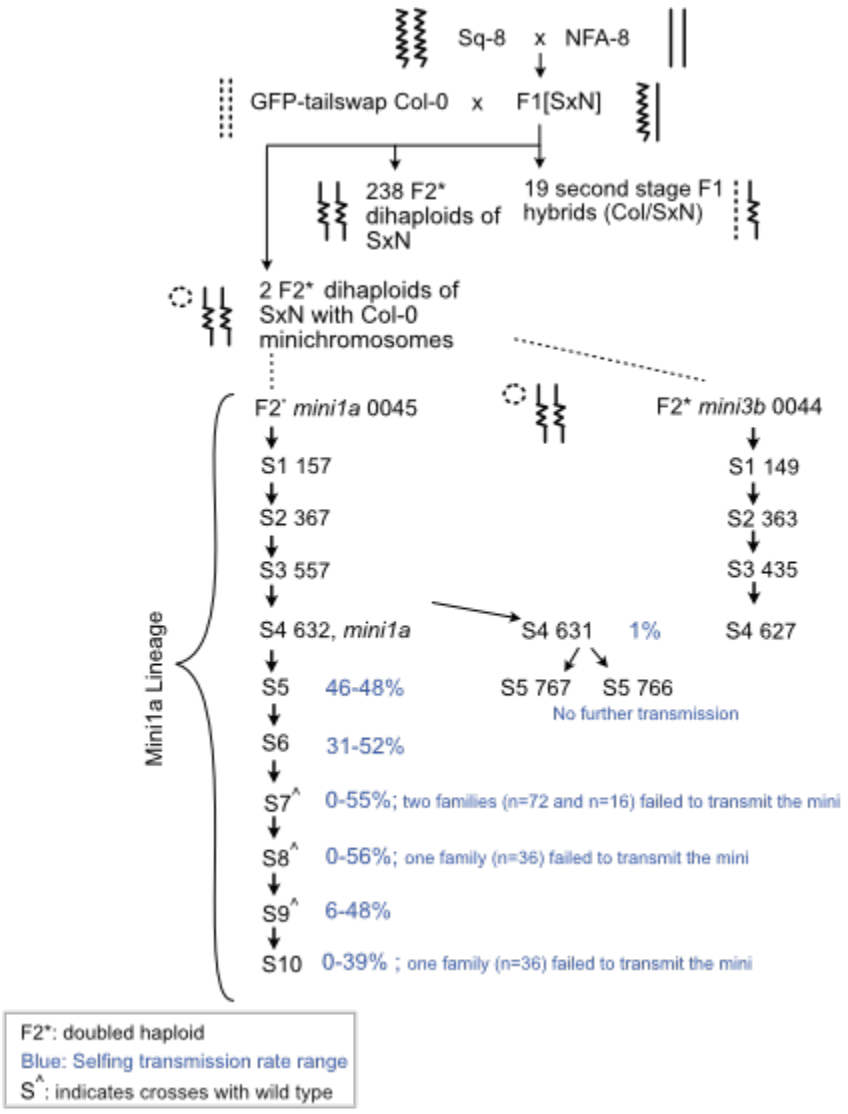

Fig. 4.4. Pedigree describing the production and characterization of minichromosomes via centromere-mediated genome elimination.
Transmission rates are summarized for the advanced lineage of the *mini1a* line. Smooth, wavy, and dotted lines represent the NFA-8, Sq-8, and GFP-TS Col-0 genomes, respectively. Second-stage F1s are the expected result of failed Col-0 genome elimination (Seymour et al. 2012). F2 generations are double haploid. The selfing transmission rate range per generation is indicated in blue. Superscripts in generations (S) indicate that crosses to wild-type (WT) were performed as well.

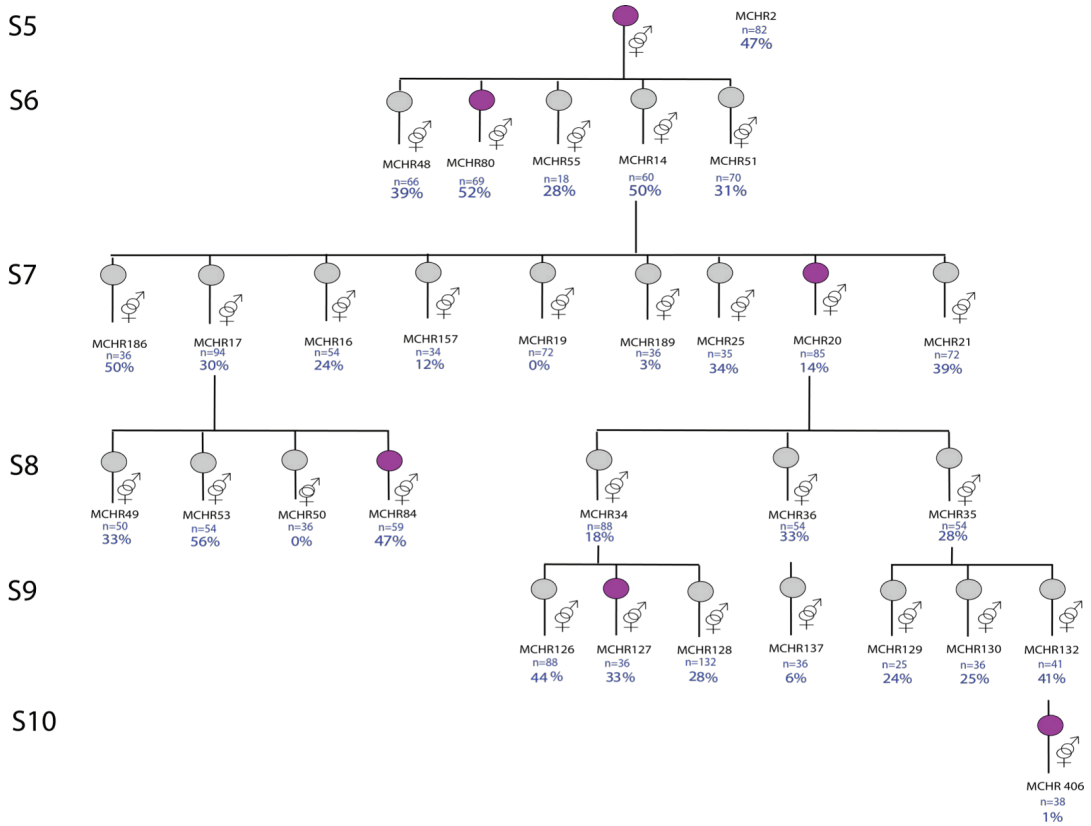

Fig. 4.5. Detailed *mini1a* lineage spanning generations S5 to S10, showing the number of individuals (n) and their respective *mini1a* transmission rates as percentages for each family in blue. Families chosen for sequencing are highlighted with a purple fill.

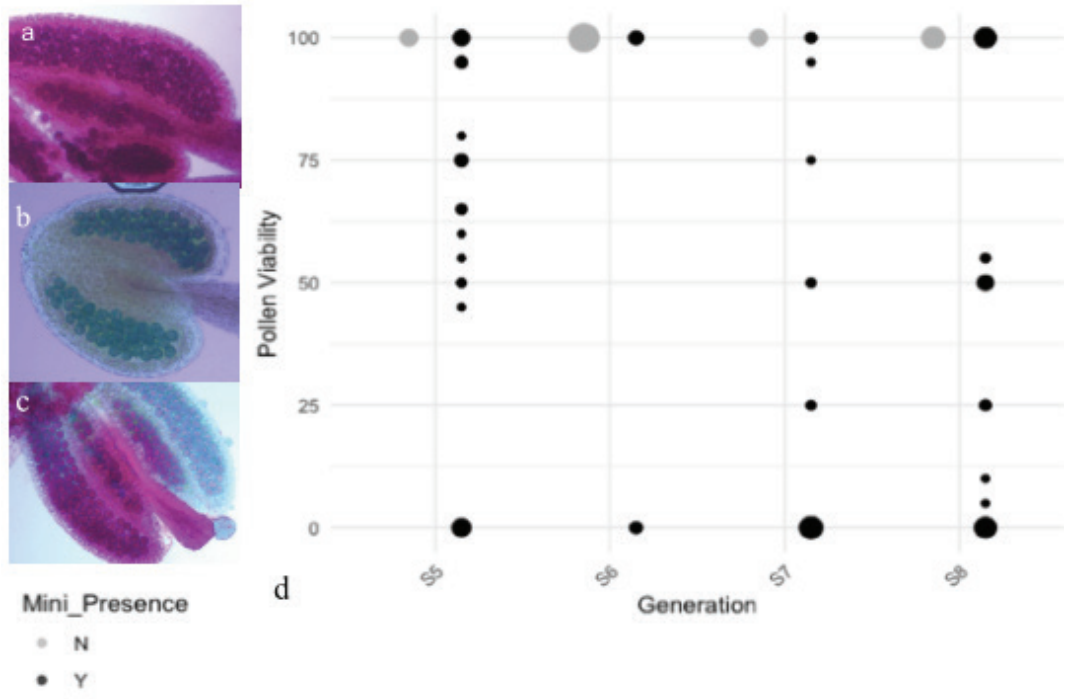

Fig. 4.6. Pollen viability of *mini1a* lines. A-C) Alexander's staining of anthers from plants carrying *mini1a* from generation S7. Wild-type pollen stains red while the aberrant pollen grains stain green. a) Displaying full viable pollen, b) Sterile pollen, c) Variable pollen viability and d) Pollen viability percentage distribution in individuals carrying *mini1a* and individuals that had failed to carry *mini1*a across generations. Dot size represents the number of individuals in each category.

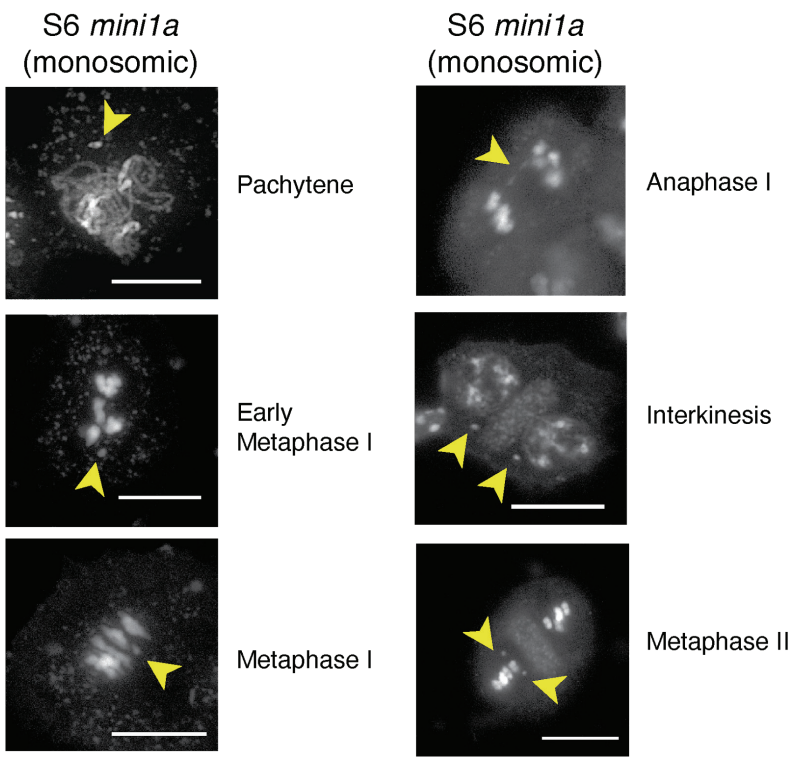

Fig. 4.7. Meiotic behavior of male meiocytes from monosomic *mini1a* in S6 lines. Yellow arrowheads indicate presumed location of *mini1a* during meiotic stage. Scale bar = 10um.

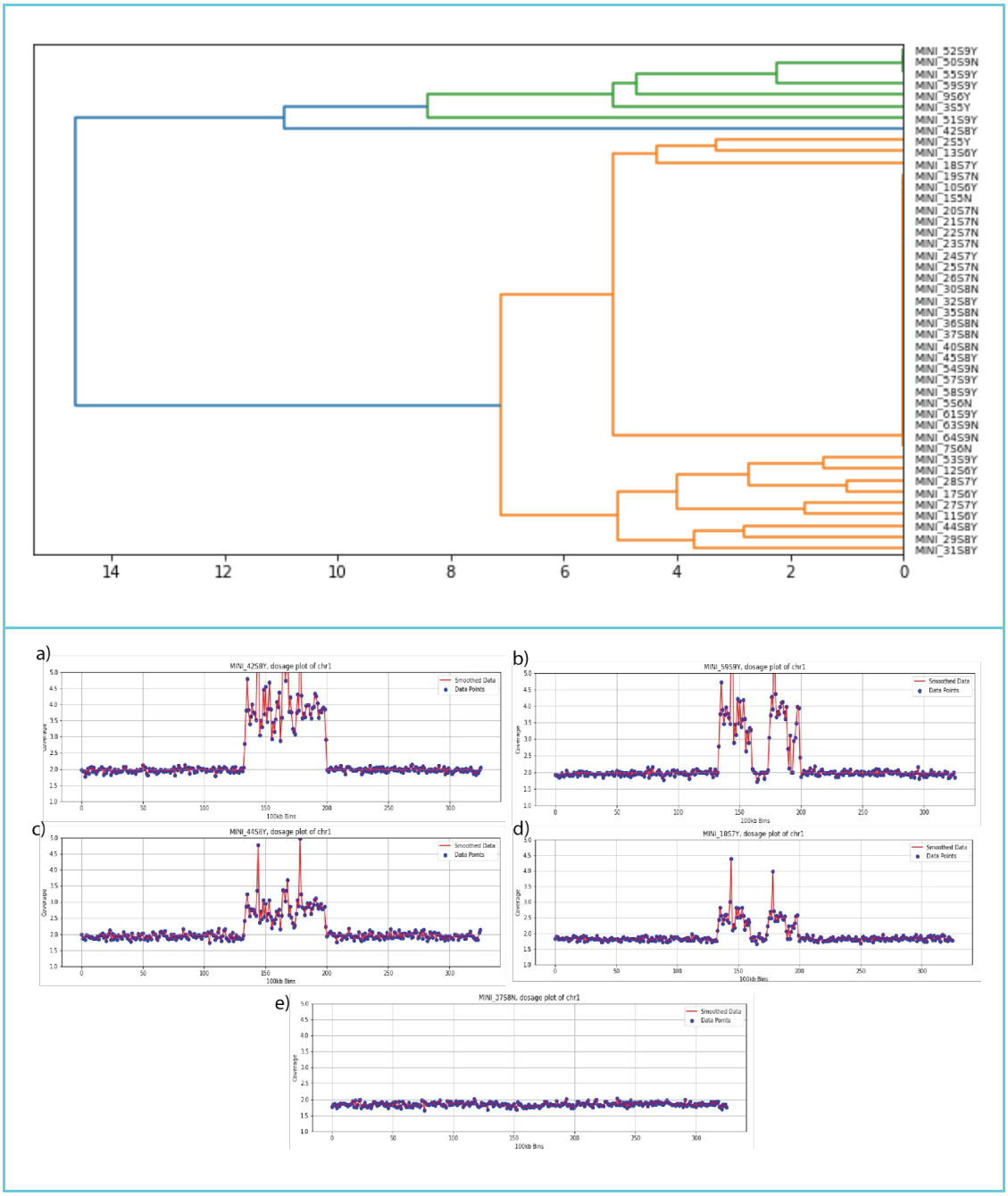
MINI_52S9Y
MINI_50S9N
MINI_55S9Y
MINI_59S9Y
MINI_9S6Y
MINI_3S5Y
MINI_51S9Y
MINI_42S8Y
MINI_25S7Y
MINI_13S6Y
MINI_18S7Y
MINI_19S7N
MINI_10S6Y
MINI_1S5N
MINI_20S7N
MINI_21S7N
MINI_22S7N
MINI_23S7N
MINI_24S7Y
MINI_25S7N
MINI_26S7N
MINI_30S8N
MINI_32S8Y
MINI_35S8N
MINI_36S8N
MINI_37S8N
MINI_40S8N
MINI_45S8Y
MINI_54S9N
MINI_57S9Y
MINI_58S9Y
MINI_55S6N
MINI_61S9Y
MINI_63S9N
MINI_64S9N
MINI_7S6N
MINI_33S9Y
MINI_12S6Y
MINI_28S7Y
MINI_17S6Y
MINI_27S7Y
MINI_11S6Y
MINI_44S8Y
MINI_29S8Y
MINI_31S8Y
14
12
10
8
6
4
2
0
a)
MINI_42S8Y, dosage plot of chr1
b)
MINI_59S9Y, dosage plot of chr1
c)
MINI_44S8Y, dosage plot of chr1
d)
MINI_18S7Y, dosage plot of chr1
e)
MINI_37S8N, dosage plot of chr1
Smoothed Data
Data Points
Coverage
100kb Bins

Fig. 4.8. **Hierarchical cluster dendrogram and chromosome dosage plot illustrating *mini1a* variation from generations S5 to S10.** Top panel: Hierarchical clustering of lines carrying *mini1a* and those failing to transmit *mini1a*, based on pattern detection within sliding windows (110-220 kb bins), spanning generations from S5 to S10. The analysis focuses on data points above the coverage threshold of 2. Bottom panel: Representative chromosome dosage plots for the different clusters observed in the top panel. Plots are based on non-overlapping 100kb bins across chromosome 1. The different categories are as follows: a) presence of two full copies of *mini1a*, b) deleted version with two copies of *mini1a* (hereafter *mini1a*Δ) c) one full copy of *mini1a,* and d) one copy of the deleted version of *mini1a,*, e) absence of *mini1a*.

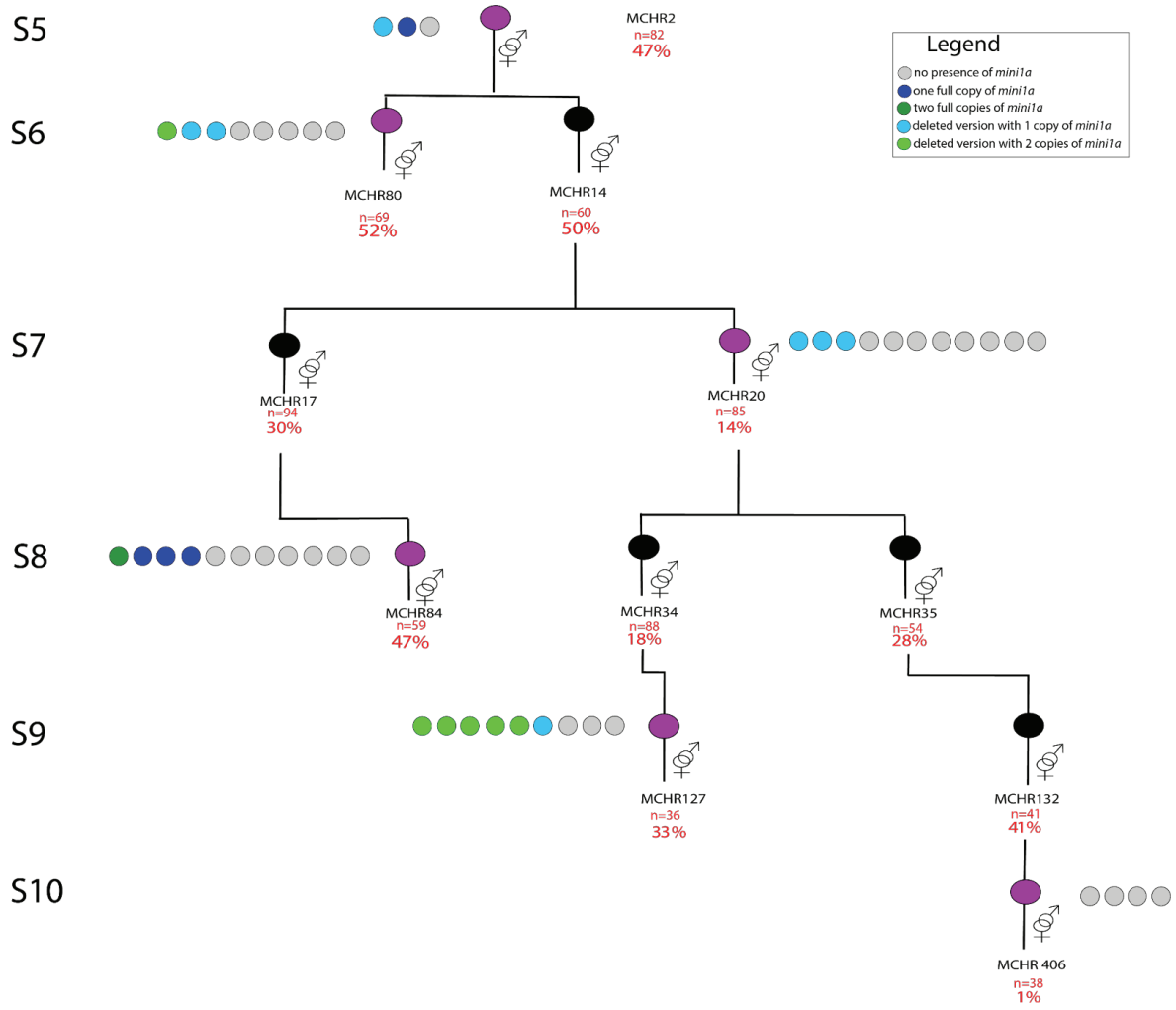

Fig. 4.9. Lineage pedigree displaying *mini1a* structural variation from generations S5 to S10. Sequenced families are highlighted in purple, while non-sequenced families are in black fill. The pedigree reveals five distinct patterns: one full copy of *mini1a*, two full copies of *mini1a*, a deleted version with one copy of *mini1a*, and a deleted version with two copies of *mini1a*.

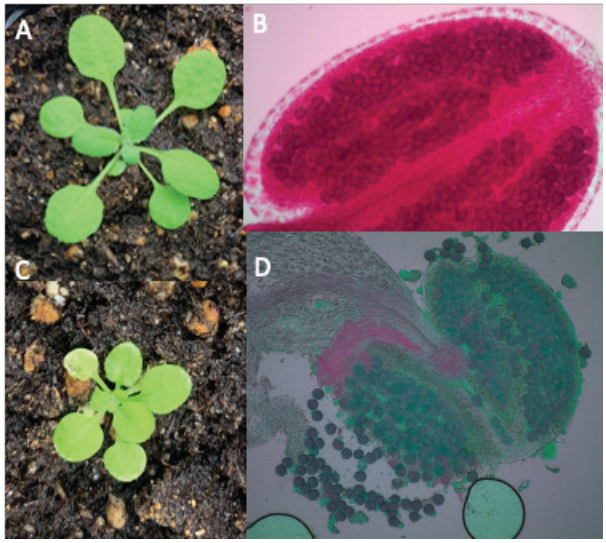

Fig. 4.10. Phenotypic comparison between mini1a lines and chlorophyll b-less mutants. A) *mini1a* line displaying a green phenotype, C) *ch1-1* (CS41) line displaying a light green phenotype. B) Alexander's staining of *mini1a* anther showing fully viable pollen. D) chlorophyll b-less mutant (CS41) anther containing sterile pollen.

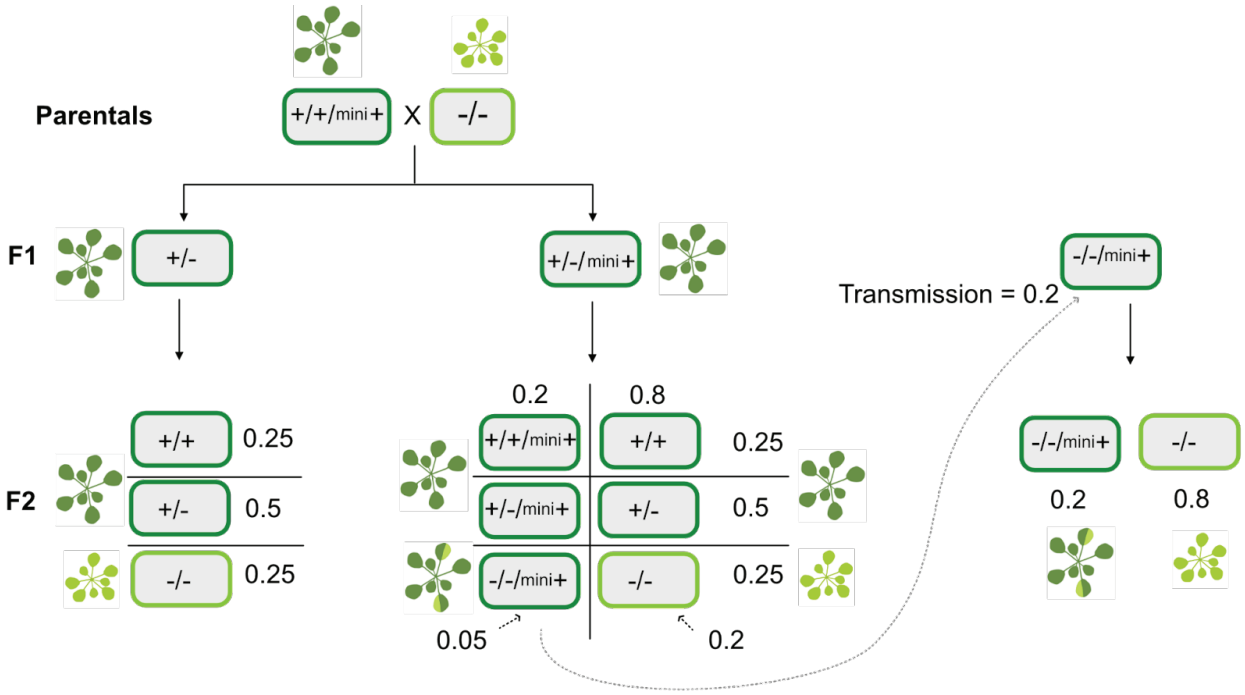

Table. Expected progeny ratio upon selfing *mini1a* lines

+/-/mini+			-/-/mini+	
Transmission rate	Frequency of light green -/-	Green : Light green	Frequency of light green -/-	Green : Light green
0	0.25	3.0 : 1	1	0 : 1
0.1	0.225	3.4 : 1	0.9	1 : 9
0.2	0.2	4.0 : 1	0.8	1 : 4
0.3	0.175	4.7 : 1	0.7	1 : 2.3

Fig. 4.11 Expected patterns of inheritance and complementation in Arabidopsis *ch1* mutants carrying the *CH1* allele on a minichromosome. Top panel, genotypes and frequencies F1 and F2 filial generation under the assumption of 0.2 minichromosome transmission rate during selfing. Bottom panel, table of frequencies and ratios under different transmission ratios. (mini+) symbolizes the *mini1a CH1* allele. A wild-type, +/+ *(*mini+*)* parent was crossed to -/-.
Selfed +/- F1 heterozygotes produced the expected 3:1 progeny.

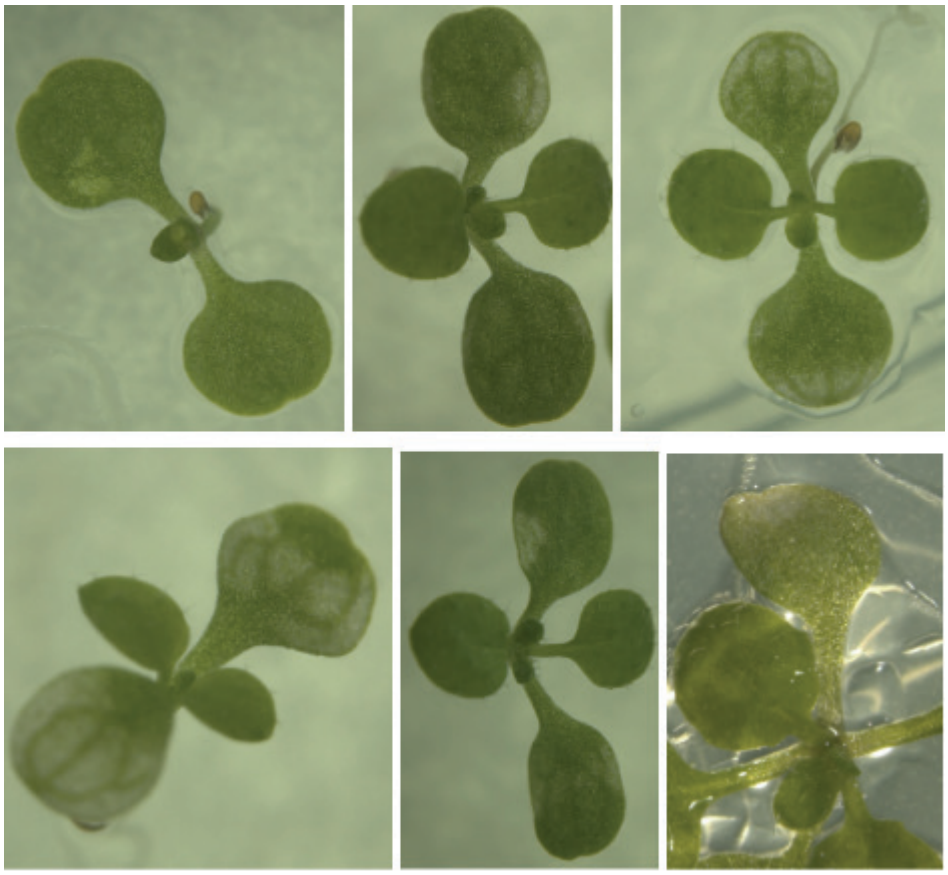

Fig. 4.12. Instances of irregular variegation in F3 individuals from crosses between *mini1a* lines with chlorophyll-b less mutants. The irregularity of the variegation may be attributed to an epigenetic silencing of CH1 gene.

Supplemental material

Supplemental Tables

Table S.4.1. Mutant lines displaying a mutation in the CAO gene.

Donor stock code number	**Mutation acronym**	**Description**	**Ecotype background***
CS3362	*ch1*, *gi-1*	double mutant	Col
CS3354	*ch1-1*, *gi-1*	double mutant	Col
CS3121	*ch1-3*	mutant	Col
CS3120	*ch1-2*	mutant	Col
CS3119	*ch1-1*	mutant	Col
CS126	*le-1*, *ch1-1*	multiple mutant mapping line	Est; Ler
CS41	*ch1-1*	mutant	L*er*

Table S.4.2. Primer sequences used for *mini1a* detection.

Name	**Sequence (5'-3')**
SNP1:13405811 F SspI	TGAGAACTCACTAGATGCGAGGA
SNP1:13405811 R SspI	GCTAAGCACTCAACTAACTTCTGTCAG
SNP3:16409164 F BstAPI	CCTCTCTTGGAGCAGTGATTGGAG
SNP3:16409164 R BstAPI	GCAAGAATTCAAGAGTCCTTTGTGGTTTG
Mini1a Fwd17.8M	CTAGTGATTTAACGTATTGACCA
Mini1a Rev13.3M	GAGATGTACCTTGTATCTTGAA

Supplemental Figures

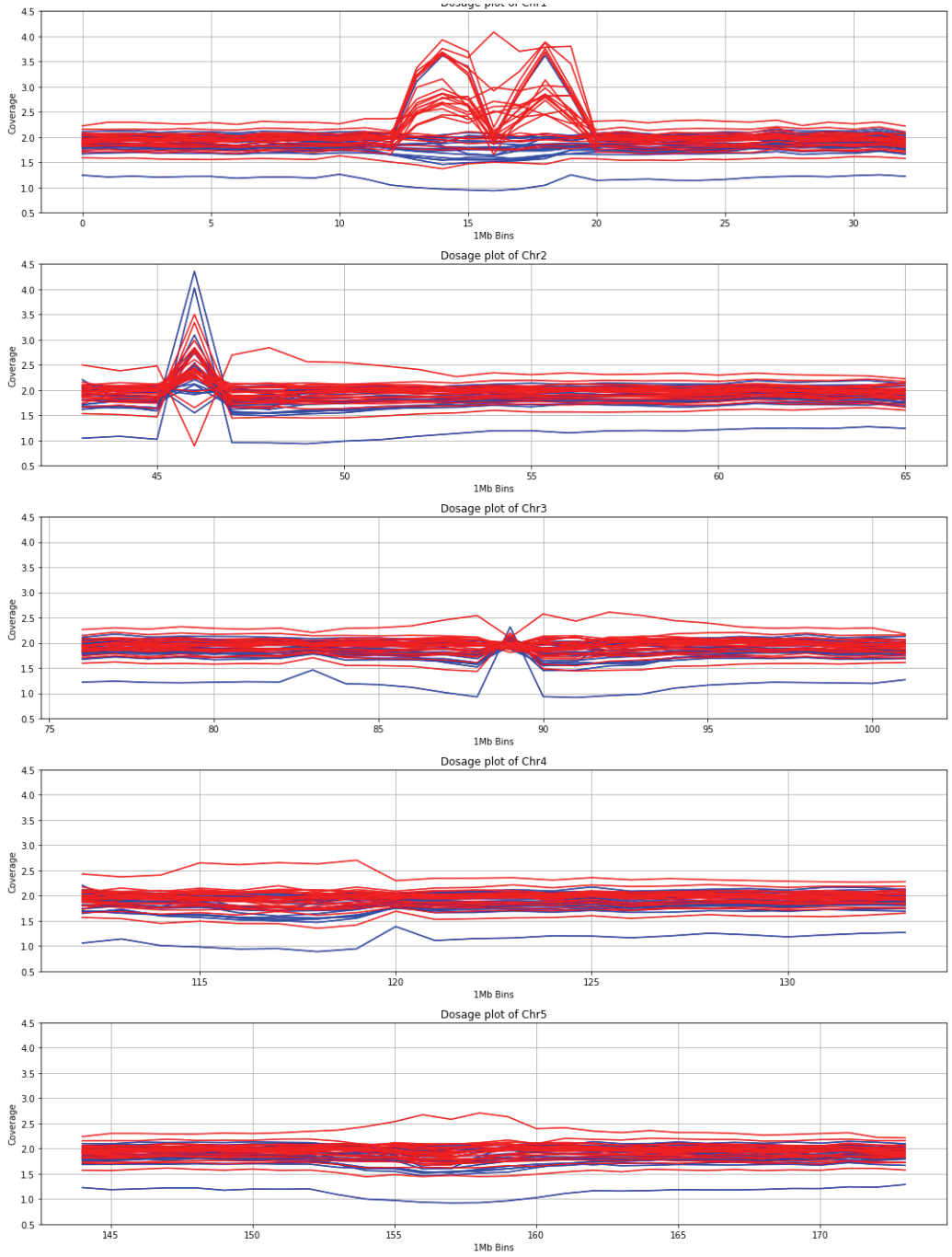

Fig. S.4.1. Overlay dosage plot of all the sequenced individuals in consecutive non-overlapping 1MB bins across all five Arabidopsis chromosomes. Two groups are defined based on the *mini1a* PCR assay: individuals who failed to carry *mini1a* are represented in 'blue', while individuals carrying *mini1a* are represented in 'red.

Chapter 5
General Conclusions

Overview of Dissertation Research

The work presented in this thesis has enhanced our understanding of the novel rearrangements arising from haploid induction crosses, and the importance of an in-depth phenotypic characterization to unveil potential agricultural applications for these new and unique chromosomal rearrangements. Minichromosomes (minis) stand out as a most interesting byproduct of haploid induction, alongside dihaploids. Therefore, a detailed characterization of their meiotic and mitotic stability transgenerationally is crucial for future applications.

This dissertation primarily addressed the following questions, using two model haploid induction systems, potato, and Arabidopsis: *i*) What genetic and genomic variations arise in the progeny of potato haploid induction? *ii*) What is the impact of the novel rearrangements resulting from haploid induction crosses on the phenotype? *iii*) What is the structure and transmission pattern of specific novel rearrangement, such as minichromosomes (minis), resulting from haploid induction in Arabidopsis? and *iv*) Can studying minichromosomes in Arabidopsis shed light on minichromosomes behavior in potato?.

These questions explore how knowledge gained from haploid induction in Arabidopsis could further the understanding of mechanisms of haploid induction in potatoes. Additionally, they investigate the similarities in byproducts, i.e. unexpected genomic outcomes, between the two species and their relevance in deciphering potato haploid induction.

In potato, while novel rearrangements resulting from haploid induction have been observed previously, they were often overlooked due to the primary focus on development of dihaploids. The Haploid Inducer (HI), a key player in this system, has not seen improvements since the release

of the IvP lines in the 1970s, despite its crucial role in efficient dihaploid production. Our study demonstrated that PL-4, a new haploid inducer, performed significantly better and exhibited a homogeneous response regardless of the genetic background of the tetraploid parents, particularly in terms of two key traits: the number of dihaploids per 100 fruits (*DH100F*) and haploid induction rate (*HIR*). PL-4 also demonstrated valuable traits for a HI, including profuse flowering and pollen-shedding capacity. Additionally, we observed that PL-4 exhibited a reduced proportion of hybrid seeds, facilitating a rapid and efficient screening process.

Taken together, the superior performance of PL-4 has the potential to boost haploid induction within breeding programs, thereby reducing production costs and accelerating the development of diploid parental lines for further breeding pipelines.

Furthermore, the byproducts of potato haploid induction have not been thoroughly characterized, especially with regards to whether specific HIs yield higher numbers of introgressions or additions. From the perspective of a traditional breeder, a Haploid inducer (HI) with this characteristic would be undesirable. However, it is possible that novel rearrangements, additions or introgressions into the dihaploid background can engender superior or novel traits, in addition to providing important functional genomic information. Therefore, we chose IvP48, which has been documented as an 'imperfect' HI because previous molecular markers and cytological analysis have suggested that, in some cases, a partial genomic contribution by the HI was retained (Clulow et al. 1991, 1993; Clulow & Rousselle-Bourgeois, 1997; Ercolano et al. 2004; Samitsu & Hosaka, 2002; Straadt & Rasmussen, 2003).

In the BB progeny, we identified a novel category of seeds—shriveled seeds. The plantlets arising from these seeds were enriched in aneuploid types, allowing the exploration of novel karyotypic arrangements. Among these novel rearrangements, we highlight BB-266, a dihaploid displaying a likely chromothripsis event. This event is characteristic of the cancer-related syndrome termed chromoanagenesis (Holland and Cleveland 2012), which refers to complex and pervasive rearrangements involving one or a few chromosomes that occur in a single catastrophic event. It is thought to result from damage and repair during the rescue of missegregated chromosomes. This event has not been observed among the byproducts of haploid induction in potato before, but it has been observed in the product of haploid induction in Arabidopsis (Tan et al. 2015; Kuppu et al. 2015) Specifically, about a third of the additions display extensive restructuring of HI-contributed chromosomes (Britt & Kuppu, 2016; Comai & Tan, 2019).

Finally, while our study has addressed the limited information on the tuber characteristics of the byproducts of haploid induction in potatoes, further agronomic traits can confirm our findings. Unfortunately, only a few instances of dihaploids carrying HI chromosomes were able to form tubers. This limitation restricts their further utilization from a breeding standpoint.

In contrast to the potato HI system, the Arabidopsis haploid induction system has been extensively studied. It has been described as involving uniparental genome elimination mediated by defective centromeric histone 3 (CENH3) (Ravi & Chan, 2010). The CENH3-based haploid induction crosses produce diverse progeny types with a high frequency (~⅓) of HI DNA additions. One of the rearranged chromosomes is referred to as “minichromosomes” (“minis”), consisting of the centromere of a regular chromosome and small portions of the chromosomal arms (Ishii et al. 2016; Tan et al. 2015). Since no minis have been described in potato haploid induction events yet,

we decided to study a particular mini, referred to as *mini1a*, which is derived from CENH3-based genome elimination crosses and was available from Seymour et al. 's (2012) study.

We analyzed the transmission rates of advanced selfing generations of *mini1a* and made the following observations: *i*) Sublineages can vary tenfold in transmission rates, estimated at 1-14% per gamete, suggesting instability and the possible formation of mini-subtypes. This was corroborated by our sequencing data of *mini1a* across generations, revealing five distinct patterns: one full copy of *mini1a*, two full copies of *mini1a*, a deleted version with one copy of *mini1a*, and a deleted version with two copies of *mini1a*. *ii*) The optimal male and female transmission rates are comparable to trisomic line transmission, ranging from 10-12%. *iii*) Optimally transmitting strains display approximately 28% transmission rate through selfing.

The confirmation of the ring structure through cytology assessment indicates that the mini-subtypes mentioned above maintain circular conformation. Our efforts to characterize mitotic stability using two approaches revealed that *mini1a* adversely affects fertility, manifesting an unusual chimeric phenotype with completely sterile and fully fertile sectors. In the second approach, which involved exploiting the visual trait (green vs light green) through the *ch1* mutation, we observed somatic mosaicism resulting from occasional loss of the ring structure or gene silencing due to position effect variegation. However, this aspect remains the subject of ongoing investigation.

In summary, this dissertation has achieved the following: *i*) compared different HIs to assess their haploid induction rate (HIR) and the influence of parental cytoplasm type on dihaploid development; *ii*) explored the byproducts of haploid induction in potato using next-generation

sequencing (NGS) techniques, and *iii*) conducted comprehensive characterizations of minichromosomes in Arabidopsis to document the potential utility of minichromosomes in plant breeding.

Literature cited

Britt, A. B., & Kuppu, S. (2016). Cenh3: An Emerging Player in Haploid Induction Technology. Frontiers in Plant Science, 7, 357.

Clulow, S. A., & Rousselle-Bourgeois, F. (1997). Widespread introgression of Solatium phureja DNA in potato (S. tuberosum) dihaploids. Plant Breeding = Zeitschrift Fur Pflanzenzuchtung, 116(4), 347–351.

Clulow, S. A., Wilkinson, M. J., & Burch, L. R. (1993). Solanum phureja genes are expressed in the leaves and tubers of aneusomatic potato dihaploids. In Euphytica (Vol. 69, Issues 1-2, pp. 1–6). https://doi.org/10.1007/bf00021720

Clulow, S. A., Wilkinson, M. J., Waugh, R., Baird, E., Demaine, M. J., & Powell, W. (1991). Cytological and molecular observations on Solanum phureja-induced dihaploid potatoes. TAG. Theoretical and Applied Genetics. Theoretische Und Angewandte Genetik, 82(5), 545–551.

Comai, L., & Tan, E. H. (2019). Haploid Induction and Genome Instability. Trends in Genetics: TIG. https://doi.org/10.1016/j.tig.2019.07.005

Ercolano, M. R., Carputo, D., Li, J., Monti, L., Barone, A., & Frusciante, L. (2004). Assessment of genetic variability of haploids extracted from tetraploid (2n = 4x = 48) Solanum tuberosum. Genome / National Research Council Canada = Genome / Conseil National de Recherches Canada, 47(4), 633–638.

Holland, A. J., & Cleveland, D. W. (2012). Chromoanagenesis and cancer: mechanisms and consequences of localized, complex chromosomal rearrangements. In Nature Medicine (Vol. 18, Issue 11, pp. 1630–1638). https://doi.org/10.1038/nm.2988

Ishii, T., Karimi-Ashtiyani, R., & Houben, A. (2016). Haploidization via Chromosome Elimination: Means and Mechanisms. Annual Review of Plant Biology, 67, 421–438.

Kuppu, S., Tan, E. H., Nguyen, H., Rodgers, A., Comai, L., Chan, S. W. L., & Britt, A. B. (2015). Point Mutations in Centromeric Histone Induce Post-zygotic Incompatibility and Uniparental Inheritance. PLoS Genetics, 11(9), e1005494.

Ravi, M., & Chan, S. W. L. (2010). Haploid plants produced by centromere-mediated genome elimination. Nature, 464(7288), 615–618.

Samitsu, Y., & Hosaka, K. (2002). Molecular marker analysis of 24- and 25-chromosome plants obtained from Solanum tuberosum L. subsp. andigena (2n = 4x = 48) pollinated with a Solanum phureja haploid inducer. Genome / National Research Council Canada = Genome / Conseil National de Recherches Canada, 45(3), 577–583.

Seymour, D. K., Filiault, D. L., Henry, I. M., Monson-Miller, J., Ravi, M., Pang, A., Comai, L., Chan, S. W. L., & Maloof, J. N. (2012). Rapid creation of Arabidopsis doubled haploid lines for quantitative trait locus mapping. Proceedings of the National Academy of Sciences of the United States of America, 109(11), 4227–4232.

Straadt, I. K., & Rasmussen, O. S. (2003). AFLP analysis of Solanum phureja DNA introgressed into potato dihaploids. Plant Breeding = Zeitschrift Fur Pflanzenzuchtung, 122(4), 352–356.

Tan, E. H., Henry, I. M., Ravi, M., Bradnam, K. R., Mandakova, T., Marimuthu, M. P. A., Korf, I., Lysak, M. A., Comai, L., & Chan, S. W. L. (2015). Catastrophic chromosomal restructuring during genome elimination in plants. In eLife (Vol. 4). https://doi.org/10.7554/elife.06516.